5-2018

Behavioral, Functional, and Shape Assessment for Temporomandibular Joint

Feng Wei
Clemson University, weifeng0715@gmail.com

BEHAVIORAL, FUNCTIONAL, AND SHAPE ASSESSMENT FOR TEMPOROMANDIBULAR JOINT

A Dissertation
Presented to
the Graduate School of
Clemson University

In Partial Fulfillment
of the Requirements for the Degree
Doctor of Philosophy
Bioengineering

---

by
Feng Wei
May 2018

Accepted by:
Hai Yao, PhD, Committee Chair
Mark Van Horn, PhD
Tong Ye, PhD
Martine LaBerge, PhD

ABSTRACT

Temporomandibular joint (TMJ) disorders affect over 10 million people in the US with an annual economic cost of more than $4 billion. Due to intriguing etiological factors of TMJ disorders, objective and accurate diagnosis is difficult and so is with the treatment. Consequently, there is the high recurrence rate. To make the situation even worse, many other types of diseases, including cancer, share symptoms and signs with TMJ disorders. Early non-invasive, objective, subject-specific and accurate diagnosis is vital because incorrect or delayed diagnosis can cause patients to miss optimal treatment times, increase unnecessary therapy expenses and even endanger patients' lives. The gold standard diagnostic criteria for TMJ disorders (DC/TMD) largely depend on subjective decisions, and therefore, it is necessary to develop a patient specific, non-invasive, and quantitative assessment system, to identify possible risk indicators for the objective early diagnosis of TMJ disorders and to determine their etiological biomechanical mechanisms by investigating the underlying biomechanical and transport pathophysiology of these indicators. As a result, significant advances in biomechanics and nutrient supply research are essential for early diagnosis and management. Common symptoms of joint sounds, limited or asymmetrical jaw movement, teeth misalignment, pain in the muscle, jaw or neck and jaw muscle stiffness indicate that an objective TMJ disorders diagnosis is necessary and should include TMJ muscle, motion and morphology assessment. Also, compared to other well-developed joint systems such as knee, glenohumeral and hip joints, TMJ has received less attention in biomechanics research because of the joint's complexity in anatomy, neuromuscular recruitment and motion. The direct *in vivo* experimental

measurement for articular space, contact force, stress distribution and nutrient supply in subject-specific TMJ components is superior to other means when a subject-specific diagnosis result is required. However, the TMJ complex anatomy, together with dense blood vessels and surrounding neuron system impedes the direct *in vivo* measurement in humans without breaking joint function integrity. The continuous development of advanced high-technologies has facilitated the development of many numerous scientific and objective diagnosis tools. Therefore, the objectives of this research are to: 1) build a non-invasive data collection system of TMJ motion, muscular electromyography and bite force and 2) determine the behavioral, functional, and morphological aspects for objective diagnosis of TMJ disorders and understanding the underlying pathology. Our central hypothesis is that TMJ properties of muscle, motion, and shape in patients are sensitive to TMJ disorders and, therefore, can be adapted to enhancing objective diagnosis criteria, functional rehabilitation assessment, therapeutic monitor and understanding the underlying pathology. **Aim 1: Determine the muscle activity pattern by calculating EMG parameters for TMJ muscles of mastication. Aim 2: Determine the feature of TMJ kinematics by collecting TMJ motion tracking data and analyzing TMJ motion. Aim 3: Determine the patient-specific TMJ 3D shape signature.** The outcome of this study will yield a data collection system for establishing an objective and subject-specific diagnosis and will build a pathway between biomechanics and the pathophysiology.

ACKNOWLEDGMENTS

I would like to acknowledge the invaluable advice, patience and support of my mentor and committee chair, Dr. Hai Yao. I also would like to acknowledge the other members of my graduate committee, Drs. Mark Van Horn, Tong Ye, and Martine LaBerge for their guidance, suggestions, time and expertise.

I would like to thank all the current and past members of the Yao Tissue Biomechanics Laboratory as well as research collaborators for their efforts and guidance. I would also like to thank Thomas Gallien and Maria Torres in the Clemson-MUSC Bioengineering program. I sincerely appreciate their friendship and efforts in establishing such a nice and compatible community.

Finally, I would like to thank my family for their generous love, encouragement and support through all my life.

TABLE OF CONTENTS

Page

Table of Contents (Continued)

Page

LIST OF TABLES

LIST OF FIGURES

List of Figures (Continued)

Page

CHAPTER ONE: INTRODUCTION

Objective and Specific Aims

The human temporomandibular joint (TMJ) is a bilateral synovial joint which is composed of condyle bone, fossa bone and TMJ disc (Figure 1). TMJ disorders (or TMD) are a category of neuromuscular and musculoskeletal conditions affecting the TMJ, the masticatory muscles, and all associated tissues (Figure 1. The American Academy of Orofacial Pain, AAOP). The most common symptoms of TMJ disorders include: joint sounds, limited or asymmetrical jaw movement, teeth misalignment, pain in the muscle, jaw or neck and jaw muscle stiffness. The most common types of TMJ disorders are internal derangement, or TMJ disc displacement, muscle pain and joint osteoarthritis.

The most commonly accepted diagnosis tool is the 2014 Diagnostic Criteria for Temporomandibular disorders (DC/TMD) [1]. However, the gold standard DC/TMD largely depends on subjective decisions, and therefore it is necessary to develop a patient specific, non-invasive, and quantitative assessment system; and to identify possible risk indicators for objective early diagnosis of TMJ disorders. Researchers can potentially determine the etiological biomechanical mechanism of TMJ disorders by investigating the underlying biomechanical and transport pathophysiology of these indicators.

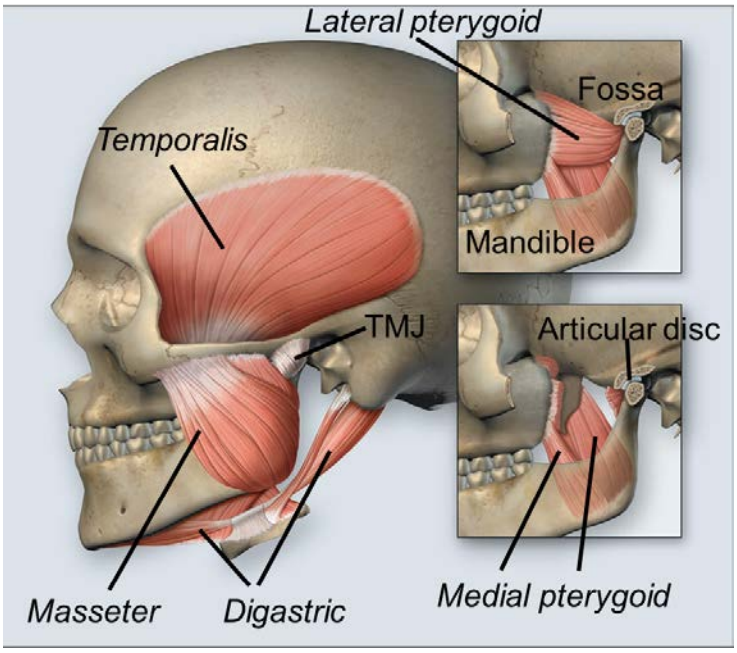

(a)

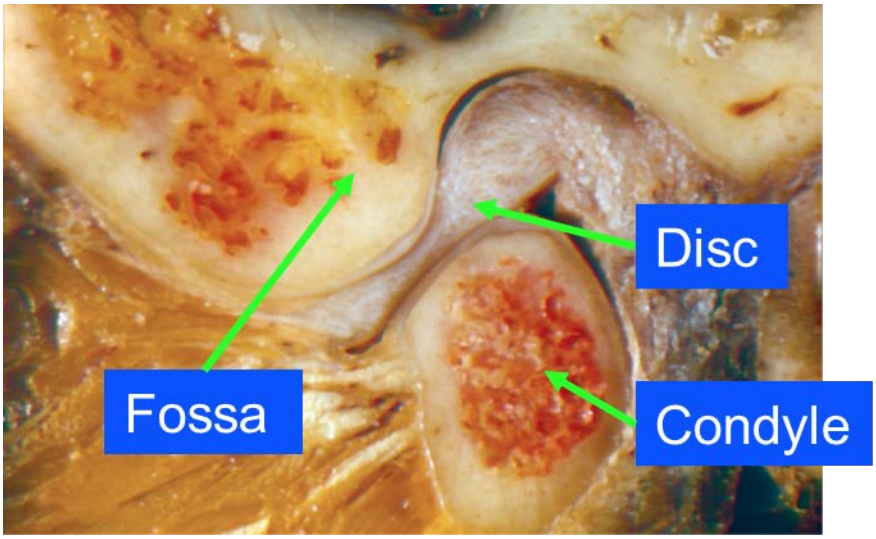

(b)

Figure 1. TMJ anatomy.
(a) TMJ and its masticatory muscles; (b) TMJ components. Modified from references [2, 3]

Compared to other well-developed joint systems, such as the knee, glenohumeral and hip joints, TMJ has received less attention in biomechanical study because: 1) TMJ has a relatively complex anatomical structure and incongruent articular surface, 2) multiple muscles with an intricate neuromuscular recruitment architecture are responsible for various oral behaviors, and 3) TMJ movement is a rotation-translation combined six degrees of freedom (DOF) movement. The complex anatomy of TMJ, together with the dense blood vessels and neuron system that surrounds it, impedes direct *in vivo* experimental measurement for articular space, contact force, stress distribution and nutrient supply in TMJ components in humans without breaking joint function integrity. These measurement properties, however, are key in understanding the TMJ wear, fatigue and degeneration mechanism. Therefore, ***the goals of this research study*** are to: 1) build a data collection system on non-invasive TMJ motion, muscular electromyography (EMG) and bite force and 2) determine behavioral, functional, and morphological properties for objective diagnosis of TMJ disorders and further understanding of their TMJ disorders pathology. Our ***central hypothesis*** is that TMJ properties of muscle, motion, and shape in patients are sensitive to TMJ disorders and, therefore, can be adapted to enhancing objective diagnosis criteria, functional rehabilitation assessment, therapeutic monitor and understanding the underlying pathology. To address this hypothesis, this dissertation established three aims:

Aim 1: Determine the patterns of TMJ muscle activity by calculating EMG parameters for TMJ muscles of mastication. Knowledge of EMG provides objective and representative information about chronic muscle pain associated with jaw loading

behaviors compared to subjective self-reporting methods. However, it is desirable to processing EMG signal to detect interesting parafunctional activities. Parafunctional activities are believed to incite the depletion of nutrient supply to TMJ disc cells and consequently lead to TMJ disorders [4, 5]. Therefore, we will record the EMG signal of the masticatory muscles. An automatic clench activity detection approached will be designed by learning from the clench activity patterns in laboratory EMG signals. Then parafunctional activities in nocturnal recordings will be identified using our designed approach. Finally, we will determine the EMG risk factors that could differentiate patients in disc displacement with chronic pain group from control group.

Aim 2: Determine the features of TMJ kinematics by collecting and analyzing TMJ motion tracking data. The accurate, quantitative recording and depiction of TMJ movement are essential for understanding TMJ function and dysfunction during TMJ movement as well as assisting objective clinical diagnosis and prosthodontics, orthodontics treatment and oral surgery. Therefore, we will: 2a) Record TMJ motion data and determine the range of motion (ROM) for inter-incisor and mandibular lateral pole. The contribution of rotation to total mandibular displacement during open/close will be analyzed and plotted. The trajectory of any mandibular joint and distance of any two mandibular points will be calculated and displayed with respect to time. 2b) Identify the location, orientation, and fluctuation for the instantaneous rotation center (ICR) or finite helical axis (FHA) in both patients and controls with respect to mandibular motion.

Aim 3: Determine the patient-specific TMJ 3D shape signature by refining the intra-articular analysis. TMJ 3D shape provides more detailed and accurate diagnosis

and assessment information than multiple planar 2D images [6]. The intra-articular space analysis is crucial for the understanding of the biomechanical and nutrition environment. The contact area will be used as an input to evaluate TMJ congruence, assess TMJ joint stability and simulate glucose distribution. Therefore, we will determine the contact area in TMJ by dynamically investigating the bone shape in TMJ 3D intra-articular space. The contact area will be calculated and displayed using a novel method.

The innovation of this study lies in its unique capability to 1) build an efficient and integrated data collection system to simplify system design, reduce interference to the TMJ movement and enhance user experiences, 2) apply laboratory EMG patterns to the detection of long term sustained clench, which is believed to obstruct the nutrient supply to TMJ disc cell and thus cause TMJ disorders, and 3) bring clinicians a non-invasive, and objective method that may develop patient-specific diagnostic tools for TMJ disorders.

Organization of Dissertation

The following manuscript is organized in chapters of related studies that combine to form the overall aims of the whole research project. All subjects gave informed consent to participate. In Chapter 2, a comprehensive overview of physiology (anatomy, and function) and biomechanics (kinematics, EMG, and shape) of human TMJ is presented. Chapter 3 illustrates a case study of the oral behaviors. The aim of this study was to develop an automated clench-detection algorithm and apply the algorithm to test for differences in nocturnal clenching in women with and without TMJ disorders. In Chapter 4, the kinematics variables were compared among three diagnostic groups to determine the risk factors for TMJ disorders during the habitual mouth open-close. In Chapter 5, a novel data

collection system was designed to collect data from five human subjects and the mandibular motion was analyzed. In Chapter 6, a new contact area descriptor is proposed, and the gender difference was determined using this new descriptor. Chapter 7 outlines the overall conclusions of this project and proposes future directions of this work.

CHAPTER TWO: BACKGROUND AND SIGNIFICANCE

TMJ and TMJ Disorders

The human TMJ is a synovial and bilateral joint with a unique morphology and function (Figure 1) [2, 3]. TMJ on each side is composed of the convex mandibular bone, the glenoid fossa of the temporal bone and the fibrocartilaginous disc filling the gap between incongruent articular cartilage surface of those two bones. The adult human TMJ disc is of biconcave shape, avascular and non-innervated. However, blood vessels do exist in the TMJ disc during the human fetal period [7].

The normal TMJ disc is seated between the posterior slope of the articular fossa eminence surface and the anterosuperior condylar head surface [8]. The disc is biconcave-shaped in sagittal plane with the thickest part in the anterior and posterior parts. The thinnest disc area is in the intermediate zone. The disc separates the condyle-fossa into the superior and inferior cavities, which are covered by specialized cells and filled with synovial fluid secreted by those cells and the synovial fringe located in the anterior part of the retrodiscal tissues. The synovial fluid serves as the medium of nutrient transport vital for cell metabolism and lubrication of TMJ movement. Inflammatory response in the retrodiscal tissues will cause retrodiscitis.

Each TMJ provides 6 degrees of freedom (DOF) movement and the two TMJs work together to support our daily activities, such as chewing, biting, drinking, and speaking. The complex TMJ movement is activated and maintained by the harmony cooperation work of a group of muscles mainly composed of temporalis muscle, masseter muscle, medial pterygoid muscle, lateral pterygoid muscle and digastric muscle. The correct muscle

action is coordinated by responding to a group of collected impulse information including the spatial position and motion information of the proprioceptors, the tissue status information of the interceptors and the pain information of the nociceptors. TMJ movement due to pathological loading is restricted by passively stretching the stabilizing TMJ ligaments: the temporomandibular ligament, the capsular ligament, the sphenomandibular ligament, the stylomandibular ligament, and the collateral ligaments.

The whole system of jaw, teeth, and their associated soft tissues is called the stomatognathic system (NIH, National Library of Medicine). Functional mandibular movement, together with occlusion and mastication, is the major concern in the stomatognathic system.

TMJ disorders are a category of neuromuscular and musculoskeletal conditions affecting the TMJ, the masticatory muscles, and all associated tissues. TMJ disc displacement and osteoarthritis are the major types of TMJ disorders.

The etiology and pathophysiology of TMJ disorders are poorly understood although multiple etiological factors including biomechanical, neuromuscular, age, hormone, psychology and genetics factors were proposed. The proposed multiple etiological factors hinder the identification of the major causal factor. The heterogenous understanding of the pathophysiology of TMJ disorders can lead to apparently inconsistent diagnosis and distinct treatment approaches. For instance, the DC/TMD [1] is the most commonly accepted diagnosis criteria. However, most part of this diagnosis tool heavily depends on subjective experiences and feelings. Thus, the diagnosis results vary among clinicians and one of the biggest challenges is to increase the statistical power of the diagnosis.

From the common symptoms of joint sounds, limited or asymmetrical jaw movement, teeth misalignment, pain in the muscle, jaw or neck and jaw muscle stiffness, it is obvious that an objective TMJ disorders diagnosis is necessary and should include TMJ muscle, motion and morphology assessment. Therefore, the ***long-term goal*** of this research is to develop a patient specific, non-invasive, and quantitative assessment system. In addition, the possible risk indicators for objective early diagnosis will be identified, and the finally the etiological biomechanical mechanism will be determined by establishing the pathways between these indicators and the underlying biomechanical/transport pathophysiology.

Clinical Relevance and Impact on Society

About 5% to 12% of the US population is affected by TMJ disorders [9], and about 60% to 90% of the general population experiences at least one of the clinical symptoms or signs of TMJ disorders [10]. The annual economic cost for TMJ disorders and orofacial pain in US alone is more than $4 to 100 billion [11]. TMJ disorders are the most common dental problems affecting non-dental area and the second most common musculoskeletal diseases after the chronic low back pain. TMJ disorders are more frequently observed in females and the sex-specific ratio of women to men is about 4:1 [12]. Females between the age of 20 to 40 have the highest predisposition towards these abnormalities and the conclusive risk factor for this propensity is still under debate. The recurrence rate of TMJ disorders is about 45.1% [13].

Common symptoms of TMJ disorders include joint sounds (clicking, grating) when closing or opening the mouth, limited or asymmetrical jaw movement, misalignment of the

upper and lower teeth, pain in the face, jaw or neck and jaw muscle stiffness. TMJ muscle pain was further divided into myalgia, myofascial pain, and myositis.

TMJ disc displacement and osteoarthritis are the major types of TMJ disorders. However, TMJ disc displacement can happen in healthy joints as well. Tasaki [14] proposed a disc displacement classification system to investigate the prevalence of disc displacement using MRI images of 600 TMJ discs from 300 subjects. It was found that disc displacement, majorly including anterolateral displacement and anterior displacement, happens in one third of the healthy subjects and in 81.9% of the patients [14-16]. The normal disc position was found in 71% of the female controls, 88.5% of the male controls, 27.2% of the female patients and 42.4% of the male patients.

TMJ disc displacement is not always harmless to TMJ components and could increase the thickness of the cartilage of the articular eminence to maintain the condyle motion path and sustain the excessive loading [17]. However, it might alter motion [18] and loading condition [19] and increase the risk of TMJ disorders [20, 21] for asymptomatic subjects. A five-stage progression of TMJ internal derangement , including clinical, imaging and surgical symptoms at five different stages, is described in literature [22]. It is unlikely that genetics factor plays an important role in disc displacement [23].

TMJ osteoarthritis, as a manifest of severely degenerative joint, is believed to be age-related [24] and less attributed to overloading [25]. TMJ osteoarthritis will cause inflammation in the synovial tissue, cartilage degeneration and subchondral bone damage [25]. Serious pain usually comes with the TMJ osteoarthritis and increases with the oral

function. Mandibular movement is limited and jaw clicking sound usually presents in the TMJ osteoarthritis.

Multiple etiological factors theory, without determining the leading factor, makes it hard to produce an accurate and objective diagnosis. Therefore, the most current treatment largely depends on conservation strategies. TMJ disorders diagnosis and treatment will benefit from the ability of quantitative EMG, motion and shape analysis because it provides a thorough understanding the normal joint function and the pathological mechanism for TMJ degeneration progression.

The study will also benefit the fields of prosthodontics, orthodontics, and oral surgery by offering an objective and precise treatments assessment over the jaw behavior, function and shape. In orthodontics, the correlation between occlusion and TMJ disorders had been discussed for a long time. In the past, malocclusion was believed to be a causal factor for TMJ disorders pathogenesis [26]. The change of teeth would affect the TMJ function since they are rigidly connected by mandibular bone. Teeth misalignment was the symptom for both orthodontics and TMJ disorders. A recent study [27] showed that the condyle bone asymmetry was significantly correlated with the occlusion asymmetry. In addition, TMJ study provides an objective assessment tool over surgery results, including teeth crossbite correction, maxillary or mandibular osteotomies, through the kinematics study. For instance, one objective of orthodontics surgery is to restore the function of teeth and jaw. It was demonstrated that the incisor motion trajectory of the subjects with crossbite presented much more motion variations than the normal subjects [28]. Therefore, the orthodontists can evaluate these variations by investigating the mandibular motion.

Moreover, it is necessary to determine the amount of autorotation before the orthognathic surgery since the mandible will move to a new position after surgery. The center of mandibular provides the way to predict the autorotation path and evaluate the impact of this autorotation on the treatment [29-32]. Finally, a more accurate computer model of the articulator could be designed to replace the inaccurate articulator that the clinicians are currently using [33]. The precise description of the kinematics from the virtual articulator computer model will provide the correct teeth occlusion so that the treatment planning and posttreatment evaluation can be faithfully reproduced with respect to the patient's actual mandibular and teeth movement. The failure to replicate the accurate determination of the axis of rotation through motion study will lead to incorrect splint usage and consequently the teeth overcorrection or under-correction [34, 35].

Parafunctional activities were believed to be a predominant factor for the pain-related TMJ disorders. Khawaja, S. N. [36] found that waking state oral parafunctional activities were substantially associated with TMJ disorders. Also, Michelotti, A. [37] found that tooth clenching was significantly correlated with myofascial pain and disc displacement. Through finite element analysis of clenching, Hirose, M. [38] concluded that disc displacement was caused by the excessive stress found in the retrodiscal tissue and subsequent tissue damage during the prolonged clenching. The sleeping disorders, especially sleep bruxism, was believed to be one of the predisposing factors leading to TMJ disorders for a long time.

Finally, the significance of TMJ disorders study is obvious from the voices of patients: "…I was in and out of the hospital wanting to die of the pain had to drop out of

nursing school, and wasn't able to tend to my four children. I just want to be normal again…I get dizzy; face and head sensitivity and severe headaches. I'm at my wits end. I don't know what to do.... Every time I'm pregnant the jaw ache/headaches come back, and then disappear for a few months. I feel scared to do anything in case I get stressed then the pain reappears…. We want the best science this country has to offer for these devastating conditions… I have had TMJ for about 3 months, and it isn't getting any better, it limits every day activities… I have pain that radiates into my ear, neck, head; all on the left side. I have struggled with dizziness for nearly 2 years" [39].

Etiology, Diagnosis and Management

Etiological mechanisms and pathological factors for TMJ disorders including parafunctional activities, mechanical environment, neuromuscular, age, hormone, psychology and genetics, have been extensively reviewed [10, 40-42]. Some of the theories, such as biopsychosocial view, are still prevalent even though they should be verified scientifically [12]. Due to intriguing etiological factors of TMJ disorders, objective and accurate diagnosis is difficult and so is with the treatment. To make the situation even worse is that many other types of diseases—such as glossopharyngeal neuralgia, trigeminal neuralgia, sinusitis, pain raised from cancer [43-49] and rheumatoid arthritis—share the symptoms and signs with TMJ dysfunction [50].

Early accurate diagnosis and in-time functional treatment is vital because incorrect or delay can cause patients to miss optimal treatment times, increase unnecessary therapy expenses and even endanger their lives. In [51], three patients with malignant tumor were reported to be incorrectly diagnosed as TMJ disorders. Only one patient recovered from

appropriate surgery. The second and the third patient died because of the misdiagnosis and the late treatment.

The requirement for establishing a widely accepted, evidence-based and effective early DC/TMD has been acknowledged as early as in 1992. However, the process was retarded because of the lack of the quantitative and reliable assessment [52]. The currently most accepted diagnosis tool in research and clinical fields is the two axes DC/TMD [1]. The criteria are consisted of two major parts: Axis I physical diagnosis and Axis II psychological status. Axis I included subject medical history check, physical examination and radiologic examination. The specificity and sensitivity has been increased for many types of TMJ disorders diagnosis such as an elevated specificity for arthralgia from 0.86 to 0.98. However, this diagnosis criteria contains lots of subjective decisions which vary among physicians/clinicians and even cause disagreement in some cases. The sensitivity is quite low for some disorders, especially 0.34 for disc displacement and 0.10 for osteoarthrosis [12]. Still, it is hard to diagnose some types of TMJ disorders using the present DC/TMD [53]. Therefore, the investigation of the objective assessment methods is captivating to assist the disease diagnosis to increase the statistical power.

Bioimaging as a visual means of objective diagnosis tool plays a crucial role in diagnosis and has been accepted by the current DC/TMD as the only objective diagnosis part. The necessity of the imaging-based diagnosis was not fully appreciated until the application of DC/TMD since the use of imaging will produce additional cost to the diagnosis and management.

Many 2D or 3D image-based, invasive and non-invasive techniques, such as arthroscopy [54], computerized tomography (CT) [55], magnetic resonance imaging (MRI) [8, 16, 55-57] and cone beam computerized tomography (CBCT) [58-60], were reported to objectively assess TMJ disorders. The clinical assessment provides comparatively limited information. Image techniques could help to confirm or exclude the disease when clinical diagnosis is equivocal. Also, additional structural and anatomical information can be obtained through image techniques.

Each of the currently commonly used imaging techniques has its own strengths and shortcomings (Table 1).

Table 1. Image techniques advantages and disadvantages.

Imaging	Advantages	Disadvantages
CT	Detailed osseous images Less expensive than MRI	Radiation No soft tissue structures such as the TMJ disc
MRI	Soft tissue determination Suitable for TMJ disc Less exposure	High cost Unavailable in clinical settings
Ultrasound	Comfortable to patients Low cost and high availability	High requirement for operation Less reliable than CT and MRI
CBCT	Rapid scanning time Image is accurate enough Low radiation dose Available in clinical setting	No disc information
Arthrography	Soft tissue	Invasive

CT and CBCT demonstrates better TMJ bone morphological assessment than MRI However, the soft tissue including TMJ disc, ligament, muscle and retro-disc tissue are invisible in CT and CBCT. The capability of MRI to provide superior contrast resolution

and capture the normal or abnormal position of TMJ disc promotes it the position of “the gold standard” in clinics. In a morphological study of comparing CT with CBCT, no significant difference was found between CT and CBCT for the TMJ morphological evaluation except the articular tubercle bone defects [61].

Arthrography and arthrotomography are used to examine the TMJ soft tissue. The diagnosis accuracy of 85% was much better than the predictive accuracy of MRI in the determination of joint intraarticular adhesion [62] and synovial chondromatosis in joint cavity. However, this imaging techniques are invasive methods by injecting a contrast media. In addition, arthrography is not suitable to detect the lateral or medial disc displacement [8]. The diagnosis accuracy of arthrography, arthroscopy and MRI with findings in TMJ open surgery was conducted in [54]. The TMJ disk position and morphology, disk perforation, joint adhesions, and degenerative joint disease were evaluated. It was found that the MRI with the accuracy of 92% joints was better than arthrography and arthrotomography with the accuracy of 75% in detection of the disk position.

Dynamic MRI has been used to detect the disc position and morphology [63-65]. However, further studies are required to assess its efficacy even with stronger magnetic field of 3 Tesla because of its poor signal intensity contrast or signal to noise ratio which is caused by the introduction of motion artifacts [66]. Finally, dynamic MRI could only provide disc position information in a single 2D plane [65]. The disc position information on other planes is not tracked. The missing information will inevitably lead to misdiagnosis [8, 67]. Contrast enhanced MRI has been used to evaluate TMJ disorders [68, 69].

However, the introduction of contrast agents will increase the diagnosis and therapeutic cost. Moreover, contrast agents will introduce mild and temporary side effects.

Recently, hybrid images based TMJ disorders diagnosis from MRI-CBCT registration became attractive because it provided both osseous and soft tissue information and enhanced the coherence between examiners [70-73]. However, it was also noted that the motion artifacts still could not be removed, the manual segmentation required experienced operators, it would double the tedious property of the segmentation work and the selection of landmark reference points would introduce extra artificial errors.

Undefined etiological factor theory and experience-based diagnosis also makes it hard to produce an effective treatment. The aim of most current available treatments is to relieve the pain (muscle stiffness, facial pain or headache) or restore the oral function by adjusting the mandible range of motion. The major types of treatments include [74, 75]: the patient education and self-care to rest the masticatory muscle and reduce parafunctional activities (e.g. clenching and tongue thrusting); the physical therapy, including exercise, thermal therapy, coolant therapy, joint mobilization and needling therapy, to relieve the muscle pain and restore the oral motor function. Physical therapy is reversible and favored by physicians; the pharmacotherapy including analgesics (e.g. ibuprofen, acetylsalicylic, diflunisal, naproxen, naproxen sodium, ketoprofen, aspirin, celecoxib and opioids) to reduce pain, muscle relaxants (e.g. flexeril, Skelaxin, Robaxin, soma, parafon, forte and DSC), antidepressants (Elavil, pamelor, norpramin, Prozac, Paxil and Cymbalta) and anti-inflammatory drugs (e.g. non-steroidal anti-inflammatory drugs or NSAID, celecoxib,

ibuprofen, naproxen and acetaminophen); arthrocentesis and arthroscopy with lavage and lysis [76]; and the surgical management for total joint replacement [74, 75].

The chronic TMJ disorders is also called chronic recurrent TMJ disorders because the episode repeats over the time. The recurrence rate of TMJ disorders runs up to 45.1% [13]. The recurrent TMJ dislocation, probably caused by the eating habit or the joint morphology, is one of such diseases that challenge the clinicians [77].

Although many types of conservative management strategies have been proposed over the years, the effective management of chronic TMJ disorders requires the development of a widely accepted clinical diagnosis criteria with high diagnosis accuracy, based on etiology and pathophysiology, to increase coherence within diagnostic subgroups and enhance the early diagnosis accuracy. In addition, without prescription labeled for TMJ disorders, different types of medicines, such as anti-inflammatory agents, opioids, antidepressants, anti-anxiety medications, are still prescribed to TMJ patients with side effects and unknown adverse risks of long-term use. For instance, the administration of NSAID will cause the well-known 'NSAID gastropathy' with the life-threatening complications of sub-epithelial hemorrhages, erosions, and ulcers [78, 79]. In 2005, US FDA requested that all NSAID products must provide label with the specification of the potential cardiovascular and gastrointestinal bleeding risks [80]. Finally, poor treatment results can still occur even when with correct diagnosis and appropriate treatment. The treatments are mainly targeted to palliate the pain or dysfunction symptoms instead of identifying the substantial etiology factors and pursuing a causative therapy. As a result, recurrence has been reported in previous literatures [77].

TMJ Anatomy and Function

Correlation between TMJ anatomy and its function

The underlying necessity for the study of TMJ anatomy lies in the correlation between TMJ anatomy and its function as proposed in "Wolf's law" from [81]: TMJ anatomy determines the mandibular movement relative to temporal fossa and the TMJ anatomy is optimally structured to meet its functional requirement. In the study of [82], it was found that the irregular mandibular movement was correlated to the asymmetrical mandibular morphology.

The TMJ function will affect the tissue anatomy. The intermittent oral behavior near or below physiological level promotes the growth, development and remodeling of TMJ tissues, while excessive pathological loadings lead to irreversible cartilage and TMJ disc degeneration [83]. For instance, TMJ disc, with the role of collagen, could maintain its morphology during the normal function. A moderate stress could stimulate the repair of the articular cartilage. It was indicated that the condyle-fossa interaction is crucial for the initial development and structure formation process of the fossa [84]. However, the sustained clenching and static biting may have contributed to mechanical fatigue failure of the TMJ disc cartilage because of a classical mechanical fatigue mechanism [85] or a combined mechanism which includes compromised disc cell nutrition due to duration of loading [4, 86], which further causes the irreversible change of the disc morphology.

TMJ Anatomy

The anatomy of TMJ has been extensively reviewed in literature [3, 60, 87]. TMJ is composed of the mandibular condyle bone, the temporal fossa bone and the TMJ disc.

Temporal fossa bone consists of glenoid fossa and the anterior articular eminence. The articular eminence has a non-uniformly distributed steepness dictating the condylar movement path and is crucial for joint load minimization [88, 89]. Thus, it is beneficial for reducing the joint tissue mechanical fatigue [90]. The posterior and superior roof parts of fossa are relatively thin compared to the anterior articular surface, indicating that the major loading force is distributed on the anterior fossa surface.

Unlike the subchondral bones (e.g. femur and tibia) covered by hyaline cartilage, the TMJ temporal bone is veneered by a thin layer of fibrocartilage with a non-uniform thickness of 0.05 to 0.5 mm. The TMJ condyle is also covered by a thin layer of fibrocartilage with thickness of 0.4-0.5 mm [3, 91, 92]. The cartilage layer is viscoelastic, devoid of blood vessels, and highly deformable. Because of the anti-angiogenic factors, such as chondromodulin-1, the cartilage layer and the TMJ disc can prevent the blood vessels invasion and maintain their functional integrity during the TMJ tissue remodeling [93]. More detailed comparison of condylar cartilage with hyaline cartilage was described in [94, 95].

Condyle cartilage is crucial for the TMJ normal function, reducing articulation friction and the bone remodeling. The importance of the articular surface topology and cartilage thickness should never be emphasized too much since it is crucial for: 1) maintaining of low surface friction and sound lubrication mode in the joint articular surface [96]; 2) the determination of contact stress and strain in the articular cartilage and subchondral layers, absorbing and transmitting the compressive load [97], and the extracellular matrix synthesis in the articular cartilage; 3) the articular surface congruence

and the joint stability; and 4) tissue engineering application [92, 98, 99]. The thickness of the articular disc and the soft tissue of TMJ bones at mouth closed has been quantitatively measured using different measuring methods and experimental protocols. Technically, the measuring techniques include needle penetration [97], slicing techniques [91, 100], optical methods [101] and imaging [102]. More details of these methods can be found in [103, 104].

The adult human TMJ disc is of biconcave shape, avascular and non-innervated. The normal TMJ disc is interposed between the posterior slope of the articular eminence and the anterosuperior condylar head surface [8]. The disc is biconcave-shaped in sagittal plane with the thickest part in the anterior and posterior parts and the thinnest area in the intermediate zone. The size of the disc is 19 mm in the mediolateral direction and 13 mm anterior-posteriorly. The thickness of the TMJ disc is 2 mm in its anterior region, 3 mm in the posterior band, 2.2 mm in the mediolateral direction and 1 mm in the intermediate area [105, 106]. In comparison, the condyle and fossa have an approximate width of 20mm and 23 mm, respectively, in the mediolateral direction. Anterior-posteriorly, the lengths of condyle and fossa are about 10 and 19 mm [3, 107, 108].

The medial and lateral parts of TMJ disc attach firmly to condylar head and merge into the TMJ fibrous capsule that connects the cartilage of temporal to the mandibular neck immediately below the condylar head. The lateral capsule surface is strengthened by the temporomandibular ligament. The upper capsular ligament connection of temporal fossa to disc is relatively lax allowing the articular disc to move freely in the upper articular joint space. Therefore, TMJ translation happens between the TMJ disc and the temporal bone

while TMJ rotation happened between the TMJ disc and the condyle bone. Another function of the capsule and capsular ligament is to form a closet in the articular cavity. This small closet entraps the synovial fluid for nutrition transport and biomechanical loading absorption. Furthermore, the inner surface of the joint capsule is lined with synovial membrane which produces synovial fluid for nutrition transport and lubrication [109]. Finally, the ligaments are filled with nerve system and blood system. The nerve system allows the sensing of the movement and position of TMJ during oral functional activities.

Anteriorly, the TMJ disc penetrates its surrounding TMJ capsule and connects to the superior head of lateral pterygoid muscle through tendinous fibers. The anterior part of the TMJ disc is more vulnerable to shear stress than the rest parts of the structure due to its comparatively low shear modulus [110]. Posteriorly, the TMJ disc penetrates the TMJ capsule and is connected to a bilaminar zone. This bilaminar zone is connected to the posterior part of the disc and is separated by loose connective tissue filled with blood, fibers, nerves and fat [111]. The whole TMJ joint is surrounded by complex nerve system and blood system: the internal carotid artery, the external carotid artery, the trigeminal nerve, the trigeminal ganglion, the deep temporal nerve, the masseteric nerve, the auriculotemporal nerve, the mandibular nerve, the maxillary artery, the superficial temporal artery, the maxillary vein and the superficial temporal vein. The blood vessels near the posterior bilaminar zone and the synovial fluid provide disc cells with nourishment and remove cell metabolite products into the circulatory system.

The surrounding attachment of the TMJ disc to the TMJ capsule completely separates the condyle-fossa intra-articular space into two compartments. Should these two compartments communicate, joint effusion would be present on MRI imaging.

The TMJ disc surface contains a fiber network arranged primarily anterior-posteriorly in the mediolateral direction, and mediolaterally in the anteroposterior direction. This fiber configuration correlates with the TMJ biomechanical functions [106].

TMJ vs other diarthrodial joints

Distinct from the subchondral bones (e.g. femur and tibia) covered by hyaline cartilage, the TMJ temporal bone and condyle bone are covered by a thin layer of fibrocartilage.

Moreover, the TMJ disc has neither blood vessels nor nerves while the knee meniscus is highly vascularized and innervated in the peripheral region [112]. In addition, a system of micro-canals exists in the knee meniscus and its possible function is to provide nutrition and fluid pressure [113], while the nutrient of the TMJ disc is provided by the blood system in the bilaminar zone, synovial fluid and the anterior disc attachment.

Furthermore, compared to the relatively static intervertebral disc, the TMJ disc moves together with the mandibular movement. As a consequence, the articular surface congruity and the resultant stress vary during the motion, leading to the possibility of the stress concentration especially at the articular eminence position where most of the joint degenerations happened [114]. The TMJ disc movement is composed of both rotation and translation of the bone at the same time [21]. The disc rotation is relative to the TMJ condyle. The translation is the condyle-disc complex relative to the TMJ temporal. One

advantage of the TMJ joint over other joints is that its movement can be tracked using the external bony markers attached to the upper and lower teeth. For knee joint, soft skin tissue is usually used to attach the external markers and this attachment method can introduce motion artifacts. To process such motion artifacts, it is usually required to design a special algorithm case by case. Such artifacts can be reduced in the TMJ joint since bony markers can be rigidly attached to the teeth.

Compared to the knee meniscus where the passive shape changing accommodates the joint movement, the TMJ disc movement is an active movement driven by the lateral pterygoid muscle and limited by the capsule as well as the TMJ ligaments. The function of the knee meniscus as a medium to smooth the incongruity of the articular surface and distribute stress over a larger contact area, to avoid stress concentration has been recognized for many years [115]. However, the capability of TMJ disc in preventing stress concentration due to surface incongruity is limited [116]. The loading condition beyond 10% of the maximum clench level will result in tissue damage.

In addition, multiple masticatory muscles are involved in the TMJ movement and their coordinate mechanism is rather complex. The uniqueness of TMJ muscle coordination is that only some muscles are involved in certain oral function. For instance, the temporalis muscle, the masseter muscle and the medial pterygoid are involved in the closed-related behaviors, while the lateral pterygoid muscle and the digastric muscle are responsible for the opening of the mouth. However, the role of the masticatory muscles can change. The EMG signal of the masseter muscle has been found to increase during the opening of the mouth due to the protective muscle co-contraction [117]. What makes the case even more

complicated is that some of the muscles are architecturally heterogeneous in a single oral activity. For instance, the fan-shaped temporalis muscle generally can be separated into three parts according to the muscle fiber alignment: the anterior vertical portion, the middle oblique portion, and the posterior horizontal portion. The length variation differs from one portion to another when the temporalis muscle elevates and retrudes the mandible. In one study, the temporalis muscle was separated into six portions because of the variations in fiber bundle length [118]. The fiber length variation was substantially smaller in the anterior portion (9%) than that of the posterior portion (14.5%) during the opening activity. Therefore, the generated force contributions differed according to each portion. The researcher concluded that each muscle portion has distinct activation mechanism and the whole muscle coordination fluctuates for distinct oral tasks.

Last but not least, TMJ is a relatively small joint surrounded by plenty of arteries, veins, and nerves. It is hard to measure the *in vivo* strain or the loading force in human without causing injury to these blood and nerve systems by using the available strain or loading measurement devices.

In summary, the TMJ functionally, morphologically and behaviorally varies from other joints. However, the investigation of TMJ could use the study methodology for the other joints.

Qualitative anatomy

Descriptive morphology characterization of TMJ components has been widely documented to characterize the disc position and relate the TMJ morphology to the TMJ disc displacement. Some researchers found that the disc morphology significantly

contributed to the presence of disc displacement [119, 120]. Others concluded that discs are distorted after the disc displacement and that the folded discs are the result of condylar movement [121]. Moreover, the severity of disc deformation is proportional to the degree of disc displacement [122]. No association between the condylar morphology and disc displacement was found in [120], contradicting to the morphometric study by [123, 124]. The diversity in the composition of the participants, the clinical diagnostic criteria, and the evaluation method contributes to the discrepancy in these findings.

In general, the TMJ disc will keep its biconcave sagittal shape during its normal function in a stable biomechanical environment. However, a harmful biomechanical environment such as abnormal occlusion, trauma, or disc displacement will result in a deformation in the disc morphology or a change of the disc thickness.

Morphometric 2D measurement at mouth closed

A morphometric TMJ analysis is beneficial for evaluating therapeutic results, designing intraoral implants, identifying risk factors differentiating patients from control subjects, and understanding the progression of TMJ dysfunction. Recently, numerous works have focused on the morphometric measurement of disc thickness, disc length, condyle length, fossa anatomy, and articular joint space through direct measurement on cadaver materials, surgically removed discs, and images.

The size of TMJ components of 115 TMJ joints [125] was examined. With increasing age, the size of the condyle bone changed from 5-11.5 mm in the anteroposterior direction and from 7.0-21.5 mm in the mediolateral direction. Also, with age, the temporal

bone was prolonged from 9.5-20.0 mm in the anteroposterior direction and from 10.0-25.0 mm in the mediolateral direction.

Histologically, the thickness of TMJ soft tissue and its regional variations over the whole TMJ area in cadavers was examined [91]. It was found that the histology treatment can cause dramatic tissue shrinkage up to 10%. The thickest condylar cartilage was 0.48 mm in the superior region of the medio-central section and the thinnest cartilage was 0.15 mm in the posterior region of the lateral section. The thickest temporal bone cartilage was 0.49 mm in the posterior-inferior slope of the articular tubercle region of the lateral part, and the thinnest cartilage was 0.01 mm in the fossa roof region of the medio-central section. The thickest part of the disc was 2.9 mm in the posterior region of the medio-central section while the thinnest part was 1.06 mm in the middle region of the lateral-central section. It was concluded that the change of articular cartilage thickness was the result of mechanical loading conditions. A late study suggested [100] that the biomechanical overloading from parafunctional activities such as bruxism caused the reduced thickness in the loading area.

In contrast, it was determined in [126] that the disc perforation is a wearing process rather than a process involving the TMJ dysfunctions which caused the TMJ osteoarthritis. The soft tissue regional thickness of condyle cartilage and disc were measured on both macro-morphometric and micro-morphometric levels. No significant differences were found between the measurements on these two levels. The author concluded that disc perforation was a process caused by the wearing mechanism instead of the parafunctional activities. The author suggested that the loading was evenly distributed in the loading area

from the observation that there was no significant condylar thickness variation along mediolateral direction.

Morphology data was also recorded for the surgically removed discs. The morphology and histology of the disc and retro-disc tissue between 17 pathologic TMJs collected from patients with TMJ disorders (16 females and 1 male, mean age of 34 years from 16 to 55 years) and 10 normal TMJs from cadavers (2 females and 5 males, mean age of 63 years) were compared [127]. The mean maximal disc thickness was 3.4 mm for surgical discs and 2.8 mm for cadaver normal discs. It was observed that some histologic features only existed in pathologic discs: 4 TMJ joints had chondrocytes in the inferior TMJ disc surface, 4 joints had a 0.7 mm surface layer of the proliferative connective tissue, 2 joints had vessels in the inferior surface of the thickened posterior band and 4 joints had splitting of the disc or/and retro-disc tissue in the inferior surface. Compared to normal TMJs, the pathologic TMJs had greater maximal fibroblast density in both the disc and the retro-disc tissue and higher vessel density in the retro-disc tissue.

Morphology data was also reported using imaging techniques. A group of TMJ quantitative measurement using MRI images with 1.5 Tesla machine from 117 TMJ joints were analyzed [16, 56]. 19% of the patients had normal disc positions, 48% of the patients had disc displacement with reduction (DDwR) and 33% of the patients had displacement without reduction(DDnR). It was concluded that the morphological change was closely correlated to the degree of anterior disc displacement by comparison.

Another study examined the correlation between anatomical/morphometric parameters and TMJ disc displacement for a group of 320 TMJs with 1.5T MRI [128].

21.9% of the discs were determined as in normal position, 51.5% of the discs were in the DDwR group, and 26.6% of the discs were in the DDnR group. It was found that the displaced discs were rounder and shorter compared to normal discs. In addition, the anterior and posterior regions were thinner while intermediate zone was thicker in displaced TMJ discs. The thickening founding in TMJ discs were also confirmed by other studies [16]. The author concluded that the disc displacement severity was associated with the condylar morphological change. The center of condylar head would move along posterior-superior direction with the progression of disc displacement. It was also found that a large tuberculum and marked eminence inclination contributed to disc displacement.

In their succeeding study [129], a set of 78 healthy TMJs were compared to another set of 159 disc-displaced TMJs to find the association between osseous change with TMJ disorders. All the joint spaces were significantly larger in normal discs. The volunteer had particularly steeper TMJ fossa eminence than patients. It was shown that women discs were shorter than men anterior-posteriorly, and women had significantly thinner anterior disc thickness and the superior joint space is significantly less than men. It was concluded that the reduced superior joint space reduction was the result of disc displacement. In addition, the author concluded that the disc thickness was increased in disc posterior band in patients. The conclusion that TMJ disc of subject with TMJ disorders was thicker than that of normal controls was supported by another study [130] by means of comparing the disc thickness of the anterior, intermediate and posterior parts in disc in cadaver heads in two groups: the balanced occlusion group and the non-balanced occlusion group. The study aimed to test the hypothesis that TMJ disc thickness increased with respect to the dysfunctional

occlusion. The author concluded that the abnormal occlusion must be properly treated before any action to manage TMJ disorders.

The disc thickening in the posterior band of patients with TMJ disorders was because of the increased signal intensity in this area where the disc was attached to the retrodiscal tissue and blood vessels in a MRI study [131]. It was postulated that the posterior disc band was firstly influenced by the disc displacement and therefore showed higher intensity in MR imaging. Thus, the nutrition environment in the disc posterior band might be worse in patients with TMJ disorders since the thickening disc will possibly block the diffusion of vital nutrients into the inner disc cells, jeopardizing the cell viability and resulting in the further progression of TMJ disc degeneration.

To study the influence of several different MRI parameters on the condyle-disc position in the TMJ articulation space, 38 normal TMJs (20 males and 18 females, median age of 40 years) were examined [132]: sagittal spin-echo T1-weigthed, oblique sagittal spin-echo T2-weighted, oblique sagittal proton density fast spin-echo, oblique axial images, oblique coronal spin-echo T2-weighted, and oblique coronal proton density fast spin-echo methods. The author concluded that the optimum MRI sequence is the fast spin-echo sequence, the favorable MRI plane is the oblique sagittal plane and the recommended imaging modality is the proton density weighted imaging. It was also found that the left and right TMJs had symmetrical anatomical structures.

To evaluate the influence of surgery on the TMJ osseous change, a group of 24 patients with dentofacial deformity were investigated at four different time periods before and after the surgery [133]: nine patients were treated with Le Fort I maxillary osteotomy

while the other 15 patients were treated with combined maxillary advancement and mandibular condyle osteotomy. As the control group, 10 volunteer controls were included. The inter-condylar distance and the condylar angle to the frontal plane significantly reduced after surgery for the bimaxillary osteotomy group. However, these changes returned towards their pre-surgery values with time. At the first week after surgery, the left and right condyle-fossa distances significantly increased for the bimaxillary osteotomy patients. However, again they went back to the values before the surgery with time.

To identify the bony features that could differentiate the patients with DDwR from patients with DDnR, a group of 12 linear, 2 angular and 8 length ratio morphometric multiple factor indices was measured and analyzed on CT images [134]. These image-based parameters, including the geometric description of both fossa and condyle shape, of 84 female DDwR joints were compared with those of 78 female DDnR joints. It was showed that post-glenoid process height, fossa depth, and absolute superior joint space significantly differed between the two groups.

Following that study, these indices of 84 patients were compared with those of 21 asymptomatic control subjects using the same experiment protocol and analysis methodology [135]. The fossa is significantly wider in patients. The ratio of the fossa width to the fossa depth for DDwRs is significantly smaller than that of the normal subjects. The condylar anteroposterior length of patients was larger, although not statistically significant, than that of normal subjects.

The TMJ morphometric parameters of 28 normal subjects were examined to evaluate the TMJ anatomical structure using 1.5T MRI [136]. A set of 8 linear indices and

4 additional modified parameters was reported. No significant sex difference was found in all those parameters.

To quantify the correlation between the TMJ biometric parameters and the disc displacement, a group of 185 patients were examined [123]. The author concluded that the narrower condyle in both anteroposterior and mediolateral directions was statistically associated with TMJ disc displacement. However, they found that the disc displacement was not correlated to TMJ pain although TMJ pain was found more frequently in patients with disc displacement. In their later study, several more morphometric were incorporated [137]. These items were evaluated in the parasagittal, coronal and axial views. It was found that the small condyle was inclined to be affected by disc displacement compared to relatively large condyle.

In summary, various 2D measurements of each TMJ component have been reported in the past. Noticeable disparity in results exists in the documents as a result of the difference in the subject composition, the measuring tools, the experiment design and the evaluation items.

TMJ joint source

Conflicting results presented in the previous published articles come from the lack of consensus over the measurement tools. Some of the studies measured using cadaver heads, some of them obtained analysis results based on the 2D CT/MRI images, and still others examined the morphology through surgically removed discs. Each method has its own advantages and disadvantages.

The use of cadaver materials could give a relatively detailed description about TMJ morphology. Furthermore, it is possible to directly measure and assess the data at any point and any TMJ component. However, the disadvantage of autopsy material is that the sample size is limited, and the gender composition cannot be controlled to match that of the population epidemiology study of TMJ disorders. In addition, the age of these persons is not on the same or similar level to the 20-40 years from the epidemiology study [138]. Quite often, both the gender and the age distribution are lacking [130]. Moreover, the clinical history of these persons could not be verified, and the diagnosis results solely on the images and dissection might be incorrect. Furthermore, it is not easy to preserve the cadaver materials and thus the available joint is commonly with the process of embalming [114]. Finally, it is impossible to evaluate the inflammation progression process and joint effusion.

The surgically removed discs could also provide precise anatomical details as cadaver specimens. The gender, age and clinical history information is usually available. However, as cadaver disc materials, these discs are severely deformed, and the sample size is limited. In addition, the surgically extirpated discs are usually incomplete discs of which some areas are missing and thus it is impossible to evaluate the disc length [127]. Finally, the intra-articular space disc deformation is lost after removal.

The non-invasive imaging analysis of the TMJ discs has no sample size limitations. The CT and MRI have been used for the TMJ joint morphology evaluation for a long time. They are widely accepted by both the clinicians and patients and these imaging techniques are recommended by the DC/TMD diagnosis protocol. However, the use of imaging

technique is not impeccable for the morphological and morphometric analysis. First of all, the TMJ disc and other soft tissue are invisible in CT images. Secondly, to increase intraexaminer and interexaminer agreement, the segmentation process requires prior complete knowledge about TMJ anatomy and structure. Automatic image demarcation cannot accurately depict the contour boundary. Distinct intraobserver and interobserver manual boundary determinations during the image segmentation will inevitably result in measurement dissension, which is especially apparent in MRI with the slice thickness of more than 2 mm. Thirdly, the lateral or medial part of TMJ disc cannot be clearly identified and sometimes is missing in MRI images due to the gap between slices and the poor image resolution [8]. These marginal parts are necessary to a precise measurement.

To reduce the third type of limitations, the individualized oblique axial MRI scan with the corrected scanning direction perpendicular to the tangent of the posterior slope of the articular eminence had been used to replace the traditional coronal scan to increase the number of scanning slices [139, 140]. It was reported that the number of images with clear disc boundary had been increased from 1.6 in the oblique axial images to 3.4 in the conventional coronal plane images. The percentage of undetermined diagnosis was dramatically reduced [139]. It was also reported that the disc width along mediolateral direction for the normal disc was 21.2 mm significantly larger than 18.3 mm of the partially anteriorly displaced disc and 18.3 mm of completely displaced disc [140].

The discrepancy also comes from the use of distinct diagnosis criteria. Some of the diagnosis results were based on visual determination while other studies made the decision based on DC/TMD or its previous version.

The inconsistence in these records is also caused by the diversity in the measurement items, evaluation parameters and the subject composition. The perspective of measurement varied in reports. Some of the studies considered sagittal measurement only while others took the data in all three planes into account. The subject constitution, gender and age distribution is also another determination factor. Some of the studies measured the data for patients only while others also collected the data for controls. As to the evaluation parameters, some studied the dimension of the TMJ components while others studied the intraarticular space distances.

In summary, the live human TMJ is preferable to the necropsy specimen. The cadaver materials are superior to the surgically removed TMJs.

2D measurement at mouth opened

The TMJ morphological features are also reported during the mandibular open stage [141, 142]. From these studies, it is obvious that the disc morphology is adapting to the mandibular movement. The motion artifacts when the mouth was opened was also noted and severely blurred the MRI image. Sometimes the MRI images must be dropped because of the poor image quality caused by the motion artifacts.

The reported disc thickness in [141] was much less than other articles because of the distinct disc demarcation on MRI images. For instance, compared to the definition in [129], the three bars in the anterior, middle and posterior parts of the disc were diminished to the area with relatively low intensity. As a result, the disc thicknesses in [129] was twice the disc thickness reported in [141] in all three locations. However, it is not explained in the literature why the author limited the disc boundary only to the relatively darken area.

In summary, the 2D measurement at mouth opened will provide additional information for the more accurate diagnosis. However, the subsequent motion artifacts and cost cannot be ignored.

2D measurement in multiple planes

Previous imaging based TMJ morphology assessment are based on 2D imaging measurement in a single plane or multiple 2D planes [142]. It has been reported that the accuracy of the diagnosis was improved because of the multiplanar analysis. It was recommended that the TMJ disc position should be assessed on the sagittal plane as well as the coronal plane.

The application of the coronal images in TMJ disc displacement diagnosis was evaluated [67]. The 158 discs came from 79 subjects consisted of 63 females and 16 males with the average age of 36 years. Three discs were incorrectly diagnosed as the laterally or medially displaced joints in the sagittal images were in normal position in the coronal plane. In addition, eighteen normally positioned discs in the sagittal plane were found to be displaced with additional diagnosis in the coronal view. These previous sagittal misdiagnoses were corrected by the disc visibility only in the mediolateral direction of the coronal view.

Accuracy of 2D measurement

The MRI sensitivity, specificity, and accuracy of TMJ disc displacement and TMJ morphological alterations were assessed on 55 TMJs from 41 subjects (24 men and 17 women, median age of 75 years) without prior knowing about TMJ health [8]. The MRI diagnosis results were verified with diagnosis results from cryo-sectioned discs. The MRI

false negative of both disc position and disc form was 5% due to disc invisibility in MRI. Bone information was correctly characterized in 93% of the discs. A total of 81.8% joints (45 joints) in the sagittal plane kept the same position in the coronal view. The coronal plane changed the disc displacement type of three joints. Seven normal joints in the sagittal view were found to be displaced in the coronal plane.

The accuracy of CBCT image based TMJ measurement was also found to be reliable after comparing with the truth value from physical measurement on the skull [143].

3D measurement

Recently, TMJ morphometric analysis from 3D reconstructed model were reported and compared with the analysis results from 2D measurement. The introduction of 3D analysis will allow the observer to measure in countless 2D views and it is a seamless integration of multiple 2D planar analysis. Moreover, it is more accurate than 2D measurement and provides more details [6, 144]. The accurate anatomical shape difference between the pathological TMJ structure and that of the controls will help clinicians precisely and quantitatively determine the morphological changes.

The 2D imaging and 3D reconstructed TMJ osseous difference between patients with facial asymmetry (3 females and 2 males, age of 24.8 years) and the controls (3 females and 2 males, age of 26.0 years) was evaluated [6]. A group of nine parameters in three orthogonal planes was evaluated on both CBCT 2D images and 3D reconstructed bone component models. For symptom-free subjects, horizontal condylar angle of the 2D measurement significantly differed between left TMJ and right TMJ but no side difference was found in all 9 parameters in the 3D measurement. For patients with facial asymmetry,

only lateral joint space showed notable difference between left TMJ and right TMJ in 2D while 4 items including coronal condylar angle, sagittal ramus angle, medial joint space, and anterior joint space presented remarkable difference between left TMJ and right TMJ in 3D. The joint space was significantly smaller in patients in all three locations. The coronal condylar angle and horizontal condylar angle of patients were much higher than those of controls. The author concluded that the 3D measurement possessed more accuracy and was more intuitive to clinicians.

In their following study, the 2D and 3D measurement of 10 normal people were assessed [59]. The same 9 parameters were reported based on CBCT data. All parameters measured in 2D were much smaller than those of 3D measurement, although CCA, CCW and PJS did not show significance. Horizontal condylar angle was found to be remarkably different between left and right TMJs in 2D measurement. The significant difference observed in 2D measurement was not found in 3D measurement. It was concluded that 3D measurement should replace 2D measurement in clinical application since it was more accurate.

Previous study only reported the morphology at several points. However, TMJ articular surface is of 3D shape with countless points. TMJ shape 3D analysis using the spherical harmonic and 3D shape distribution model description (SPHARM-PDM) method was invented to solve this problem [145, 146]: the condyle head was aligned in the parameter space using spherical harmonics and then the distance between two surface models was evaluated using statistical method. The registration procedure of this method is different from the landmark point, curve or surface-based alignment method [138]. The

selected landmarks in the later method probably significantly deformed before and after surgery or with the tissue remodeling. Therefore, it is quite often impossible to find the corresponding features varied over time for the later method. The best fitted landmark will introduce huge errors leading to less meaningful or even wrong diagnosis. The SPHARM-PDM method has been applied to evaluate the diagnostic group difference and longitudinal rehabilitation assessment [147, 148]. However, one of the major problem with this approach is that the shape of the input 3D model must be of the spherical topology. Therefore, it is suitable for the condyle head shape analysis but may not be the optimal choice for the comparison of the fossa shape.

In sum, 3D TMJ shape provides extended and more accurate diagnosis and assessment information than multiple planar 2D image, although 2D measurement is directly available to clinicians.

Articular eminence

The shape of articular eminence was qualitatively categorized into four types: box, sigmoid, flattened, and deformed [149]. The box shaped eminence had a deep fossa and steep articular eminence. The sigmoid shaped eminence had a s-shaped surface with a relatively shallow eminence. The flattened eminence had a smooth and shallow eminence. The deformed eminence presented osseous deformation in the eminence part.

Quantitative descriptors included articular steepness and eminence depth. Articular eminence steepness as one evaluation item was important because it determines the movement path of the condyle-disc complex [150].

Distinct definitions for the steepness of the articular eminence or the eminence angle were reported in literature. On one hand, the eminence angle was defined as the sagittal angle between the tangent line at some point on the posterior eminence surface or the so-called best fit line and the horizontal Frankfort plane [151-154]. On the other hand, it was defined as the angle between the line connecting the fossa zenith to the eminence nadir point to the horizontal Frankfort plane in sagittal plane [155, 156].

The slope of articular eminence and its relationship to TMJ disorders had been debatably discussed for a long time. Controversial conclusions regarding the articular eminence steepness as the etiological factor for TMJ disc displacement had been reported.

In the viewpoint of the positive correlation, the eminence steepness is believed to be the predisposing factor for the disc displacement. The biomechanical theory of disk displacement proposed in [157] stated that, when the condyle was pulling back to the fossa roof, the disc must rotate forward further than the condyle so that the condyle-disc-eminence contact was maintained if the eminence was steeper. Therefore, the disc displacement was caused by a steeper eminence. At the end, the author used two eminectomy surgery examples to demonstrate the application for this theory.

This theory had been applied to the eminectomy surgery to treat the internal derangement of 36 TMJs for 30 patients [152]. After surgery, 5 anterior displaced discs without reduction returned normal position, the rest discs were still in partially or completely displaced position. The 1-year follow up study results showed that the symptoms of 24 patients were reduced and one patients felt worse than before. However, the consequence was the unnecessary surgery and damage to the articular surface, as

implied in its reviewer comments. Moreover, the surgery results did not support the biomechanical theory proposed in [157] since the symptoms could be reduced as long as the intra-articular space was increased surgically [153]. Furthermore, it was suggested that the disc displacement was caused by the incapability of the retrodiscal tissue to resist the abnormal stretching force [111]. Finally, the theory was not plausible when the correlation between disc anatomy and articular eminence [153, 158] was taken into consideration.

The TMJ morphology and its correlation with disc displacement were evaluated in [159]. All subjects were categorized into four groups: DDwR, DDnR, normal controls and patients without disc displacement. It was found that, the eminence steepness was higher in the DDwRs than that of the normal. However, it was also found that the eminence steepness of the DDnRs was close to the normal controls. The medial side steepness was larger than the central and lateral part.

Opposing to the previous biomechanical theory proposed in [157], the negative relationship believed that the disc rotated with respect to the condyle and the condyle-disc complex slid along temporal articular surface during the mandibular movement. It was claimed in this view that the normal disc had steeper articular eminence and therefore the TMJ disc could rotate back farther along condyle to avoid the disc displacement during the mouth opening. It was also hypothesized that the eminence steepness decreased with tissue remodeling during the progression of disc displacement.

In a study to find the correlation between the articular eminence steepness and the disc displacement [153], the lack of osseous change and disc displacement in the healthy controls was validated using the radiography method at first. The author then evaluated the

eminence steepness of 119 joints (85 displaced discs and 34 normal discs) based on radiographical analysis between patients with TMJ disk displacement (50 women and 21 men, average of 28 years) and normal TMJs of the controls (18 women and 16 men, average of 28 years). The author measured the lateral, central and medial articular eminence steepness in the sagittal plane. It was found that the patients with disc displacement had a more flattened eminence than the asymptomatic volunteers (patients: 56.1˚ laterally, 60.2˚ centrally, 58.9˚ medially; controls: 64.9˚ laterally, 64.4 centrally, and 65.4˚ medially). The lateral difference was statistically significant, indicating the most vulnerable TMJ region. Osseous change due to the tissue remodeling and osteoarthrosis was proposed to be the predisposing factor for the difference of the eminence steepness. No gender difference was found.

Also, the eminence steepness of the patients with disc displacement was 39.0˚, which was less than the 44.0˚ for the asymptomatic volunteers in another study [129].

Still a third group held the opinion that no correlation existed between the two phenomena. No association between articular eminence steepness and the disc displacement was found through the comparison among 20 TMJs with DDnR, 20 TMJs with DDwR, and 20 normal TMJs from 59 patients [155]. The lateral TMJ side was found to be flatter than the medial and central sides. It was also found that the DDnR group had least convexity or prominence among the three group. The rotation and translation of TMJ components were measured based on MRI [158, 160]. The correlation between eminence steepness and rotation/translation parameters was examined. No correlation was found between articular eminence steepness and the rotation or translation in [160]. No significant

correlation was found between the eminence steepness and the TMJ movement in the group DDwR [158]. The condyle translation was correlated with the eminence steepness in the group DDnR [158]. It was found that disc rotation was significantly smaller in the group DDnR than the group DDwR [158], indicating the disc rotated backward with the progression of TMJ disorders and thus contradicting the biomechanical theory [157].

Another commonly used evaluation item for articular eminence was the depth of eminence: the vertical distance between the fossa zenith to the eminence nadir point. The eminence depth was reported to be 8.4 mm for the patients with disc displacement and 8.8 mm for the normal volunteers [129].

The impact of eminence on muscle forces was also reported. It was demonstrated in [89] that the joint reaction force increased with the increase of the eminence steepness and that the muscle forces was not sensitive to the eminence angle between 20˚ and 50˚. The temporalis muscle significantly decreased and pterygoid muscle increased at the eminence angle of 70˚. Unfortunately, the TMJ disc was not modeled in the musculoskeletal model. It is impossible to verify the influence of the TMJ articular eminence steepness on the disc displacement through the model.

The correlation between the teeth attrition and the shape and size of TMJ was reported in [161]. The author measured the eminence height as the morphological description for 155 cadaver skulls. Furthermore, the author used the eminence curvature to express the shape because the depth measurement varied significantly among skulls. The curvature descriptor had extensively high reproducibility. The teeth attrition was found to associate with the TMJ shape and morphological change. The teeth worn group had flatter

eminence with greater radii and a wider radii distribution. The teeth unworn group had a more concentrated radii distribution, indicating that the eminence shape did not change too much. The teeth worn group had a less eminence height. It was observed that the males had deeper eminence than females and that their shape were similar.

TMJ masticatory muscles

The TMJ muscles of mastication are a group of muscles mainly composed of the temporalis muscle, the masseter muscle, the medial pterygoid muscle, and the lateral pterygoid muscle. The insertion, origin, function and innervation of these muscles are listed in Figure 2 and Table 2.

The coordination patterns of TMJ masticatory muscles activate and maintain TMJ movement and different types of oral activities through muscular isotonic contraction, isometric contraction, and controlled relaxation [162].

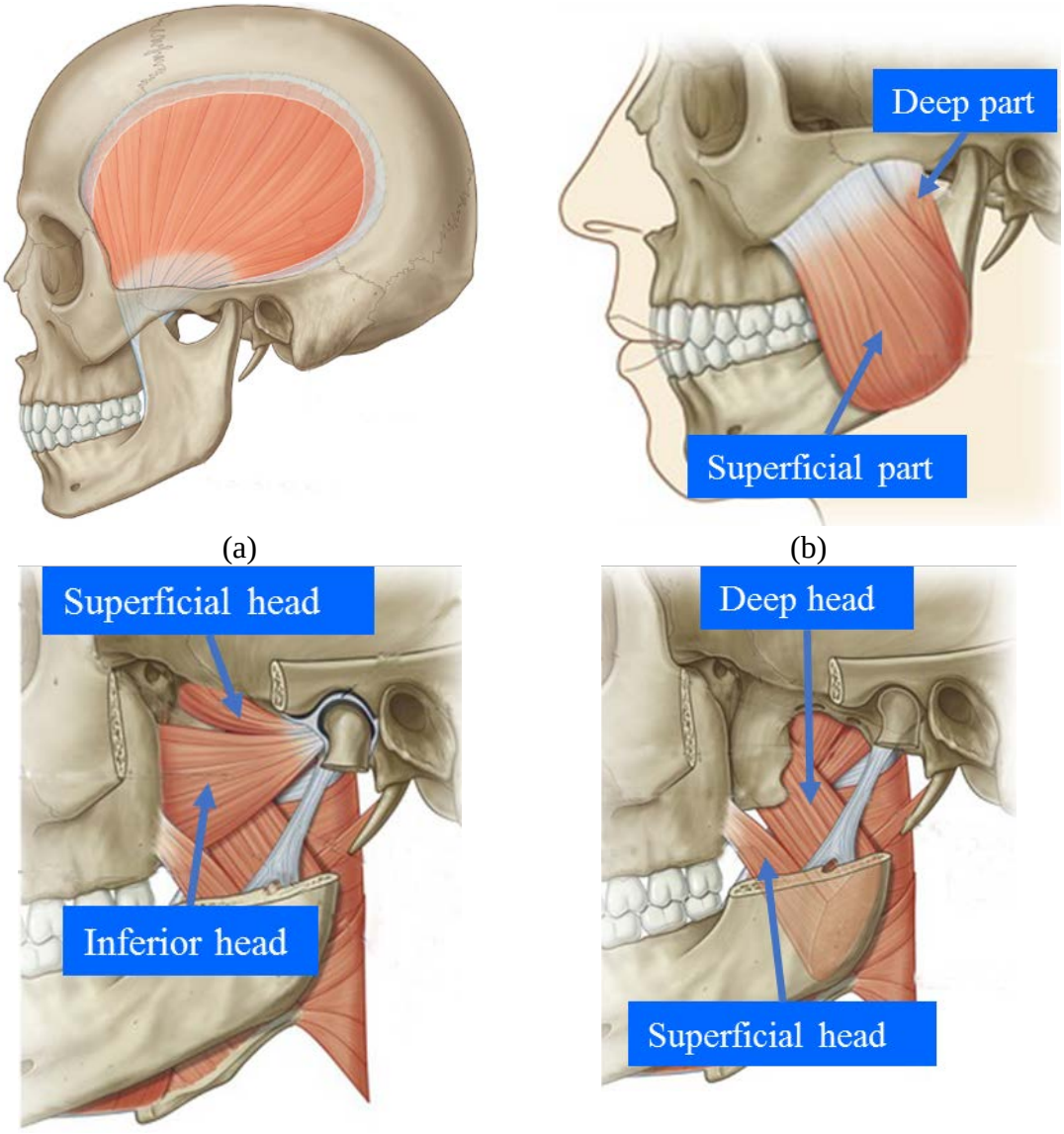

Figure 2. Muscles of mastication.
(a) Temporalis muscle; (b) masseter muscle; (c) lateral pterygoid muscle; (d) medial pterygoid muscle. Modified from reference [162]

Table 2. Muscle origin, insertion and function of the masticatory muscles.
Modified from reference [162]

Muscle	Origin, insertion and innervation
Masseter	Origin includes both zygomatic arch and maxillary process Insertion includes lateral surface of mandibular ramus Innervation: masseteric nerve from the anterior trunk of the mandibular nerve [V_3] Responsible for mandible bone elevation
Temporalis	Origin includes temporal fossa and temporal fascia Insertion includes coronoid process of mandible and anterior margin of ramus of mandible almost to last molar tooth Innervation: deep temporal nerves from the anterior trunk of the mandibular nerve [V_3] Responsible for mandible elevation and retraction
Medial pterygoid	Origin: the deep head includes medial surface of lateral pterygoid plate and pyramidal process of palatine bone; while the superficial head includes tuberosity and pyramidal process of maxilla Insertion includes medial surface of mandible near angle Innervation: nerve to medial pterygoid from the mandibular nerve [V_3] Responsible for mandible elevation and lateral movements
Lateral pterygoid	Origin: the upper head includes infratemporal fossa roof; while the lower head includes lateral surface of lateral pterygoid plate Insertion includes TMJ capsule in the region of attachment to the articular disc and to the pterygoid fovea on the neck of mandible Innervation: nerve to lateral pterygoid directly from the anterior trunk of the mandibular nerve [V_3] or from the buccal branch Responsible for mandible protrusion and lateral movements

The temporalis muscle, masseter muscle, and medial pterygoid muscle are involved in the closing of the mouth, while the lateral pterygoid muscle and the digastric muscle are responsible for the opening of the mouth. However, the EMG signal of the masseter muscle was found to increase during the opening of the mouth due to the protective muscle co-contraction [117]. The contribution of the lateral pterygoid muscle (LPM) to TMJ disorders, especially the disc displacement, is still under hot debate. Some studies insisted on the role of LPM in contributing to TMJ disorders [163, 164], while others found no relationship between the LPM insertion type and the disc displacement [165].

The digastric muscle is also crucial for normal oral functions although it is usually not considered as one of the masticatory muscles [162].

Condyle surface area and disc displacement

The correlation between condylar size and disc displacement has been reported. The condyle head area was measured for 96 females with average age of 15.1 years in both the coronal and the axial planes [166]. The horizontal condyle area of 85.8 mm^2 for DDnRs was much smaller than that of 106.7 mm^2 for the DDwRs and that of 111.1 mm^2 for the normal group. The author concluded that the disc displacement induced the smaller condyle size, which was confirmed by a MRI study [167] and an animal ex vivo study [168].

Gender difference

In one study, the gender difference of the TMJ anatomical properties was reported in a group of 51 symptom-free subjects (26 males and 25 females, average age of 42 years from 22 to 77) [169]. The male condyle width of 20.7 mm was extensively larger than the female condyle width of 18.2 mm. In another study, the gender difference was evaluated

among cadaver materials (9 females and 7 males, average age of 79 years) [138]. A shape and trait model combining the anatomical landmark point coordinates and the image signal intensity was created to compare the anatomical differences. It was found that females had a statistically smaller condyle head size versus males, especially in the mediolateral direction. However, in the superior region, it was found that females had a relatively larger condylar head.

With regard to the condyle shape, the female was more frequently convex than that of male [169]. The male condyle showed a much more pronounced mediolateral width of 20.7 mm versus the female condyle width of 18.2 mm.

Gender difference of the eminence inclination was reported as well. The articular eminence steepness of males was found to be significantly greater than that of females on CBCT images [154] using two methods: the best fit tangent line method (males: 49.66°, females: 47.58°) and the fossa zenith-eminence nadir method (males: 40.19°, females: 37.99°). The eminence depth of males was larger than that of females (males: 7.33 mm, females: 6.69 mm).

On the other hand, no significant gender difference was found between 14 females and 14 males on any of the eleven MRI morphology measurement items: the fossa width, the fossa depth, the postglenoid process height, the eminence height, the posterior joint space, the anterior joint space, the maximum longitudinal diameter of the condyle, the maximum transverse diameter of the condyle, the distance between the lateroposterior point of the oval foramen and the anteromedial portion of the TMJ disc (DOF) and the maximum length of the lateral pterygoid muscle (lPM), and the maximum length of the

medial pterygoid muscle (mPM). [136]. Also, no gender differences were found for the eminence steepness in the lateral, central, and medial sides [153]. Finally, no gender differences were found for either the eminence steepness or the eminence depth [170].

In summary, there is little agreement over the gender differences regarding the TMJ anatomy in the literature. The possible discrepancy of these reports may be explained by the differences in subject composition, experimental design, evaluation items, definition of evaluation items, and measuring tools.

Animal

Generally, it is difficult to acquire *in vivo* human TMJ data from live humans due to ethical concerns regarding possible irreversible detrimental complications during experimentation. Also, the TMJs from surgery are limited in quantity, and those TMJs ae usually degenerated. The cadaver specimens are hard to obtain and preserve, and their quality is limited by gender and age distribution. Moreover, the availability of cadaver specimens from each progression period of TMJ disorders is a problem. On the other hand, disc properties comparison across various species provide tissue engineers with an invaluable database to choose the animal with the closest desired properties. Therefore, the possibility to obtain animal TMJs with similar anatomical, biomechanical, and genetic properties for tissue engineering and regenerative medicine applications has aroused significant interests among clinicians and researchers [95, 110, 171, 172].

In one study, the TMJ disc biochemical composition, morphology, and biomechanical properties were compared among four types of animal discs and human disc using the identical set of experiment configurations [173]. The size of human disc was

23.60 mm in the mediolateral direction and 14.0 mm in the anterior-posterior direction. Morphologically, the closest species to the human was the pig, with an average anteroposterior length of 27.0 mm and mediolateral length of 13.9 mm. The largest disc was the cow disc, and the smallest disc was the rabbit disc. In biochemical composition comparison, the human disc was similar to other species in both collagen and glycosaminoglycan (GAG) content but had significantly lower DNA than other species, probably due to the old age. In biomechanical testing, the human disc had the highest tensile modulus, with the weakest region at the center of mediolateral direction, following by the pig disc. The compression test showed that the human disc was most proximal to the pig disc, and both had a lower compression modulus than other species. The inconsistency of eating habit was thought to contribute to this difference since both of them are omnivores. The softest disc part was the lateral disc along the mediolateral direction. Goat disc had the highest compression modulus due to its richest GAG content. It was found that the disc size for, GAG and collagen content, and compressive moduli at equilibrium for the pig disc are closest to those parameters for the human TMJ disc. Therefore, the author indicated that the pig disc is an optimum model for the applications of TMJ disc experiments and tissue engineering when human TMJ is unavailable. This conclusion has been confirmed by other researchers [174].

However, the limitation for animal material is that the striking anatomical and biomechanical property variations still exist between human TMJ and animal TMJ no matter how closely correlated they are in morphology and biomechanical properties. In addition, each component of the whole TMJ, including TMJ bones and correlated soft

tissues, must be compared to reach the conclusion that a specific animal TMJ shares similar structure and function with human TMJ. Furthermore, even if certain lineage, morphological and biomechanical adjacency occur, these findings alone cannot establish the functional consistency across species [175]. Thus, when substituting animal TMJ for human TMJ in tissue engineering or surgical treatment, researchers should account for potential or likely species-specific diversity, disease pathology and immune response. The appropriate therapies for the animal may not be suitable for human patients.

Moreover, significant size variations of porcine discs were observed. It was found that the porcine TMJ disc length along the anteroposterior direction was 20 mm for normal porcine disc and 18 mm for deformed porcine disc, and that the disc length along the mediolateral direction was 38 mm for normal porcine disc and 35 mm for the deformed porcine disc [176]. Both these two lengths of the pig disc were greater than the values in another study [173] in which the porcine TMJ disc length along the anteroposterior direction was 13.9 mm, and the disc length along the mediolateral direction was 27.0 mm. The differences might be explained by the selection of dissimilar specimens and diverse testing conditions.

Furthermore, the thickness of the porcine TMJ disc was dramatically different from the human TMJ disc. The regional thickness of the porcine TMJ disc [176] was: 5 mm for the normal disc and 5.5 mm for the deformed disc anteriorly, 2.5 mm for the normal disc and 3.25 mm for the deformed disc in the intermediate zone, and 7.5 mm for the normal disc and 9.25 mm for deformed disc posteriorly. All these data were substantially larger

than that of human TMJ disc as indicated in the data obtained from TMJ disc anatomical measurement in human cadavers or MRI images of the human disc.

In addition, anatomical TMT bone structure similarity between rat TMJs and human TMJs through dissection and CT scanning has been evaluated [177]. It was found that the bone structure in rat was similar to that of human TMJ. The author concluded that the mouse TMJ could be used to replace human TMJ for clinical and research applications. However, it was also reported that no articular eminence exists in the rat TMJ, and that the condyle axis is placed along the sagittal direction. The condyle axis is transversal in the human TMJ. These two anatomical differences are determining factors affecting TMJ mandible function in these two species. As a result, the human is an omnivore and the rat is a carnivore. Indeed, it has been pointed out [175] that the carnivorans have unequivocally distinguishable mandibular anatomy and functional movement pattern compared with those of humans due to rat's distinct diet preference.

The anatomical head similarity has been assessed between the human and the pig [178]. It was found that both have an incongruent articulation joint surface. However, it was also observed that caudal borders in the fossa and the retroarticular process are missing in the pig. TMJ. These findings also have been recognized by another investigator who has assessed the pig TMJ anatomy on micro level [179]. It was found that the pig TMJ retrodiscal tissue is fibro-fatty, while human retrodiscal disc tissue is highly vascularized.

In summary, animal TMJ cannot substitute the direct study towards human TMJ, although the use of animal TMJ might help researchers to further understand TMJ morphology, function, and biomechanical properties. Notable variations exist in reports

due to the difference in experimental design. Admittedly, animal material is an alternative option when it is impossible to obtain corresponding human TMJ data by current available techniques without destroying the functional integrity of the human joint. For instance, the contact strain and stress data could only be experimentally gathered on animals because the placement of the invasive instrumentation can impair the joint biomechanical environment. Thus, surgical treatments must be verified in the animals before applied to humans.

TMJ Disorders and Behavior

For the past six decades, the electromyography devices including polysomnography (PSG), needle and surface EMG devices have been used in clinical and research fields to measure and evaluate the influence of oral behaviors on TMJ disorders for diagnosis and on TMJ chronic pain treatment because these devices can provide subject-specific, non-invasive or minimum-invasive, objective, numerical, and repeatable data on the masticatory muscles [180, 181].

The hypothesis of EMG assessment is that the intensity and duration of muscular activation for certain types of oral activities are significantly different between subjects with TMJ disorders and controls.

Parafunctional activity vs TMJ disorders

The relationship between oral parafunctional behaviors and TMJ disorders is still under debate [182, 183]. Literature suggests that the intensity of masticatory muscles activity related to parafunctional jaw loading behaviors, such as teeth clenching and grinding, is associated with the development of TMJ disorders [182]. It was suggested that

frequent repeated clench or bruxism promoted tensile or shear stress on the articular surface, leading to TMJ fatigue [184]. However, data from laboratory recordings of muscle behaviors in TMJ disorders and control subjects did not confirm this association [183]. Yet, inconsistency among findings may be due to differences in, and limitations of, study design, data collection, and analytical methods. For instance, muscle activities data in laboratory conditions might be quite different from those in natural settings.

Laboratory vs ambulatory

Masticatory muscle signals can be recorded in both the controlled laboratory environment and the natural ambulatory condition. Laboratory recordings usually have better recording quality because the recording is performed under instruction in the laboratory with less environmental noise around. Also, data analysis of laboratory recordings is much easier than ambulatory recordings because oral behavior log book and instruction program could help registration by matching the recording timeline to the log book timeline. In contrast, no reliable log book can generally be obtained in ambulatory recordings and subjective report is the only clue over the oral activates in most cases. However, laboratory recordings also have the following drawbacks: the lack of individual and meaningful oral tasks since all subjects follow the same instructions; the subjective limitations of time, speed and amplitude on oral tasks; and the inclusion of some meaningless oral tasks. Moreover, the recordings do not represent occlusion activities in real life. Alternatively, ambulatory recordings include behaviors in a more natural environment, but it is difficult to extract oral activities over a sufficiently long duration because there is no oral behavior log book for ambulatory recordings. Also, there are

usually background noises that mask some of meaningful signals. A wise combination of these two types of recordings will assistant in identifying meaningful oral activities in an objective way.

Oral activity recognition

The raw EMG data contain both positive and negative values because the data result from an alternating current signal in which the motor unit action potential distributes evenly around zeros. The mean value of the raw EMG data approaches zero. The raw EMG signal provides limited information for oral activity detection. The amplitude and frequency of the EMG signal are the two most critical sources of information for signal processing. The amplitude of the EMG signal reflects the muscle strength or force, while the frequency of the EMG signal indicates the fatigue. Therefore, to obtain meaningful analysis results in time domain, the raw EMG signal must be rectified first by computing the absolute value or the root mean square value. The absolute amplitude of EMG signal without normalization is meaningless because the EMG signal is influenced by many factors including the muscle anatomical and physiological structures, the action potential distance to electrodes, skin preparation, and electrode configuration. The EMG signals can vary significantly at different times even for the same person. Therefore, it is necessary to normalize the EMG signal so that it is possible to compare data among subjects and at different times. To remove the noise in the signal, a moving average or low pass filter is frequently applied to smooth the input EMG signal.

Recently published data [185], based on ambulatory EMG recordings, showed that subjects with and without TMJ disorders produced masticatory muscles activities which

were predominantly at low intensities associated with jaw loads in the range of 1-2 N. However, the type of jaw loading behaviors which accounted for these muscle activities were not determined. Parafunctional loading of the mandible has been considered to significantly hinder the nutrient supply to TMJ disc cells and, therefore, have clinical relevance with respect to development of TMD-related myofascial pain [4, 186]. The most commonly reported computerized approach to identify onset and duration of behaviors recorded by surface EMG is a threshold-based estimation method, where one of the three amplitude criteria are employed to detect events (Table 3).

The fixed amplitude criterion uses an a priori defined EMG threshold to identify onset and cessation of events. The inability to customize the threshold for each individual makes the fixed amplitude criterion less popular in research field. The peak amplitude or maximum voluntary contraction (MVC) criterion uses the maximum recorded root-mean square (RMS) EMG values to express the individual-specific EMG threshold as percentages of MVC. However, this criterion is problematic given that MVC is sensitive to training and visual feedback and does not standardize load magnitude amongst subjects. The statistically-based amplitude criterion uses EMG recordings, to identify resting-state baseline or background EMG activities at first and then expresses onset and duration of behaviors relative to specified standard deviations above the resting-state data [187]. The original hypothesis is that this criterion coupled with individual-specific EMG calibrations, such as jaw muscle activity per unit of bite-force (μV/N), enables unique characterization of a wider range of jaw loading behaviors.

Table 3. EMG oral behavior detection methods.
Threshold-based estimation methods. A: amplitude, D: duration (unit: seconds), L: linkage (unit: seconds), MVC: maximum voluntary clench, PSG: polysomnography, electromyography.

Article	Muscle	Device	Threshold	Method
[188]	Masseter	PSG	A: 40% MVC or 40 μV; D: 1.5; L: 3	Manual
[189]	Masseter	EMG	A: 20 mV	Analog device
[190]	Masseter	EMG	A: 5 μV; L: 3	Analog device and manual
[191]	Masseter and digastric	PSG	A: 20 μV; D: [0.5, 1.5); L: 2.5	Manual
[192]		EMG	A: Ordinary movement; D: 2; L: 1	Analog device and algorithm
[193]	Masseter	PSG	A: 2* background or 75 mV; D: 0.25-2 phasic, >2 tonic	Manual
[194-196]	Masseter	PSG	A: 40% MVC peak (raw); D: 2	Manual
[197]	Suprahyoid, temporalis, masseter and tibialis	PSG	A: 40% MVC peak (raw); D: 0.25-2 phasic, >2 tonic; L: 3	Manual
[198]	Masseter	PSG	A: 20% MVC	Manual

[199, 200]	Masseter	EMG	A: 13.1% (7%-22% MVC peak); L: 5	Algorithm
[201, 202]	Masseter, temporalis and anterior tibialis	PSG	A: 20% RMS of MVC; D: 0.25-2, >3 bursts for phasic, >2 for tonic	Manual
[203, 204]	Temporalis	EMG	A: 30% MVC peak; D: 2	Algorithm
[205]	Chin/suprahyoid, masseter and anterior tibialis	PSG	A: 20% RMS of MVC; D: 0.25-2, >3 bursts for phasic, >2 for tonic	Manual
[206, 207]	Masseter and tibial	PSG	A: 20% RMS of MVC; D: 0.25-2, >3 bursts for phasic, >2 for tonic	Manual
[208]	Temporalis	EMG	20% of calibrated force, which equals to force at 60% MVC peak	Algorithm
[187]			3SD, SD is the standard deviation of background noise	Algorithm

Mandibular Movement and Functional Assessment

Mandibular movement

Mandibular movement includes several different typical oral tasks including the jaw open/close movement, protrusion, retrusion, and laterotrusion. Protrusion is the anterior mandibular movement while retrusion is posterior mandibular movement. Laterotrusion is the mandibular lateral movement in a sideward direction, for instance, from the left position to the right position.

Motion tracking vs dynamic MRI

Compared to the static imaging method recommended by DC/TMD [1], image and tracking combined with 3D motion study provides a whole set of dynamic information about TMJ movement so that the time points when possible irregular TMJ movement positions happen can be determined and analyzed. For instance, 3D motion can provide disc position information at any plane or multiple planes simultaneously in a way that is user-friendly. The TMJ disc displacement can be determined in the mandibular three-dimensional kinematics study. Furthermore, kinematics study provides surgeons a monitoring system to determine the process of an active treatment and determine whether any further procedure is required. In addition, the rehabilitation of jaw function through orthognathic treatment requires that the jaw restores its function and one of the objective functions is that the mandibular movement can be corrected. In orthodontics, one of the targets is to restore the jaw functional occlusion surface or centric relation position after the orthodontic treatment including inlays, onlays and denture management [209].

Dynamic MRI is promising because it provides dynamic recording of the habitual mandibular movement but dynamic MRI is limited by its clinical availability, resolution, signal to noise ratio, sampling frequency [66, 210] and cost. Furthermore, dynamic MRI can only provide TMJ motion information in only one single plane, making it hard to detect the disc displacement in other two planes. For instance, the images in the sagittal view could not be used to detect lateral or medial disc displacement. It was found that the slice thickness of dynamic MRI is too large compared to that of CBCT. Consequently, the medial or lateral disc portion cannot be captured, leading to the incorrect diagnosis results [8, 67]. Moreover, one-time image scanning, as required in the motion study, minimizes the invasion to subjects from the multiple series of image scanning at different mandibular positions taken in dynamic MR imaging techniques. Finally, the posture of the supine position during scanning, the use of head fixation and the scanning environment will cause interference to the natural mouth movement. It is preferable for both subjects to be scanned in a friendly environment where they can maintain a standing or sitting posture to obtain the natural mandibular movement. The head movement should not be restricted because head motion happens in every second of daily life.

The optimum dynamic MRI protocol was determined by comparing the result of the conventional coronal technique with that of a new oblique-axial MRI for the continuous recording of TMJ motion [139]. The following scanning parameters were finally determined: fast field echo with echo planar image acceleration, repetition time T_R = 60 ms, echo time T_E = 17 ms, flip angle = 20º, field of view (FOV) = 140 mm, rectangular FOV = 50%, slice thickness = 5 mm, scanning matrix = 128, reconstruction matrix = 256,

number of signal average = 4. The time for a single scanning of TMJ was 500 ms. The scanning time for a single open/close movement was 6-7 s, which was much longer than the time for a mouth to complete one natural open/close cycle. The images were of bad quality because of the low signal-to-noise ratio as well as the motion artifacts.

The application of dynamic MRI to TMJ study was also reported in [65, 211]. The scanning rate was up to 15 frames per second, or 66.7 ms for a single scanning. The scanning resolution was $0.75\times0.75\times5$ mm^3. The subject was asked to do the close and maximumly open mouth task. It took the subject 10-13 seconds to complete a maximum open-close cycle. While the scanning speed had been extensively improved, the oral tasks instruction video, which aims to keep pace with the imaging speed and to obtain satisfactory image quality, prevented the volunteers from using the subject-specific and natural speed in performing those oral tasks. The oral task speed of 10 seconds per cycle was still much slower than the habitual oral activity. Finally, the motion artifacts were noted and image quality was not comparable to the static MRI.

Incisor motion vs mandibular movement

Literature has shown that the TMJ movement pattern of patients with TMJ disorders significantly differs from that of the controls [18, 212, 213]. For instance, the DC/TMD adopted incisor range of motion, or distance limit as one of the most important diagnosis items for TMJ disorders [1].

Incisor motion has been widely reported in the literature. The incisor chewing movement pattern in the frontal plane was categorized into 8 patterns [214] as in Figure 3. Pattern I had a streamline-shaped trajectory with a line shape on mouth opening and a bow

shape on mouth closing. Pattern II had a line deviated to the working side on mouth opening and a curve with more variation in curvature on mouth closing. Pattern III is a circular shape with incisors deviated to the balancing side on mouth opening and similar trajectory of the pattern I on mouth closing. These first three patterns were recognized as the normal types while the rest five patterns were considered as abnormal occlusion occurring in patients with TMJ disorders.

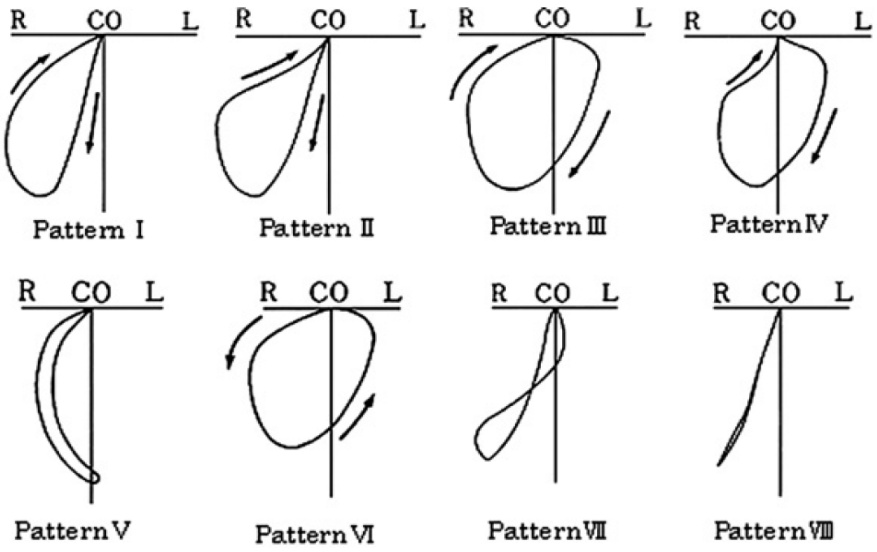

Figure 3. Eight types of chewing patterns of the interincisal point in the frontal view. The first three types are for normal subjects while the rest are for patients with TMJ disorders. R: right jaw side L, left jaw side. CO is the centric occlusion. Modified from reference [214]

The well-known Posselt envelope (Figure 4) describes incisor movement in three two-dimensional planes. It includes the incisor excursion during maximum open and close, lateral movement and protrusion/retrusion.

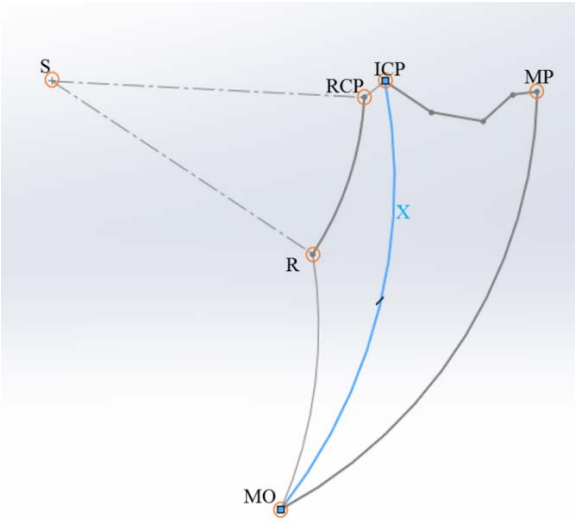

Figure 4. Schematic of the posselt envelope for the mandibular incisor motion envelope. S is the condyle hinge axis. RCP is the retruded contact position. ICP is the intercuspation position. MP is the maximum protrusion. MO is the maximum opening. R is the retrusion opening. X is the rest position. Modified from reference [215]

Table 4. Interincisal distance (unit: mm).
R is the right TMJ, L is the left side TMJ, F is female, M is male.

Article	Maximum opening	Lateral movement	protrusion
[216]	33.12±7.55 F patients 50.14±9.93 F controls	10.51±2.79 patients R, 11.57±3.10 controls R 9.18±2.75 patients L, 11.11±2.64 controls L	6.23±1.98 55 patients 9.84±2.02 controls
[217]	46.60±0.91		
[218]		11.45±0.40 R 10.98±0.43 L	9.32±0.28
[219]	M: 57.5 ±6.3 F: 52.1±4.1		
[220]	M: 58.6±6.6 F: 53.3±5.7	9.1±1.9 M R, 9.5±1.6 F R 10.0±2.1 M L, 9.7±1.6 M R	M: 9.0±2.0 F: 9.0±1.8
[221]	Adults: 56.9±4.3 Children: 51.8±4.6		

The incisor range of motion for maximum opening, lateral movement and protrusion has also been recorded using various measuring devices in literature (Table 4).

However, discrepancy exists in the results due to the difference of sample composition, measuring tools and experiment conditions.

The underlying assumption for using incisor motion to assess TMJ function is that both incisor and TMJ are rigid parts of mandible. Therefore, it is presumed that the incisor motion could completely express the TMJ joint function.

However, this assumption is not plausible theoretically as well as experimentally. Theoretically, the limited 3 degrees of freedom of the incisor motion is not adequate to explain the complex 6 degrees of freedom mandibular movement. The non-superimposed two markers define 5 degrees of freedom. To completely define the 6 degrees of freedom, at least 3 noncolinear markers are required.

Experimentally, the role of the incisor movement in the evaluation of the whole mandibular movement has been questioned [222-225]. The relationship between the condylar movement and the incisor movement was evaluated in [217]. It was found that the same incisor motion result can be achieved by various types of mandibular movement, and therefore the incisor motion alone cannot thoroughly or accurately reflect the whole TMJ movement. It was also noted that the condylar rotation was mildly associated with the incisor displacement. No association was found between the condylar translation and the incisor displacement. The same conclusion was supported by their later study [225].

The discrepancy in the investigations comes from the difference in the subject composition, the experimental design (e.g., some take the maximum opening-closing as the sole oral task while others also include the lateral movement and protrusion), the

measuring techniques, the assessment items (e.g., linear incisor distance, 3D movement paths, condylar translation) and the diagnostic criteria.

In summary, the DC/TMD recommended incisor movement could provide only limited information for the accurate diagnosis for the TMJ movement. Direct investigation of the whole mandibular movement via a combination of the data from a jaw tracking system with data from an image system is required.

Tracking device

The literature has reported various jaw motion tracking devices and corresponding experimental protocols. Some of the reviews were presented in the past [226-229]. The continuous development in advanced mechanical, electronic and optical high-technologies have facilitated the development of the scientific and objective diagnostic tools. The accuracy of quantitative measurement has been extensively improved. According to the data acquiring mechanism, seven major types of tracking devices have been reported:

1. Mechanical devices (e.g., the case gnathic replicator and the face-bow recording device). The disadvantage of mechanical devices is that they interfere with the natural mandibular movement.

2. Photographic methods (e.g., the cinematography). Photographic methods do not require the head fixation. The defects are that they need strong light, only 2D planar movement can be captured, a heavy face-bow is required, head fixation is required, and there is interference to the natural mandibular movement.

3. Roentgenographic methods [230]. There is no interference with this method. However, the problem with this method is that the low image contrast can only be improved

by increasing the x-ray radiation. Such increased radiation exposure to the patients is not permitted by the IRB review committees if an alternative exists.

4. Electronics and telemetric methods (e.g., the Cadiax compact [231]). These data collection systems are more accurate and more robust than mechanical device.

5. Ultrasound tracking system (e.g., the commercial system SICAT [232-236] shown in Figure 5). This system is relatively affordable for patients and relatively light weighted. In addition, it does not take much space allowing the application in clinics. However, the problem with the ultrasound tracking device is that the attachment of sound transmitter or receiver to the soft tissue of the head or face will produce relative skin-bone displacement and thus introduce errors during the recording. Moreover, the recording environment must be quiet enough so that no disturbance will be recorded.

6. Magnetometry devices. Two major types of magnetic commercial products, the mandibular kinesiograph and sirognathograph, have been usually applied in clinical settings in the literature [237]. A thorough description over the principles of these two systems can be found in [237]. Additionally, a third type of the magnetometry device electrognathography was reviewed and it was concluded that the application of this device was promising [238].

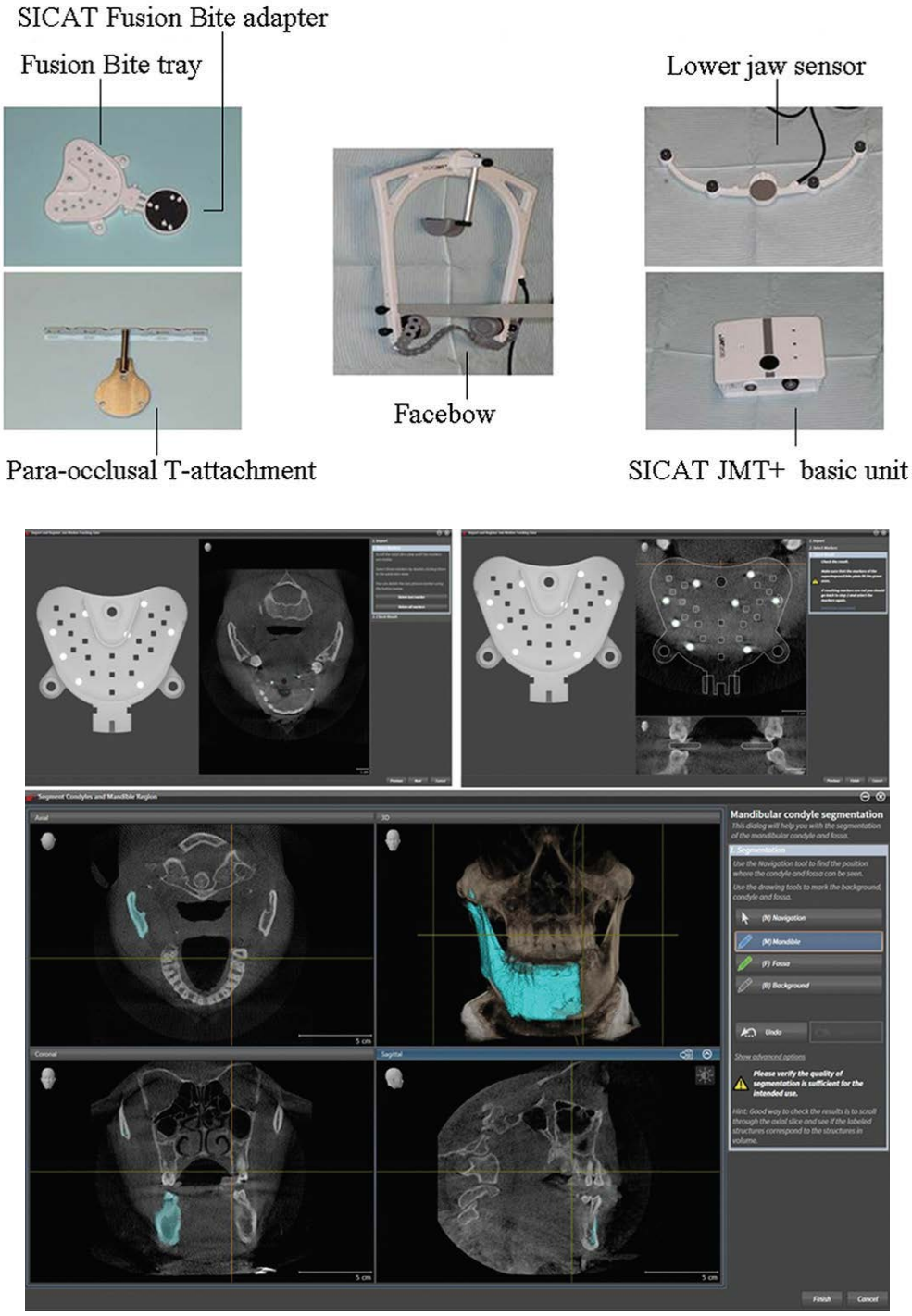

Figure 5. SICAT tracking device.
The reconstructed model from CBCT image is combined with the TMJ motion trajectories to build the TMJ motion model. Modified from reference [234]

The advantages of these magnetic devices are that they are relatively light-weighted (weight of magnet: 2g), no impairment to the occlusion surface or the natural mandibular movement and do not take much space allowing the application in clinics. The defects of these devices are also apparent: the magnetic tracking device is sensitive to the presence of the metal sources in the tracking field, and it is not suitable for patients with metal implants; the head fixation was required during the recording; the device movement relative to skin during recording must be considered; and only the incisor movement is tracked [239].

The magnetic devices are less accurate than the optoelectronic devices. The accuracy of the two popular magnetometry devices (kinesiograph and sirognathograph) was compared [237] through a clinical test on a 27-year-old woman with no symptoms of TMJ disorders. The author found that the measured value of a 5-mm protrusion was 3.5 mm, a value of 26 mm for a 22-mm opening, and a value of 31 mm of a 42-mm opening using mandibular kinesiograph. Therefore, because of the inherent distortion in the kinesiograph, the sirognathograph was chosen as the tool to track the mandibular movement [240]. A list of functional oral activities including resting posture, swallowing, speech, chewing, maximum opening, protrusion and lateral sliding were analyzed. Then the device was used to evaluate the incisor functional movement trajectories in the normal subjects and the patients with malocclusion: the trajectories area of natural chewing, swallowing and speech of the overjet/overbite patients before surgery were more dispersedly distributed compared to that of post-treatment by filling a missing mandibular molar with a fixed bridge. The increasing posterior support led to more symmetrical incisal movement in frontal plane. The frontal incisor trajectory of patients with vertical dimension

problem were found to be wider after treatment. It was also reported that the recording device moved relative to head during the chewing and maximum opening.

The error of the sirognathograph was evaluated [241] and found that the device produced severe errors for the maximum opening-closing due to its non-linearity when the magnet vertical displacement was beyond 40 mm.

7. Optoelectronic methods (e.g., Optotrak). Optoelectronic devices detect the three-dimensional positions of optical markers in 3D space by analyzing consecutive video image sequences.

Compared to electromagnetic methods, optoelectronic methods do not restrict the normal mandibular movement. However, the optoelectronic method is not flawless. It requires that the reflective side of the tracking markers are visible to the cameras during the whole recording process, which is not suitable in some cases. For instance, it cannot be applied to study the natural mandibular movement of a rat jaw because the natural movement of a live animal cannot be instructed as that of a human subject. By properly setting the experimental protocols, these limitations of the application in the jaw motion research could be avoided.

The accuracy of four types of tracking systems was compared [242]: optoelectronic, optoelectronic + CT, electromagnetic and electromagnetic + CT. It was found that their accuracies are comparable to each other, although the optoelectronic device (linear accuracy: 0.022 mm; curvilinear: 0.12 mm) was a little superior to the electromagnetic device (linear accuracy: 0.046 mm; curvilinear: 0.39 mm).

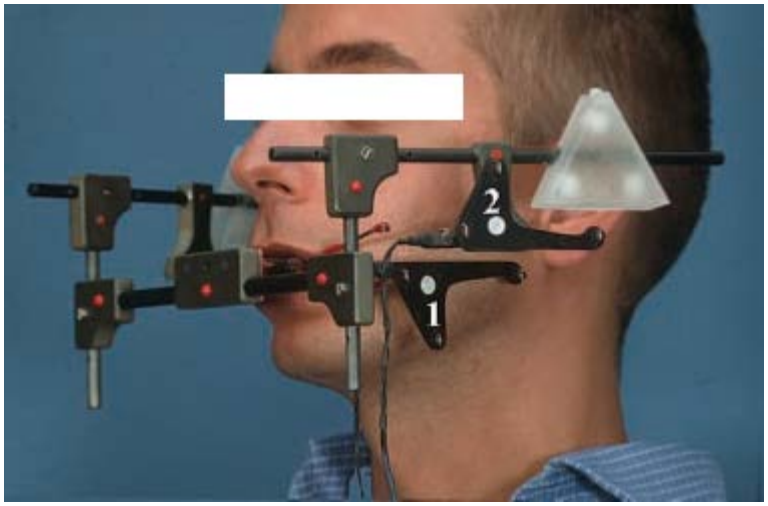

Figure 6. JAWS-3D tracking device.
The subject closed the mouth to register the motion marker with image markers. Two triangular target frames with motion markers are attached to the mandibular teeth (1) and another to the precision locator of the side arm of the face bow (2). MRI imaging markers were placed in a white plastic triangular frame. Modified from reference [243]

Optoelectronic tracking systems can be divided into two types, based on the type of tracking markers: the tracking system with active markers and the tracking system with passive markers. An active marker-based tracking system usually produces better signal since it makes use of the light from the LED markers. However, it has the problem of interference to the habitual mouth movement since it requires power supply and power cables for the jaw LED markers. A passive marker-based tracking system usually emits infrared light (λ = 850 nm) from LED of high-speed infrared cameras to the jaw retroreflective markers and captures the marker spatial coordinates by detecting the reflected light from the markers. Compare to the tracking system with active markers, a passive wireless marker-based tracking system takes less room and has no disturbance to the jaw movement. However, it has the risk of losing marker when the signal of the marker is too weak or when the marker is totally blocked.

The literature has reported the accuracy of various data recording systems. The linear accuracy of an active jaw tracking system JAWS-3D [244] (Figure 6) with active LED markers was 0.17 mm and the angular accuracy was 0.7º. The accuracy of a tracking system OKAS-3D [245] with active markers was 0.13 mm. The accuracy of a tracking system with active markers [246] (Figure 7) was 0.20 mm. The accuracy of a tracking system with passive markers [212, 247] (Figure 8) was 0.15 mm.

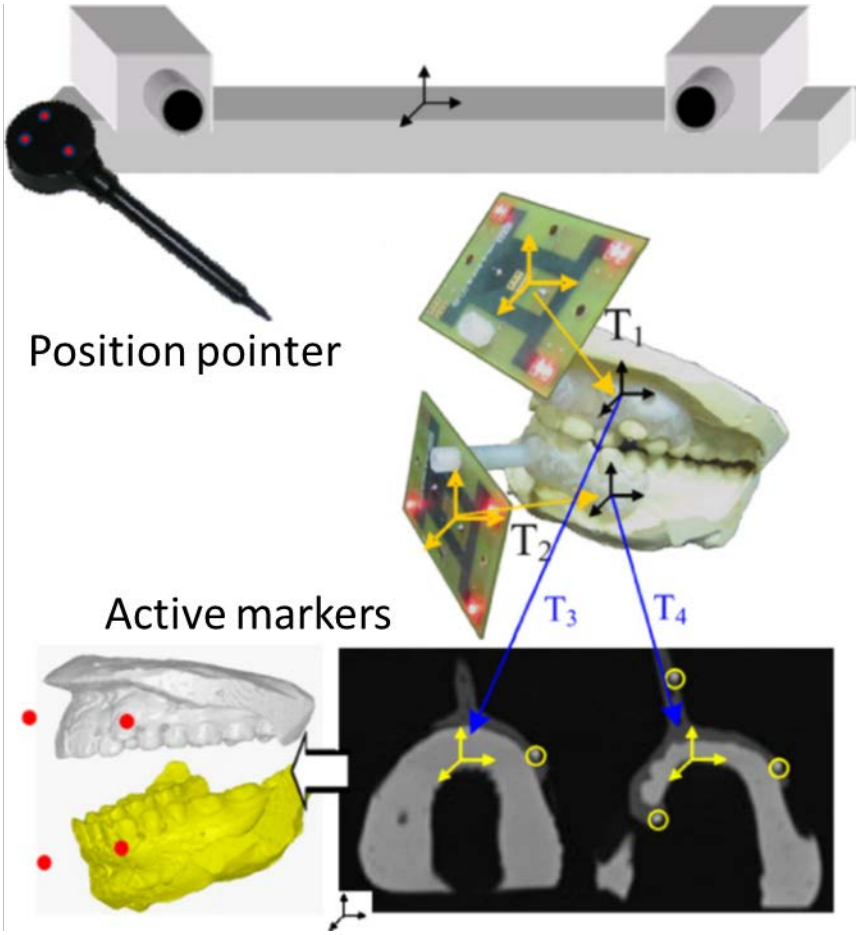

Figure 7. Active optitracking device with a position pointer.
The position pointer is employed to determine the spatial relationship between the imaging system and the motion tracking system. Modified from reference [246]

Figure 8. Passive optitracking device.
No electricity cables and EMG are available. Modified from reference [212, 248]

Some basic requirements [249] for a tracking device include: reproducibility, non-invasiveness, no interference or non-obstructiveness to the natural jaw movement, free head movement without fixation during the whole recording, simplified design, ability to perform distinct types of oral tasks including empty motion and mastication tasks, ability to integrate with other data collection system, and best user experience.

The placement of markers is paramount for the reliability of the experiment data. Tracking markers were put on the face or elsewhere on the skin in some experiments as skin markers, while others attached the markers to the human teeth as the bony markers. The difference between these two approaches has been reported. Some authors preferred the bony marker to the face marker. The possibility of using chin marker motion as the indicator was evaluated [250] for mandibular movement and compared with the movement of a marker attached to the teeth. It was found that the motion of these two markers was coherent. However, significant vertical displacement difference was found in the open-close movement. It was concluded that markers attached to the soft tissue could be used

only if the relative movement of the soft tissue to the bony markers was obtained in advance. On the other hand, others held an optimistic opinion on the use of the face marker. The tracking system error resulted from the placement of retroreflective markers on the glabella, the tragi, and the frontotemporal was evaluated [251]. Compared to the error of 0.35 mm of the bony marker, the error for the skin marker was 0.49 mm, indicating the suitability of the skin marker. Apparently, the difference lies in the selection of skin position to place the marker: the chin has relative large movement while the glabella hardly moves with the mandibular movement.

Registration of image and motion tracking coordinate systems

Most studies on TMJ kinematics and dynamics focus on either the trajectory path of a single point (e.g., the incisor point) on the mandible [252] or several mandibular points simultaneously [253] (Figure 8). To avoid the labor-intensive and time-consuming image scanning and reconstruction work from images, a motion tracking system was designed with an extraoral mandibular marker frame rigidly glued to the teeth and the frame had three non-linear tracking markers. Two more tracking markers around the tragi or the condyle lateral pole were positioned by palpation. A last marker was attached to the glabella [253] (Figure 8). The cranial reference plane was constructed with the glabella marker, and the two condylar lateral pole markers. The mandibular reference plane was composed of the markers on the extraoral mandibular marker frame. The coordinates of the incisors and the tragi markers in extraoral teeth coordinate system were determined using a marker pointer. To determine the lateral pole position, the tragi marker was shifted 15 mm along the medial direction. However, this device is problematic: the tracking

devices in literature ignored the imaging and thus cannot provide a patient-specific 3D TMJ model. Moreover, the displacement of the tragi marker was noticeably large and thus cannot be considered as a marker location for the cranial reference plane construction. Therefore, in their later study [251] (Figure 8), they improved the design by placing two extra markers on the frontotemporal as the cranial markers while still used the two tragi markers for the condylar lateral pole.

However, the study of one or several points movement only provides limited information over the mandibular movement. It is still impossible to determine the motion of other points on the whole condyle. One limitation is that it is impossible to know the intraarticular space situation. The whole condyle motion and the intra-articular space, as indicated in other parts of this dissertation, are extremely important for the establishment of a correct and objective diagnosis for TMJ disorders.

One possible way of assessing the entire mandibular movement is to assign the experimental motion data to a generic model [89]. The advantage of using the generic model is that there is no need for reconstructing a time-consuming 3D model for each subject and that it is easy to determine the location of the markers on the 3D model. However, one of the limitations is that all subjects share the same anatomy and the diagnosis will not be patient-specific although the motion is subject-specific. Thus, the diagnosis can be inaccurate.

The combination of image anatomy with motion trajectory provides the spatial information of more places other than the tracking markers. Moreover, it is possible to predict the motion condition of some points whose location cannot be accessed by the

marker pointer. For instance, it is impossible to attach the markers directly onto the condylar superior surface of a live human to obtain the condyle motion relative to fossa, critical for clinical diagnosis and management. The method reported in research is to attach markers to the skin or teeth so that the motion condition of the marker set connected to the mandible could be obtained. Then, with image-motion registration, the condylar movement could be deduced from the motion of that marker set.

Image-motion registration is to determine the spatial correlation between the imaging markers and the tracking markers in 3D space. Image-motion registration includes two major type of registration methods: rigid registration and non-rigid registration. It is assumed in the rigid registration that the set of markers used for image and the set of markers used for image are rigidly connected. Therefore, only translation and rotation are considered in the 4×4 transform matrix of the rigid registration. Non-rigid registration is usually used to describe the deformation of the soft tissue such as the motion in the lungs and heart. For non-rigid registration, markers are usually put on the structure with least deformation. The transform matrix of the non-rigid registration must consider the affine factor or scaling and shearing factors.

Recently, several image-motion registration methods, including point-based registration, intensity-based registration, surface matching, statistical shape-based registration, and deformable registration, are reported in the image guided surgery field for the post-surgery evaluation and the surgical procedure planning [254, 255].

Image-motion registration methods are also applied to study the three-dimensional mandibular movement. According to the registration device used, three major types of methods have been reported.

The first type of method is dependent on the use of a coordinate measuring machine [243, 244, 256] (Figure 6). A set of 3 non-linear spherical markers with MRI contrast media in the image scanning and a motion tracking frame consisting of three LED markers was placed. The relative position of these two sets of markers was determined using a 3D coordinate measuring machine.

The commercially available real-time data recording device SICAT [232-236] (Figure 5) used two sets of markers: one set of radiopaque markers for the CBCT system and the other set of markers for the jaw motion tracking system. The relative spatial relationship was automatically determined using commercial software with preset spatial configurations. The system was relatively small and suitable for clinical use since ultrasound motion tracking system was introduced: the position of four ultrasound transmitters in the front of SICAT fusion bite tray was tracked.

The second method is to use a marker pointer or track probe to determine the spatial relationship between the two sets of markers in the tracking system. A track probe was employed to measure the spatial location of the implants in the tracking system [246] (Figure 7). Then the transform matrix can be calculated to establish the relationship between the tracking system and the imaging coordinate system. The motion trajectories of those tracking markers were transformed into the image coordinate system. A similar method [242] was reported to track the mandibular motion.

Both the previous two methods use one set of markers for image and another set of markers for motion tracking. The whole data collecting system is rather complex.

The third type of registration method is to design a shared marker with a dual purpose for both the image scanning system and the motion tracking system. In this way, only one set of markers is required. Thus, a lot of space for placing the markers can be saved. The weight of the marker frame can be reduced as well. The possible interference due to the heavy weight of the marker frame could be avoided. Moreover, it spares room for placing the electrodes for muscle EMG recording. Finally, compared to the method of using the coordinate measuring machine [243, 256], there is no manual or computational alignment step to determine the spatial relationship between the image marker and the tracking marker since these two sets of markers are purposely designed to be located at the same position. Therefore, the tracking marker material must be positioned on top of the imaging marker material so that the tracking camera can capture the marker. The challenge lies in the design of a marker which is visible in both imaging system and tracking system. This method has been widely reported in real-time image guided surgery. Such a multimodality marker consisting of an infrared marker and a concentered tungsten sphere marker for the surgery intervention was reported [257].

Simultaneous data recording and data synchronization

The simultaneous multiple dataset recording allows the operator to collect multiple sets of data simultaneously. For instance, it is possible to extract the neuromuscular-activation mechanism (e.g., which muscles are involved and how strong they are) for different types of oral tasks.

Table 5. Simultaneous data recording.

Article	EMG	Motion tracking
[252]	Surface EMG Temporalis and masseter bilaterally	Magnetometry Kinesiograph Incisor movement
[258, 259]	Surface EMG Temporalis and masseter bilaterally	Magnetometry device Incisor movement
[260]	Surface EMG Temporalis, masseter and digastric	Sirognathograph Incisor movement
[239]	Surface EMG Temporalis, masseter and suprahyoid	Optoelectronic; passive marker Mandible movement
[261]	PSG Temporalis and masseter bilaterally Right digastric and mentalis	Optoelectronic; active marker Mandible movement
[247, 253, 262]	Surface EMG Temporalis and masseter bilaterally	Optoelectronic; passive marker Mandible movement
[263]	Surface EMG Temporalis and masseter bilaterally	Sirognathograph Incisor
[264]	Surface EMG Temporalis and masseter bilaterally	Magnetometry kinesiograph
[265]	PSG Masseter bilaterally	Mandible movement

The muscle configuration during dynamic movement will help explain how the muscle pain affects the mandibular movement. In addition, the muscle-skeleton synchronized data can simplify and improve the detection of oral behavior. For instance, it is hard to differentiate smile and moderate clench solely based on the EMG signal amplitude since their signal amplitudes are comparable. However, the additional movement could distinguish these two oral activities. The simultaneous EMG and motion recording is possible and has been reported in literature (Table 5).

In summary, the previous studies used a trigger pulse, multiple signal channel data acquisition or a global timing device to synchronize the motion tracking data and the EMG data. The challenge lies in the harmony combining of the two systems so that the motion tracking device will not disturb the EMG data recording system.

Kinematics descriptor: range of motion (ROM) vs functional axis/center of rotation (AoR/CoR)

Two major quantitative joint kinematics descriptors have been reported in the literature. One descriptor is the range of motion analysis and the other is the axis of rotation or the center of rotation (AoR/CoR).

The mandibular range of motion is to investigate the displacement or translation range of motion (ROM) of several points on mandible such as the condyle poles and the mandibular incisor. In addition to the ROM translation, another paramount ROM evaluation item is the joint rotation angle ROM describing the joint rotation limit. The functional joint rotation angle and translation assessment is to estimate the rotation and translation of the whole mandible which is usually interpreted as a rigid body.

The translation component derived from the trajectory of incisor point, incisor ROM analysis, and mandibular incisor analysis has been used for diagnosis [214]. Incisor ROM analyses performed during pain free opening, maximum unassisted opening, maximum assisted opening, lateral excursion, and protrusion are also most important mobility assessment items in DC/TMD diagnostic criteria [1]. The mandibular ROM analysis of the whole open-close procedure permits the incisive characterization of the normal mandibular motion and the comparison with the motion parameters of the patients. Finally, the ROM analysis can be applied to compute the action line length change and thus the force magnitude of the ligaments and muscles with respect to the mandibular movement so that their roles during the mandibular movement can be identified. From the ROM analysis, it is possible to determine the well-known controversies over whether the ligament plays a role during mandibular movement.

Three methods have been reported to express the joint rotation angle in three-dimensional space: the Euler angle, the joint coordinate system method, and the helical axis theory. The helical axis method will be described as one of the method for the determination of the AoR/CoR, which is also defined as the transverse horizontal axis in the prosthodontic terms.

In the Euler angle method, the condyle-fossa movement is a combination of the translation and the rotation components. It is desirable to extract the two parts and determine how each of them responds to the progression of the TMJ disease. Decomposition of mandibular movement into translation components and rotation components has been reported in literature [266]. The fossa-condyle complex movement

was consisted of the translation movement in upper compartment and the rotation unit in the lower compartment. The translation is between the TMJ disc and the temporal bone while the rotation unit is between the condyle bone and the TMJ disc. The rotation component can be further decomposed into three Cardan-Euler angle sequences of flexion-extension, adduction-abduction, and axial rotation around the local coordinate system built on the fossa bone so that it is able to determine the rotation angles of the mandible bone in three orthogonal planes. Because of independency property of the three Cardan-Euler angles, the decomposition has twelve possible rotation sequences and the sequence of XYZ is most commonly used.

The joint coordinate system (JCS) with a floating axis is well-known in the biomechanics field for its capability to express joint angle with clinical, anatomical and functional meaning [267-270]. In this expression, one coordinate axis from each of the two original segment coordinate systems is extracted to construct two coordinate axes of the new JCS. These two coordinate axes are called body fixed axes. The third coordinate axis is the cross product of these two extracted coordinate axes of the new JCS. The third constructed axis is called floating axis. It should be noted, however, that the wo extracted coordinate axes of the new JCS are not necessarily perpendicular to each other and that the new JCS is not an orthogonal coordinate system. Based on this definition, the joint flexion-extension, abduction-adduction, and external-internal rotations are defined. The relationship between the JCS and Euler angle is that the JCS corresponds to Euler XYZ sequence of flexion-extension, abduction-adduction, and external-internal rotation provided only the tibial is moving relative to the stationary femur as the reference frame

[267, 268, 271]. This method, intuitive to clinician and physicians, has been implemented in various software, including the commercial Visual3D (C-Motion, Inc. Germantown, USA and the biomechZoo [272]. However, one of the challenges is to standardize the selection sequence of the body segment coordinate system although it was stated that the method was sequence independent [267] and the choice of the reference point on each body segment so that a coherent diagnosis could be achieved. The distinct selection of the reference points will result in inconsistence in interpretation and diagnosis [268, 271]. To this end, much effort has been documented to improve this method so that it could be applied in various human joints and that the results could be comparable among studies in the past decades [268-270]. The application of this method to describe the mandibular movement was reported [273].

The correct and accurate determination of AoR is crucial in both the biomechanical field and the clinical field. The correct determination of the functional center of rotation (CoR) in the 2D or 3D joint motion and the instantaneous axis of rotation (AoR) in the 3D joint motion is fundamental to establish a set of reliable joint motion parameters and build up a subject specific diagnosis based on the identification of the abnormal subtle motion factors. The determination of AoR or CoR to the joint anatomy provides the mean joint center or hinge axis. The AoR or CoR information could be used for joint functional assessment.

In biomechanics, the AoR or CoR variables could also be used for the muscle/ligament efficacy evaluation since the AoR or CoR is the functional lever arm for the masticatory muscles and ligaments. In clinical field, the Aor or CoR provides the way

to evaluate surgical results and the application of surgical stents or splint for optimal implant guidance [274]. Accurate determination of AoR is relevant for dental articulator design and prosthesis [33]. An accurately designed articulator representing the functional mandibular movement will help the dentist and technician to precisely evaluate oral function and restore after surgery. The determination of AoR is also necessary for the orthognathic and orthodontics surgery procedure planning and evaluation [33, 209, 275-277]. The degree of the AoR discrepancy between the simulated or computed AoR and the actual patient AoR during the mandibular movement, especially when the opposing teeth are about to contact, is the major impact factor contributing to the failure in osteotomies surgery, prosthesis design, and splint device construction [32, 34, 35, 276, 277]. For instance, it was graphically demonstrated [276] that the molar mesial-buccal cusp moved to a different point in real situation rather than the expected location in the articulator. The inconsistence magnitude due to the inaccuracy of the articulator was quantified. It was demonstrated that both the incisal and molar occlusion errors linearly increased with the misalignment of the articulator rotation center to the assumed mandibular rotation center. It was showed in [278] that there was notable error in the maxillary position after surgery if the AoR was inappropriately calculated. In addition, the application of AoR to predict the mandibular autorotation after surgery is also reported [277, 279, 280]. The mandible will move or autorotate to a new position after surgery. It usually takes some time for the autorotation to complete the autorotation process and the AoR prediction helps shorten this surgery time. However, it is necessary to accurately locate the AoR position.

The accurate, patient-specific, objective and non-invasive diagnosis based on the analysis joint motion requires that the CoR or AoR determination is sensitive to the individual subtle motion pattern so that the subject-specific kinematics irregularity patterns, such as AoR inclination relative to the condyle mediolateral poles, distance to the condyle pole, ratio of translation to rotation, and axis distribution dispersion, in patients can be captured. The reproducibility and irregularities of the CoR or AoR calculated from the screw axis were evaluated [281] for the diagnosis and surgical treatment plan for 113 subjects including 42 malocclusion patients without muscle pain and 15 malocclusion patients with muscle pain. It was found that the AoR was more concentrated around normal position in the control subjects than the patients with TMJ muscle pain. It was found that the mandibular fixed hinge axis was more abnormally distributed in patients and the distribution was improved after therapy [282]. On the other hand, it was observed that the AoR range of 4.1 mm for a patient with DDnR was smaller than the normal range of 5.6 mm [283]. However, the AoR range of 24 mm for a patient with DDwR was significantly larger than the normal range.

In addition, the difference in muscle activation will be expressed by the variation of the joint AoR properties. The inaccurate evaluation of the AoR and CoR inevitably results in imprecise estimation of the kinematics, force, moment arms and moments of the joint muscles, leading to faulty interpretation and risky diagnosis. In clinical application, the incorrect determination of the AoR will cause the severe errors in surgery [279]. The AoR has been used for the calculation of muscle moments by determining the lever arm and functional assessment of masticatory muscles. The joint muscle moments of two

methods were compared [284]: one was from the stationary hinge axis by connecting the condylar lateral pole and the condylar medial pole while the other was from the instantaneous AoR from the Reuleaux technique, at mouth rest position and the mouth normal opening position of 18°. The muscles included masseter muscle, anterior temporalis muscle, posterior temporalis muscle and the medial pterygoid muscle. At rest position, it was found that the moment arm of the instantaneous AoR was 1.76 times as large as that of the fixed hinge axis. Consequently, the total moment significantly differed between the two methods. Also, it was found that the muscle contribution varied a lot between the rest potion and the opening position when instantaneous AoR was adopted. For instance, the role of the masseter muscle and the medial pterygoid muscle reduced when the mouth activity change from the rest to the opening position. However, little increase of the muscle contribution of the masseter muscle and the medial pterygoid muscle was found from the rest potion to the opening position when fixed hinge axis was employed, contradicting the known function of these masticatory muscles. Therefore, to obtain correct analysis results, it was recommended to use the instantaneous AoR. The limitation of this study was that the muscle force was set to a constant value and did not change with respect to the muscle length.

Two major CoR and AoR determination methods, the kinematics constraints-based transformation method and the marker trajectory-based fitting method, have been reported and reviewed in the investigation of synovial joints kinematics. Most of these methods are introduced to reduce the limitation of the motion artifacts from the skin-bone relative

movement which is estimated to range from a few millimeters to about 40 mm [285] and could be reduced in the TMJ movement study by the current available technologies.

The first type of AoR detection methods, the rigid body transformation method, is based on solving kinematics constraints includes the helical axis method, the Schwartz approach [286] and the symmetrical AoR approach [287] or the symmetrical CoR estimation approach [288]. The helical axis theory is the most widely used method although it has several limitations. For instance, the tracked motion trajectory must be smoothed to remove artifacts before the calculation since the helical axis is quite sensitive to the small angle of rotation or the pure translation. However, the smoothing will probably remove the motion irregularities which is crucial for the identification of abnormal joint movement. In addition, the determination of an appropriate helical angle interval is vital for the precise computation of the position and direction of the helical variables. It is well-known that the appropriate time interval is necessary for the determination of the average velocity determination over a joint movement: a long-time interval will ignore the detailed path of the motion trajectories and thus result in incorrect results, while a short-time interval will lead to extremely high velocity probably due to the noise instead of the true joint motion displacement. The choice of helical angle interval is similar to the that of the time interval. The helical axis method is usually used as the reference method to which the new methods are compared. The International Society of Biomechanics recommended the use of the helical axis method for accurate locating the CoR of ball joint and the AoR of hinge joint [269, 270]. According to the helical axis theory, the spatial rigid body movement could always be considered as a combination of a rotation around an AoR and a translation along

that same AoR (Figure 9). This rotation axis is also referred as the helical axis, screw axis or twist axis. When the joint movement is studied at infinitely small time-intervals, the helical axis is continuous in time domain and rotation axis is said to be instantaneous helical axis. However, if the joint movement is calculated at finite time intervals, only limited number of helical axes will be extracted. The rotation axis will be called as finite helical axis (FHA) or mean helical axis (MHA).

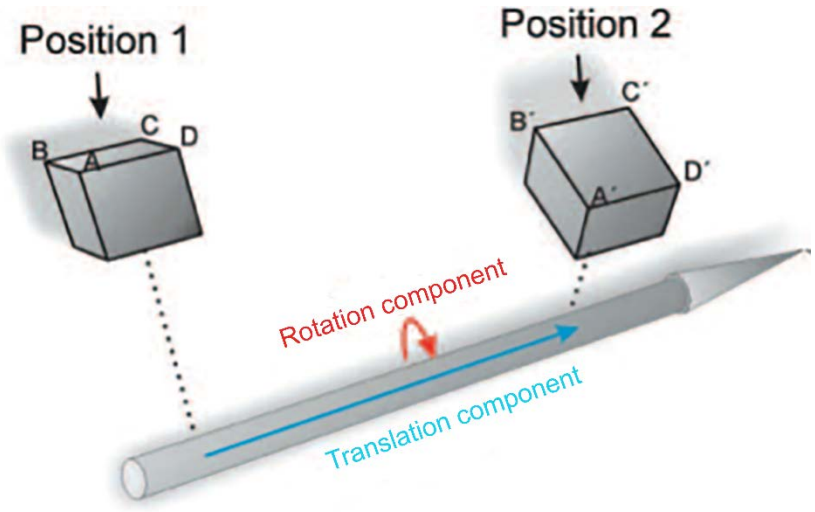

Figure 9. The rigid body movement around the helical axis (HA).
The rigid box ABCD in the figure moves from position 1 to position 2. The movement contains both rotation and translation. An imaginary HA may be constructed to describe this movement. The rigid body movement can be decomposed into the translation along the HA, and the rotation around the HA. The blue component is the translation vector, while the red arrow the rotation around the helical axis. Modified from reference [289]

The second type of AoR detection methods, the trajectory fitting method, assumes that the trajectory of markers at any two successive steps is of circular shape to determine the hinge axis in the knee or finger joint and that the trajectory is of spherical shape to determine the ball-socket rotation center in the hip or glenohumeral joint. The Reuleaux method originally described in [290] was the most intuitive fitting method in 2D

kinematics. The procedure is shown in [283] Figure 10: two landmarks (point A and point D) are selected and the displacements of these two landmarks when the segment is moving are plotted as the chords of the trajectory circles. The perpendicular bisector lines to these chords are then drawn. These two perpendicular bisector lines intersect at a point which is identified as the center of rotation. More recent details about this method could be found in [291].

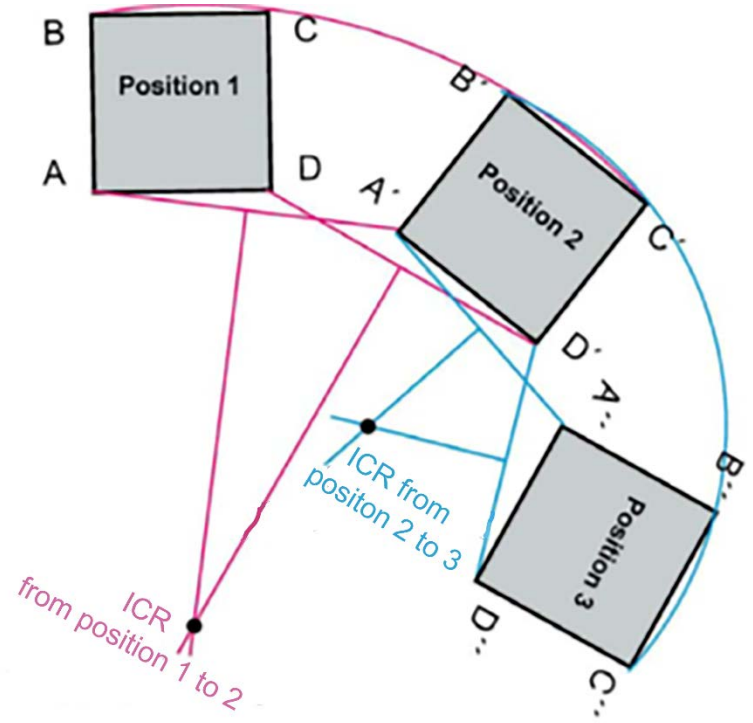

Figure 10. The Reuleaux technique for determining the axis of rotation.
A rigid body moves from the initial position (position 1) to the positions 2 (red color) and 3 (blue color). Each of the upper corners of the square move along colored circular paths around a given center. Modified from reference [283]

Based on the Reuleaux method, a method of minimizing the sum of all displacements to find the rotation axis for the hinge joint was described [292]. The author compared the results of this new method with the results from the FHA method. It was found that the new method had improved rotation axis position estimation when the notable

skin movement presented. It was also observed that the new method was not so good as the FHA method in the rigid body movement. It was found that the performance of the method [292] heavily depended on the appropriate selection of the time interval [293]. The calculated AoR angle error increased with the reduce of the frame distance. A closed-form solution of the CoR for the hip joint and the AoR for the knee joint was found [293]. The limitations for the fitting method was that it introduced and dramatically magnified the estimation error caused by the measurement noise. It was reported that the estimation error was more than 40 times the measured point coordinates errors [291]. In addition, it does not take the rigid body nature of the segment movement into consideration.

The systematic assessment of these CoR or AoR methods through the computer mathematical model simulation [287, 288], the mechanical analog device simulation [294], *in vivo* shoulder joint experiment [295], and *in vivo* knee experiment [296] are also reported.

On one hand, the rigid body transformation method is reported to surpass the fitting method. The performance of a list of eleven CoR estimation methods [288] and seven AoR estimation methods [287] were compared. It was found that only the Schwartz approach [286] and the symmetrical AoR or CoR method did not require the movement transformation of one segment into the coordinate system of the other segment to compensate the effect of the second segment movement. The innovation of the symmetrical AoR or CoR method over the traditional helical axis is that the influence of the skin movement artifacts could be reduced without the requirement of the transformation. It was also found that the geometric sphere or axis fitting method outperformed other methods in

CoR estimation and that the symmetrical CoR method shared the same formula with the FHA method when one segment was in the stationary state. However, the symmetrical CoR method was the optimal method with least CoR estimation error and the estimation error of the FHA method was extremely close to that of the symmetrical CoR method when both connection segments of the ball joint were moving. A later combination of the symmetrical AoR and the symmetrical CoR method, with the name of the OSSCA method, enhanced the reliability of the joint center and axis estimation [297]. The major purpose of the three symmetrical methods and the Schwartz approach is to minimize the impact of the skin movement artifacts on the transformation. Moreover, these methods are built for calculating a relatively concentrated AoR or CoR which is stationary in the segment local coordinate system and not suitable for the calculation of the discretely distributed instantaneous AoRs or CoRs moving relative to both the global coordinate system and the segment coordinate system during the segment movement.

One the other hand, it was also reported that the fitting method outperformed the rigid body transformation method in the AoR estimation. The hip joint center estimation of two fitting methods and two rigid body transformation methods with the same reference coordinate system were compared [298]. It was found that the sphere fitting methods had better performance than the rigid body transformation methods.

In TMJ kinematics field, the 2D mandibular CoR of the mandible movement is majorly determined using the Reuleaux method or fitting method [277, 283, 299, 300] while the 3D AoR parameters is determined using the helical axis method [18, 281, 289, 301-303]. The FHA parameters describing the mandibular movement is shown in Figure

11. The xy-plane is the horizontal plane. The xz-plane is the sagittal plane. The yz plane is the coronal plane. The d_{CP} parameter is the distance from condyle reference point to the FHA axis. The variables x_d and z_d are the components of d_{CP} along the coordinate system. T is the translation of the mandible along the FHA axis. θ_x and θ_z are the components of the FHA rotation. Finally, the rotation angle around the helical axis is expressed using Φ but it is not shown in Figure 11.

The mandibular axis of rotation was also simplified to 2D using a dimeric link chain method [304]. Although 2D motion description is simplified, it loses the motion information in other planes and the correlation among the motion in these planes. It is also possible to miss the abnormal mandibular movement in other planes. In addition to these methods, terminal hinge axis between the condyle latera poles was also widely used [282]. However, this concept of the fixed hinge axis contradicts the real mandibular movement of both translation and rotation [305], leading to serious errors in the Le Fort I osteotomy surgery [279]. This hinge axis should move around with respect to the mandible anatomy. Finally, there is kinematic center describing the mandibular movement [306, 307], which was found not to be associated with the TMJ anatomy or the intraarticular space [308] and, therefore, its usage is limited.

There is little consensus regarding the location of the AoR in literature. Some of the reported AoR position relative to the condyle center are listed in the Table 6 in the radiograph or the cephalometric condyle pole through the clinical palpation method.

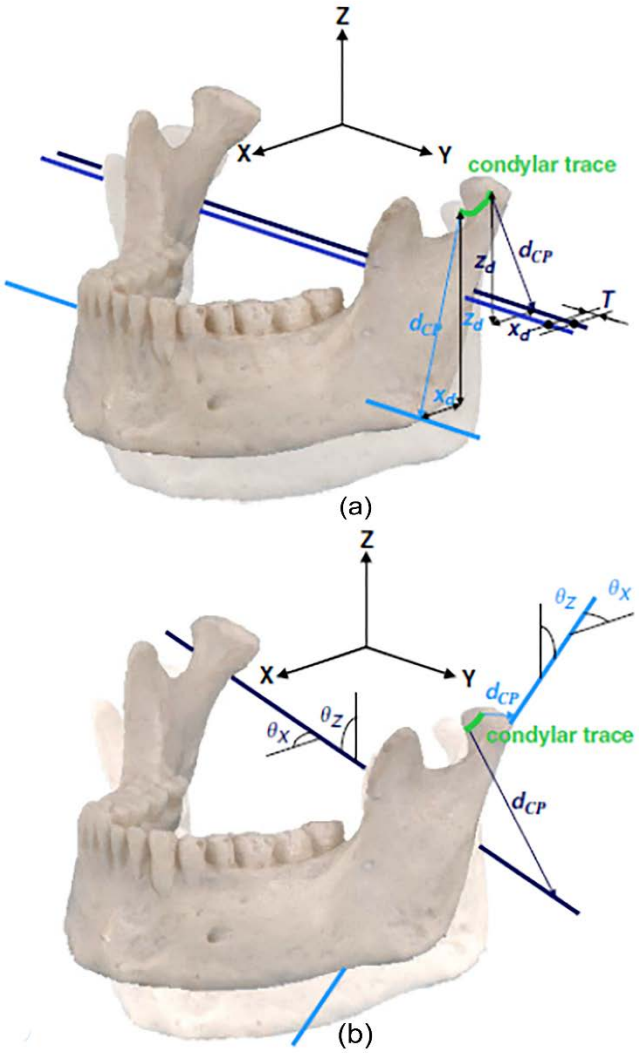

Figure 11. Definition of mandibular FHA parameters in 3D space.
x-axis is the anteroposterior direction, y-axis is the mediolateral direction, and z-axis is the superior-inferior direction. (a) The d_{CP} parameter is the distance from condyle reference point to the FHA axis. The variables x_d and z_d are the components of d_{CP} along the coordinate system. T is the translation of the mandible along the FHA axis. (b) θ_x and θ_z are the components of the FHA rotation. Modified from reference [18]

Table 6. AoR determination method and its location.

Article	Method	Location relative to the condylar pole
[29, 31, 309]	Tracing	Condyle summit
[279]	Reuleaux	5.0 mm posteriorly, 14.9 mm inferiorly with 10 m opening
[280]	Reuleaux	Mastoid process region 32 mm posteriorly, 28 mm inferiorly
[32]	Reuleaux	2.5 mm posteriorly, 19.55 mm inferiorly
[230, 310]	Fixed hinge axis	Condylar center
[311]	Geometric fitting	Condylar center
[301]	Helical axis	4.7 mm (anteriorly) to 27.6 mm (posteriorly) 12.4 to 43.7 mm inferiorly during the whole maximum opening process
[18]	Helical axis	normal TMJs: 5 to 28 mm (anteriorly), 12 mm (superiorly) to 44 mm (inferiorly) clicking joints: 33 mm (anteriorly) to 58 mm (posteriorly), 12 mm (superiorly) to 63 mm (inferiorly)

In summary, ROM analysis provides the border movement information of any mandibular point for the clinical diagnosis and the ligament and muscle length change during the mandibular movement for the dynamics study. However, ROM analysis has low repeatability among different studies because of the cross-talk effect risks: a small change of the choice in reference coordinate system would apparently cause appreciable difference [312], giving rise to the misinterpretation and inconsistent diagnosis. In addition, ROM analysis study the movement of one or several chosen points and the results of ROM analysis severely depend on the choice of the reference point. Lower diagnostic results would be possible depending on the selection of the reference point on TMJ [313-315]. To reproduce the same diagnostic results, the exact same coordinate system and reference point must be picked up with extreme caution among different researches. Compared to ROM analysis, FHA describes the comprehensive rigid body movement and elucidates how the motion of incisor is correlated to the mandibular movement. Furthermore, FHA is not dependent on the choice of reference point and the selection of reference plane. Finally, FHA is not affected by the body size and thus normalization is not required. However, FHA obtains less advocacy in clinical settings because it does not always correspond to an anatomical location. Therefore, the relative position and orientation of FHA with respect to the reference condyle points and the anatomical reference system is usually computed.

In addition to the previously described Euler angle-based ROM analysis and FHA method, a third kinematics description approach exists in clinical use: the projected angle. The projected angles method simplifies the motion analysis procedure by projecting the movement into three interested 2D planes. This 2D planar analysis is intuitive to and can

be easily accepted by the clinicians. However, it is not reliable and incorrect since the kinematics results largely depend on the choose of the reference frame [316]. The distinct definitions of the reference frame will lead to dramatic inter-observer inconsistence [317] and thus contradicting diagnosis results. In the kinematics of other joints, The relationship between the 2D frontal plane projection angle and the 3D movement analysis was evaluated [318] for both the hip joint and the knee joint. It was found that the 2D projected angle analysis reflected only 23-30% of the 3D movement. It was concluded that the 2D projected angle analysis could not be used for application with high accuracy requirement.

To employ and extend those techniques into our study and to improve the past tracking devices, the data collection system and data analysis system will be designed for the current research. Specifically, the motion study will include both the ROM Euler and JCS evaluation and the AoR or FHA determination at the normal mouth opening and the maximum mouth opening. The analysis results of TMJ disorders patient group will be compared with controls using the statistical method to identify potential risk factors for TMJ disorders.

Gender difference

The incisor distance during maximum opening was reported to be larger in males [219, 225, 319]. However, no such findings were reported in other studies [306, 315].

Discrepancy also existed in the mandible rotation during maximum opening. It was found that male had a significantly larger mandibular sagittal rotation of 37.5˚ than the 31.4˚ for the females [225]. However, this conclusion of larger rotation angle for the males

was not supported by other studies [219, 320-323]. The difference in the subject composition might explain the discrepancy.

The mandibular condyle center translation also had little agreement in literature. It was found that the males had significantly larger translation especially in the anteroposterior direction [225]. However, no significant difference was found in [219]. Again, the subject age distribution and the great group variation might explain the inconsistence.

Contribution to the following study

Finally, motion study provides indispensable kinematics input for follow-up contact mechanics, dynamics and disc nutrition diffusion study. For instance, the muscle length change with respect to motion is fundamental to muscle force computation using force-length-velocity relations [324, 325]. Motion study also enables the intra-articular space analysis and thus the determination of disc position during the TMJ movement. The contact area on TMJ disc calculated from intra-articular space analysis is a necessity for the joint congruence assessment and the glucose consumption simulation in TMJ disc. It is believed that the mandibular movement causes the articular surface congruity variation and thus leads to the stress concentration and articular cartilage damage especially at the crest portion of the fossa eminence where the joint degeneration is commonly observed [114].

Intra-articular Space Analysis and Shape-based Contact Area

The biconcave shape of the articular disc is conformed to the convex condyle head and the convex fossa eminence. Therefore, the existence of the biconcave TMJ disc compensated the TMJ articular surface incongruity between the mandibular condyle and

the fossa at mouth closed and between the condyle and the articular eminence when the mouth is opened.

Intra-articular space

In biomechanics field, Intra-articular space distance analysis allows the calculation of contact area and joint congruency. Based on contact area and joint congruence, joint stability, articulation surface friction, and contact stress distribution can be estimated. It is also possible to predict the solute diffusion and nutrition distribution in TMJ disc, the development of cartilage degeneration and the TMJ pathology [4, 114, 326, 327].For instance, the decrease of the intra-articular space distance due to excessive open-close, clench and other parafunctional activities, will increase the intra-articular pressure and produce the reactive oxidative species that inhibit the biosynthesis of the hyaluronic acid and cause the hyaluronic acid degradation. The degradation of the hyaluronic acid will lose its capability to prevent the lysis of the surface-active phospholipid layer, the principal part of the boundary lubricant, by inhibiting the phospholipase A_2 [328-330]. The intermittent oral behavior near or below physiological level promotes the growth, development and remodeling of TMJ tissues, while excessive pathological loadings lead to irreversible cartilage and TMJ disc degeneration [83]. Also, the knee joint stability was tested to find its correlation with the joint congruency in eight autopsy specimens under anteroposterior and rotatory load [331]. The author compared the joint anteroposterior laxity under compressive loading, no loading, cutting of tissue structures with compressive loading and cutting of tissue structures without loading. The author also compared joint rotatory laxity under compressive loading, no loading, cutting of tissue structures with compressive

loading and cutting of tissue structures without loading. It was observed that the joint stability depended largely on the joint soft tissue structures including knee menisci, ligaments, and capsule. However, under the condition of compressive loading, the joint stability was more affected by the congruence of the articular surface for both rotation and anteroposterior movement. Moreover, the dependence of the joint stability on joint congruence increased with the applied compressive loading.

Clinically, the joint congruence helps to establish the normal physiological articulation and to identify the abnormality in the pathological state. The vibration sound analysis due to the joint incongruency was reported [332, 333] and used as a frequent diagnosis item in the EMG study. The increase in joint congruence promotes stress distribution within the articular surfaces. The load maldistribution or stress concentration was believed to contribute to the human joint osteoarthritis [334]. In addition, the abnormal stress concentration due to the articular surface incongruity led to the degenerative lesions and was usually found at the crest of articular fossa eminence [88, 114].

Image based analysis

Intraarticular space has been evaluated for the articulating surface distance between condyle and fossa in images. The TMJ morphological and biometric features on the basis of CT images was evaluated [169]. A group of 51 symptom-free subjects were recruited (26 males and 25 females, average age of 42 years from 22 to 77). The eight morphometric measurement items in the coronal plane and the sagittal plane were obtained. Three additional indices, including the lateral stability index reflecting the joint stability, the coverage index indicating the joint constrained condition, the frontal centering index

indicating the lateromedial shifting degree and the sagittal centering index indicating condylar anteroposterior position in fossa cap were introduced. The asymmetries of the left and right TMJs were evaluated for those biometric parameters. The condyle width along mediolateral direction was 19.34 mm and the left TMJ was significantly wider than the right TMJ. The fossa width was 22.99 mm. No side difference was detected. It was found that the male condyle width of 20.7 mm was extensively larger than the female condyle width of 18.2 mm. The coronal intraarticular space was 2.24 mm laterally, 2.78 mm in the center and 3.02 mm medially. No remarkable side difference was found in those three coronal intraarticular spaces. The lateral, central and medial intraarticular spaces varied remarkably with condyle morphology including flat condyle and convex condyle. The intraarticular space was exceptionally wider in men in both the sagittal plane and the coronal plane. The fossa depth was 4.52 mm and the right side TMJ had notably deeper fossa than the left side TMJ. The lateral stability index was 0.8 and the joint was determined as stable accordingly. The right TMJ with stability index of 0.83 was much more stable than the left TMJ with stability index of 0.85. The coverage index was 0.19 and the joint was unconstrained. The coverage index was found to be extensively affected by condyle morphology. The convex condyle had a higher coverage index than that of the flat condyle. The sagittal centering index was 0.9 and the joint was determined as centered joint. The author concluded that the joint stability should be assessed using lateral stability index on coronal plane instead of the sagittal plane. More studies have been summarized in the previous part of “Anatomy and function”.

In vivo measurement

The *in vivo* direct measurement of the human TMJ contact area without disrupting the function integrity has been proven extremely difficult due to its intricate anatomy in an extremely small region although there are *in vivo* experiment reports of intra-articular pressure by inserting needle into articular space of TMJ joint [328, 335, 336] and invasive *in vivo* strain and force data of Baboon [337], macaques [338, 339] and miniature pigs [340-342] using strain gauges and piezoelectric film. In addition, the introduce of prosthesis will cause harmful corrosion because of its different material properties of with the condyle bone.

Contact area: contact mechanics

Shape descriptors, including surface curvature, have been broadly applied to measure the congruence of carpometacarpal joint (CMC joint) articular space. Some contradicting results were concluded due to the different designs of the study and distinct analysis methods. The hertz model is the mostly widely used model to evaluate congruence. By using stereo-photogrammetry to reconstruct the CMC joint articular surface frozen cadaver hands of eight females and five males, defining the relative principal curvature as congruence index based on the hertz theory and averaging the principal curvature over the whole articular surface because of the difficulty to compare the curvature on a point-by-point basis, it is found that women CMC joints are less incongruent than male joints and consequently the contact area in women CMC joints will be smaller than that of male joints under similar joint loading conditions. The smaller contact area in women joints will lead to higher stress distribution and stress concentration which trigger a cascade of CMC

pathology pathways to osteoarthritis [343]. However, the elastic half-space perquisite of the hertz contact theory generally cannot be met in human joints. Based on the winkler elastic foundation contact model, an elastic layer with thickness of 2 mm to mimic the cartilage is placed on the solid foundation. By reconstructing the 3D model from CT images of 34 women and 25 men and applying the elastic foundation contact model, it is found that there is no gender difference after normalization to joint size and that there is no significant correlation between joint congruence and the early joint osteoarthritis [327]. Unlike CMC joint, the cartilage thickness of TMJ fossa and condyle is relatively thin. The contact area of TMJ is comparable to the size of TMJ condyle and fossa. The curvature of TMJ articular surfaces is relatively large and non-uniformly distributed. Moreover, there is a deformable and moving soft TMJ disc between the articular bones. The TMJ disc is a biphasic viscoelastic material and cannot be simplified as a spring as in the elastic foundation contact theory. The deformation and motion of the TMJ disc also prevents the application of the elastic foundation contact theory which assumes no interaction between the elastic units. These inherent geometrical and anatomical properties limit the application of these contact theories to model TMJ.

Surface congruence in TMJ

Another way of the TMJ joint articular surface congruence estimation is through the examination of the distances between fossa and condyle surfaces or disc and condyle surfaces in intra-articular space. To evaluate the congruity of growing TMJs of 52 specimens, the frontal planar distances of 17 points distributed between lateral pole and medial pole are graphed with respect to their positions [114, 344]. The articular surface

congruency is normalized by subtracting the 2D mean distance from those 2D distances. The thickness of the soft tissues of the articular eminence and temporal fossa was uniformly set to 1.5 mm. In their later study, it was demonstrated that the cause of this surface incongruity was the shape of the growing articular eminence and that the consequence was the local stress concentration [116]. It was also found that the one of the disc function as the media to reduce the condyle-fossa articular surface incongruity was limited.

Stress field in 3D intra-articular space

The studies of joint congruency and contact area in 3D space are possible with 3D intra articular space analysis [345]. The contact area or stress-field calculation is described as a circle composed of 10 to 30 minimum distances between condyle and fossa. The radius of this circle is the standard deviation around the centroid of the stress field (Figure 12).

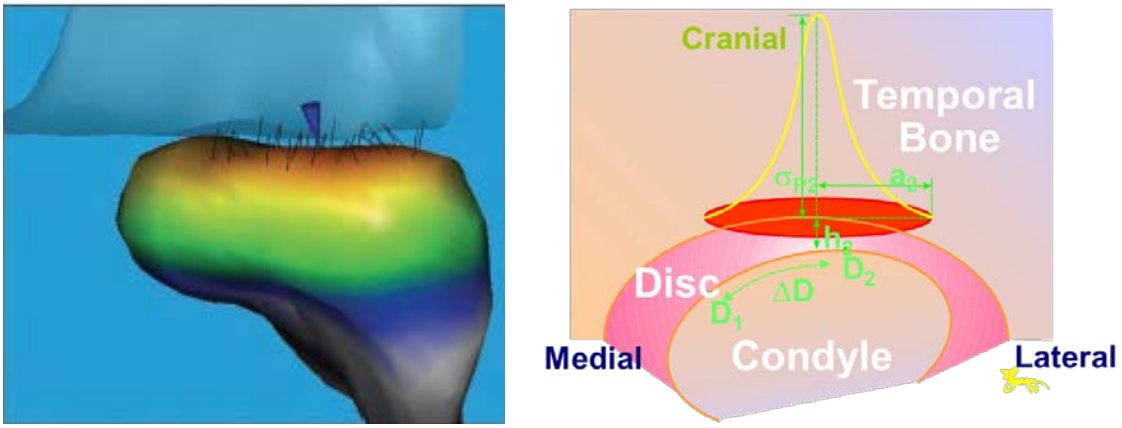

(a) (b)

Figure 12. Definition of the stress field, or the contact area descriptor I.
(a) The stress field consists of a set of 30 minimum distances between condyle and fossa. (b) The minimum condyle-fossa distance *h* is defined as the mean value of those 30 minimal distances. The centroid is center of those 30 minimal distances. The mean radius *a* is standard deviation of those 30 minimal distances. The surface congruency determines the position of the centroid of the stress-field. The peak stress (σ) and shape of the stress distribution curve over the stress-field are dependent on the velocity of translation, as well as on *a* and *h*. Modified from references [345, 346]

However, the later study [346] (Figure 12) and our preliminary data show that the shape of the contact area is more like an ellipsoid than a circle. Consequently, the subsequent contact stress distribution, the work done to cartilage and energy density [85] might deviate from the previous reports due to the algorithm update of the contact area. For instance, the ellipsoidal shaped contact data show that the loading area along mediolateral direction is longer than that of anteroposterior direction, which conforms to the condyle anatomical features and enables the major stress distribution along long mediolateral direction. However, should an idealized stress field circle be used to statistically depict the contact area and remove the eccentric property of the contact area originated from TMJ anatomy, the condyle and disc would have the same contact area along any direction and the contact stress would have more distribution along anteroposterior direction and less distribution along mediolateral direction, leading to possible stress concentration in conflict with *in vivo* contact properties and contradicting the TMJ anatomy [114, 116, 347]. Moreover, the stress field is located out the condylar anteroposterior anatomical boundary if the standard deviation is too large due to the elongated condylar shape in that direction, which is a common finding in the morphometrical measurement TMJ studies. In addition, the increase of the cartilage pressurization and the tissue fatigue due to localized compression and stress concentration is ignored. Furthermore, the application analysis of glucose diffusion in TMJ disc may also be more accurate by improving the contact area calculation. Finally, this method of

calculating the contact area with joint movement was adopted in the knee joint [348], the glenohumeral joint [349] and the CMC joint [350] as shown in Table 7.

Table 7. Contact area determination based on distance threshold.

Article	Joint	Distance (mm)
[351]	Human CMC	1.5
[348, 352]	Human knee joint	2
[353]	The bovine shoulder joint and knee joint	2
[350]	Human CMC	0.25
[349]	Human shoulder joint	0.1

Therefore, to extract the contact area based on exact scalar value on each point and element, this study will split the condyle and fossa articular surface into finite elements and then calculate the distance on each element and each point. After that, the points with scalar less than specified value will be located and the area containing these points will be separated from original fossa and condyle model. In addition, we will compare our extraction method with the contact area calculation method in literature. Finally, our previous studies showed that TMJ disc cells had relatively low solute diffusivity while the cell density was comparatively high, especially in the medial and anterior regions [86, 172, 354, 355]. It was hypothesized that parafunctional activities, including sustained joint loading due to clench and bruxism, might impede the nutrition transport in the TMJ disc and expose the TMJ cells to harsh nutrient environment. We will demonstrate the application of contact area to glucose diffusion simulation with and without parafunctional

activities (e.g., clenching) in TMJ disc since it is believed that glucose diffusion is the limiting nutrient for the survival of TMJ cells [4].

TMJ Biomechanics, Tribology, and Transport

Importance

The failure of the Proplast-Teflon TMJ implant from Vitek, Inc. as a management means to TMJ disorders was reported in [356] and many other surgeons. It was incorrectly thought that the polyethylene to be suitable for non-load-bearing joints [357]. Consequently, more than 26,000 problematic implants had been administrated even before the US food and drug administration (FDA) issued the recall [358]. Lesson from the failure of this TMJ disorder treatment confirmed the necessity to investigate the TMJ biomechanical environment.

In vivo measurement and simulation

The TMJ loading condition has been investigated using the *in vivo* measurement and the computer simulation. *In vivo* synovial fluid pressure measurement demonstrated that up to 15 mm Hg pressure was produced in pig TMJ cavity during mastication [359]. The synovial fluid pressure in upper TMJ compartment of 35 TMJs from 35 patients (28 females, 7 males, average age of 31.23 years) was measured [336]. It was found that the maximum opening produced a negative pressure of -53.82 mm Hg and the clench activities produced a positive pressure of 63.90 mm Hg. It was also found that females produced much higher pressure than males (females: 73.70 mm Hg, males: 31.42 mm Hg). Direct loading measurement in Macaca arctoides using piezoelectric film was reported by [339]. It was found that the force was 13-18 N during incisal biting and 4-13 N during molar

chewing. The strain was calculated and the condyle forces were calculated with prosthesis in the baboon [337]. It was found that the reaction force was up to 33 N corresponding to the biting force of 32.5 N during the incisal biting. Our simulation results in the published article showed that TMJ the interstitial fluid pressurization could sustain up to 80% of the compressive loading [360].

Composition

The human TMJ disc biomechanical composition was characterized in [361]. The average volume fraction of water in the human TMJ disc was 80% of the wet weight. The collagen took 62% and was influential for maintain the disc shape. GAG took 3.2% of the dry disc weight. The percentage of water was higher than human articular cartilage while the GAG content was lower in human disc. Therefore, the TMJ disc was less stiff and more permeable than human articular cartilage [83, 92].

TMJ disc cell types included elongated fibroblast-like cells, round chondrocytes-like cells, and fibro-chondrocytes. The animal TMJ discs at different ages were investigated [362]. It was found that cell type changed from fibrous to fibrocartilaginous with age. More chondrocytes-like cells were observed in the older animals. Three surgically removed discs from three female patients were examined [363]. The cells were selected from the central disc region since this region was less affected by TMJ disorders. It was found from morphology under transmission electron microscope that all cells are fibroblast-like cells except one chondrocytes-like cell.

Biomechanical characterization

Three types of loading conditions happen on TMJ disc and condylar cartilage included compression, tension and shear stress. The TMJ is a loading bearing joint, therefore, the TMJ disc and condylar cartilage sustain the compression stress. The lateral pterygoid muscles, ligaments, capsule and retrodiscal tissue stretch the disc during the oral activities, leading to tensile stress. Because of the incongruence of the articular surface and the extracellular matrix variation over the disc, the disc and condyle cartilage have non-uniform deformations over the whole disc. These factors result in shear stress, which could lead to fatigue and permanent disc degeneration.

TMJ tensile biomechanics characterization had been fully examined for the TMJ disc [106, 364], the condyle cartilage [92, 98, 365], and the retrodiscal tissue [111, 366]. The Young's modulus of human TMJ disc, condylar cartilage and retrodiscal tissue were region dependent. The porcine, bovine and canine TMJ discs were much stiffer than human disc [106]. The Young's modulus of the human TMJ disc was larger than that of the porcine retrodiscal tissue [111]. From the viewpoint of the retro-disc tissue, its tensile moduli have been proven to be relatively low to resist the abnormal pulling force resulted from displaced disc [111]. The Young's Modulus of the human TMJ disc was close to the Young's Modulus of the porcine condylar cartilage in one study [365] but much stiffer porcine condylar cartilage was reported in another study [364]. The reason for the contradiction was the distinct testing configurations including the strain rate, the experiment temperature, and the specimen preparations.

Compression test was also documented on both the TMJ condyle and TMJ disc. Proteoglycan, located in the anterior band, the posterior band and the intermediate zone, played the major role in resistance to compression [367].

Shear test was conducted to test the shear response of the TMJ condylar cartilage and TMJ disc to shear stress. The condylar cartilage dynamic shear properties were firstly tested with respect to the loading frequency and the strain level [368]. The condylar cartilage thickness was 1.25 mm measured using needle penetration method. It was found that the shear modulus increased with the increasing loading frequency and the increase of strain amplitude. Direction dependent shear property of condylar cartilage was validated in [369]. It was found that the shear modulus along anteroposterior direction was only 1/5 to 1/3 of the shear modulus along mediolateral direction. Therefore, the TMJ disc mediolateral strip is softer than the disc strip along anteroposterior direction. Probably, it is the shear stress from the mediolateral translation of the stress field during mouth open/close that leads to the articular cartilage degeneration [345, 370].

The effect of loading direction and frequency on the TMJ disc was tested [371]. It was found that the shear modulus increased with the increase of loading frequency. It was also observed that both the complex shear modulus and the storage shear modulus along anteroposterior direction were greater than those of mediolateral direction. The loss shear modulus was larger, although not statistically significant, along anteroposterior direction. The regional viscoelastic shear properties of porcine TMJ discs was measured [110]. It was found that the anterior disc band had relatively low equilibrium shear modulus than other regions (lowest in the anterior band: 2.5 kPa, highest in the posterior band: 3.88 kPa). This

relative softer anterior disc region was caused by the regional collagen fiber alignment distinction that anterior TMJ disc band had more isotropic collagen fibers with a significantly lower coherency coefficient through the scanning electron microscope study [355], similar to that of the human disc [106]. The shear stress of porcine discs was tested [372]. It was also found that the posterior band was the stiffest disc region. Together with the observation in MRI that the condyle-disc contact area located in the posterior or posterior-intermediate region and the collagen disorganization in this region [106], it was hypothesized that the stiffer property made it hard for the posterior region to disperse the applied stress to neighbor regions, resulting in localized stress concentration. The localized stress concentration will cause tissue fatigue (e.g. disc perforations and osteoarthritis.). Because of the collagen disorganization, the osteoarthritis will reduce the shear modulus and the TMJ disc will suffer even worse biomechanical function, leading to TMJ dysfunction.

In conclusion, TMJ disc is subjected to multiple types of loading conditions during its movement. Regional material properties result in region-specific responses to the biomechanical stimuli in TMJ disc. A moderate stress could stimulate the repair of the damaged articular cartilage. However, the sustained clenching and static biting may have contributed to mechanical fatigue failure of the TMJ disc cartilage because of a classical mechanical fatigue mechanism [85] or a combined mechanism which includes compromised disc cell nutrition due to duration of loading [4, 86], which further causes the irreversible change of the disc morphology.

TMJ tribology

Many types of diarthrodial joint lubrication modes have been proposed to explain experiment data and can be modeled mathematically to compare with experiments in literature: fluid-film lubrication in which a lubricant thin layer of less than 1 micron formed the high pressure and separated the articulation surfaces, self-pressurized hydrostatic lubrication or weeping lubrication, boosted lubrication and boundary lubrication.

The lubrication of TMJ articulation was also supported by the present of synovial fluid, TMJ disc and articular cartilage in the articular space. It was found that no single lubrication existed in TMJ bearing surface. For instance, the boundary lubrication alone cannot account for the extremely low friction coefficient of 0.0154 for articular cartilage [96] and 0.007 for disc [184] measured in TMJ and the observed time dependence of the friction coefficient. A combination of boundary lubrication and weeping lubrication was supported in literature [329].

The existence of ‘weeping lubrication’ was validated in the articular surface and refuted the mechanism of the squeeze film in TMJ articulation [184]. It was found that the friction increased with loading time and it was suggested that frequent repeated clench or bruxism promoted tensile or shear stress on articular surface, leading to the TMJ fatigue and dysfunction. Also, it was found that the fluid flowed from inner disc part to the disc bearing surface, removing the possibility of the squeeze film lubrication in TMJ articulation.

Synovial fluid was the overriding factor for sound joint lubrication. Both the hyaluronic acid and the lubricin in the synovial fluid are principal for joint lubrication. For

instance, it was found that TMJ joint without synovial fluid had 1.5 times larger friction and that the friction increased to 3.5 times for eroded joint [96]. The present of hyaluronic acid reduced half of the joint friction.

Articular cartilage played a crucial role in lubrication and preventing joint fatigue. It was found that the static energy dissipation fundamentally reduced but no significant change was found in the dynamic energy dissipation without the cartilage [373]. The accumulation of energy caused joint disc deformation, articular cartilage degeneration and joint fatigue [85]. Also, the conclusion of the chronic loading condition on TMJ function was confirmed by our simulation results in the published article [360]. In the simulation, the introduction of biphasic theory could accurately describe the confined compression creep. It was found that elongated loading condition caused solid matrix deformation in TMJ disc and larger ploughing force, leading to irreversible deformation to the collagen network, tissue swelling and articular surface degeneration.

TMJ transport

TMJ nutrient transport is crucial for the TMJ disc cell viability and the matrix remodeling. The major transport mechanism in the TMJ disc is the diffusion driven by the concentration gradient so that the nutrients around the periphery of the disc with high nutrient concentration can diffuse into the disc center with low nutrient concentration. The previous study also found that the TMJ disc had lower solute diffusivities through the ECM than other cartilaginous tissues [86, 172, 355]. In addition, the cell density and oxygen consumption rate are higher in the TMJ disc than in the articular cartilage [354]. Therefore, the TMJ disc cells are under vulnerable conditions and the possible major metabolic

mechanism is through the glycolysis [4]. It is hard to measure the solute concentration directly *in vivo*. With the finite element method, mathematical model provides the way to simulate the molecular diffusion in the TMJ disc.

Our previous studies showed that TMJ disc cells had relatively low solute diffusivity while the cell density was comparatively high, especially in the medial and anterior regions [86, 172, 354, 355]. It was hypothesized that parafunctional activities, including sustained joint loading due to clench and bruxism, might impede the nutrition transport in the TMJ disc and expose the TMJ cells to harsh nutrient environment. We will demonstrate the application of contact area to glucose diffusion simulation with and without parafunctional activities (e.g., clenching) in TMJ disc since it is believed that glucose diffusion is the limiting nutrient for the survival of TMJ cells [4].

In summary, the TMJ components resist compression, tension and shear stress during it functional six degrees of freedom movement under physiological loading condition. These loading stress conditions below 0.07 MPa are necessary for maintaining its functional integrity and tissue hemostasis after injury [116]. While abnormal loading condition of clenching and bruxism, even at low level, resulted in TMJ cartilage fatigue due to a classical mechanical fatigue mechanism or a combined pathology pathway including disc cell nutrition destruction due to abnormally frequent loading, which will further promote the permanent disc deformation.

Proposed Research and Scope of the Project

Proposed research and scope of the current research project. The proposed project will quantitatively assess the EMG, motion, and shape of the TMJ, which will bring an

objective and non-invasive diagnosis tool to TMJ disorders diagnosis. To achieve this goal, a novel and simplified EMG-Motion-Force data collection system with light weight devices and tools will be developed by putting imaging markers in the same positions with passive motion tracking markers. Therefore, the process of registration will be simplified without using intermediate markers as used in literature. Also, the system will be customized to own the capability to synchronize the EMG recording with motion tracking so as to remove redundant EMG signal at the beginning and the end. This study will provide objective and quantitative assessment to orthodontics surgery and prosthesis. A novel contact area calculation method with more physical meaning will be presented. Finally, this project will set the foundation for the continuing TMJ dynamics and TMJ disc nutrition study by providing vital EMG, motion and shape data.

CHAPTER THREE: CASE STUDY OF HUMAN TMJ MASTICATORY MUSCLE – ACTIVITY PATTERN THROUGH ELECTROMYOGRAM STUDY

Introduction

Published self-reported data suggests that the abnormal intensity and frequency of self-reported masticatory muscle activities associated with parafunctional jaw loading behaviors, such as teeth clenching and grinding, is a factor in the development of TMJ disorders (TMD) [182, 204, 374]. However, data from polysomnographic recordings of muscle behaviors in TMD and control subjects contradicts this association [183, 202]. The inconsistency amongst findings may be due to differences in, and limitations of, study design, data collection and analytical methods [36, 208, 375]. More specifically, previous reports characterizing parafunctional activity usually employed data collection methods of self-report questionnaires [37] or ecological momentary assessments [376]. Given the subjective influences of self-reporting methods [375], laboratory polysomnography (PSG) or ambulatory electromyography (EMG) may provide more objective and representative methods.

The advantages of ambulatory EMG over PSG include greater ecological validity, lower costs, and ability to record awake- and sleep-state data. Recently published data [185], based on ambulatory EMG recordings, showed that during the day and night, subjects with and without TMD produced masticatory muscle activities predominantly at low intensities, associated with jaw loads in the range of 1-2 N. Subjects with TMD differed from control subjects by the amount of time their masticatory muscles were active at these

low levels. However, the type of jaw loading behaviors which accounted for diurnal and nocturnal muscle activities were not determined.

Methods and criteria for computerized detection and characterization of the onset, duration, and intensity of jaw loading behaviors are limited [377]. The most commonly reported computerized approach [378] to identify onset and duration of behaviors recorded by surface EMG is a threshold-based estimation method, where one of three amplitude criteria are employed to detect events. The fixed amplitude criterion uses an a priori defined EMG threshold to identify onset and cessation of events but it does not customize the threshold for each individual, so it has been used less often. The peak amplitude or maximum voluntary contraction (MVC) criterion uses maximum recorded root-mean square (RMS) EMG values to express individual-specific EMG thresholds as percentages of MVC [204]. However, this criterion is problematic given MVC is sensitive to training and visual feedback [379], and does not standardize load magnitude amongst subjects. The statistically-based amplitude criterion uses EMG recordings, first to identify resting-state baseline or background EMG activities and then expresses onset and duration of behaviors relative to specified standard deviations above resting-state data [187, 378]. This criterion coupled with individual-specific EMG calibrations, such as jaw muscle activity per unit of bite-force (μV/N), enables unique characterization of a wider range of jaw loading behaviors.

The objectives of this pilot study were to: (1) record temporalis EMG from two clinically-defined diagnostic groups of women with/without (+/-) both TM joint (TMJ) disc placement (DD) and chronic pain (myalgia/arthralgia, P) in both laboratory and natural

settings; (2) use laboratory recordings to develop and validate an automatic detection method for the onset and duration of sustained teeth clenching; (3) apply the automated clench-detection methodology to define nocturnal epochs of clenching behaviors in ambulatory temporalis EMG recordings; and (4) use the pilot data to determine the number of subjects required to detect diagnostic group differences in temporalis clenching behavior. Based on time-logs of each epoch, subject-specific bite force (N) vs muscle activation μV/N calibration data were used to estimate the magnitude (N) of the loading behavior per epoch. Statistical analyses tested the hypothesis that there were diagnostic group differences in frequency (total number, number/hour), duration (s), and intensity (N) of teeth clenching behaviors.

Materials and Methods

Subjects

This pilot study was approved by the Institutional Review Boards of the University at Buffalo and University of Missouri-Kansas City. All participants volunteered for this pilot study. Subjects were recruited at the University at Buffalo School of Dental Medicine, and gave informed consent before enrolling. Given the higher incidence of TMD in women [380], this pilot project focused on night-time clenching behaviors in women.

Cone beam computed tomography (CBCT) and magnetic resonance (MR) images were used with Research Diagnostic Criteria for TMD by calibrated examiners to categorize subjects [1, 381]. Subjects were excluded from participation if they reported a history of rheumatic diseases, presented with CBCT evidence of degenerative joint disease of the TMJ, had multiple missing teeth or large dental restorations, were pregnant, or were

unable to perform the variety of tasks in the study protocol. This pilot investigation focused on equal numbers of age-matched women in two diagnostic groups: a +DD+P group containing subjects with both bilateral TMJ disc displacement and chronic pain, and a -DD-P group containing healthy control subjects without disc displacement and pain.

Laboratory EMG recording

Each subject presented for two laboratory EMG recording sessions, separated by a minimum of 3 nights during which ambulatory EMG recordings were completed. As previously described [185], at each laboratory session subjects had surface electrodes placed for bilateral EMG recording from the anterior temporalis muscles using standardized techniques. EMG outputs were amplified, filtered, and digitally recorded, along with outputs from a custom pre-calibrated force transducer. During each laboratory session, subjects performed static and dynamic biting tasks on the force transducer positioned between the molar teeth on one side at a time [185]. RMS EMG values of temporalis muscle activities (μV) versus bite-force (N) from the biting tasks were plotted, linear regression applied and slopes (μV/N) calculated for each subject and session. Subjects then performed a set of 15 tasks (Table 8, Oral Task Collector, OTC) of common functional and parafunctional oral behaviors, over a period of approximately 20 minutes, following written and pictorial instructions via a laptop computer. These tasks were chosen to test the ability of an automated algorithm to detect clenching behavior from amongst 14 other behaviors that produced similar temporalis muscle EMG characteristics.

Table 8. List of oral tasks.
The oral tasks that subjects performed whilst EMG signals were recorded in each of the two laboratory sessions. Modified from reference [382]

	Oral Task Collector Calibration Activity	Duration (s)
1	Moderate sustained clench	5
2	Rhythmic clenches (~1 Hz)	15
3	Molar tapping (~1 Hz)	15
4	Static incisor bite on saliva ejector	5
5	Rhythmic incisor bites on saliva ejector (~1 Hz)	15
6	Grind on right canine	15
7	Grind on left canine	15
8	Dynamic jaw play (right-left movement)	15
9	Smile	5
10	Right side dried meat chewing (~1 Hz)	15
11	Left side dried meat chewing (~1 Hz)	15
12	Right side gum chewing (~1 Hz)	15
13	Left side gum chewing (~1 Hz)	15
14	Dynamic right molar bites on saliva ejector	15
15	Maximum clench	5

Ambulatory EMG recordings

At the first laboratory session, participants were trained to prepare their skin, position surface electrodes, and operate portable EMG recorders to collect right anterior temporalis EMG data as described previously [185]. Briefly, EMG surface electrode signals were band pass filtered (20 – 1000 Hz) and amplified (5000x) by means of a custom built portable digital amplifier with input impedance of 250 MΩ, noise level of 0.7 μVolt, and common mode rejection ratio of 100 dB. Subjects were instructed to self-record in their natural environments for at least 5 hours for each of 3 nights and to keep a diary of start and stop times of the recording periods. Subjects returned equipment and data at the second laboratory session.

Clench detection algorithm

To extract data from each OTC EMG recording, the 15 predefined tasks (Table 8) and segments of background EMG activity signals were first identified visually (Figure 13a) then concatenated to create an EMG event list data file (Figure 14a). This was aided by hand-written timing logs and/or audio recordings of timing signals generated by the OTC program. The RMS EMG value of Task 15 (maximum clench) was used to normalize muscle activities, and the normalized RMS value of the background EMG activity was calculated for the limited purpose of defining standard deviation (σ) thresholds.

A clench-detection program was developed (MATLAB, MathWorks, Natick, MA) to identify and measure sustained clenches based on the event list. This program ran on the palmetto cluster in Clemson University. Steps for determination of sustained clenching included the envelope calculation, the square wave generation, and the duration check. The envelope of each predefined task was computed by rectifying and low-pass filtering the clench event signal (Figure 13b). By setting the amplitude threshold to 4σ (Figure 13b, dashed lines) and assigning 1 and 0 to the time samples whose envelope values were above and below 4σ, respectively, the square wave for each task was obtained (Figure 13c). A sustained clench episode was defined as a signal whose square wave occurred for longer than 0.5 seconds. The start and stop times of each identified epoch of clenching behavior were logged to reference with the raw EMG signals, and subject-specific laboratory calibrations of temporalis muscle activity (μV) per N of bite-force were used to estimate magnitude of clenching load for each epoch.

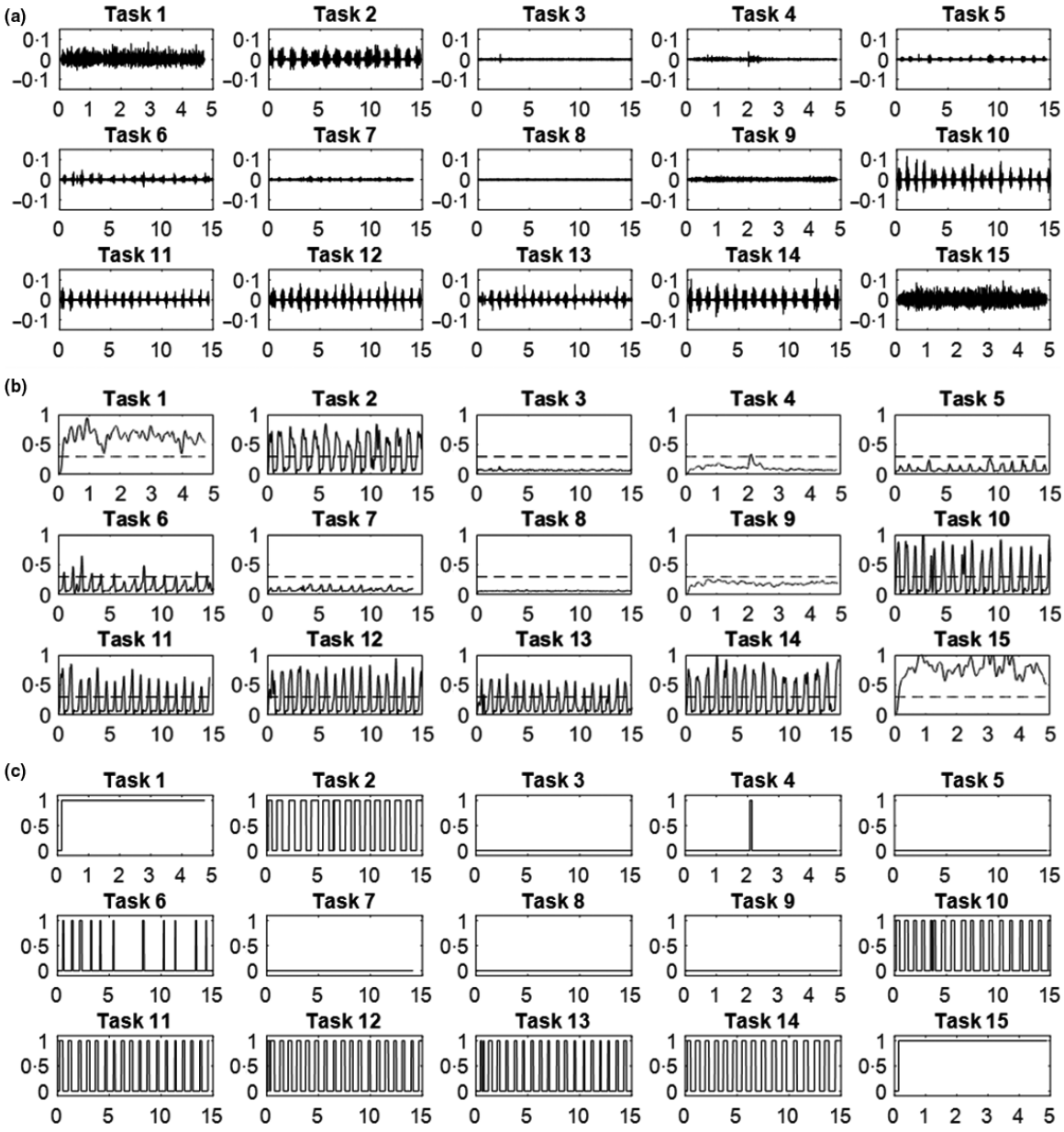

Figure 13. Steps to develop the clench-detection algorithm.
a) EMG activity (mV) versus time (seconds) from the 15 pre-defined tasks performed by a subject during one laboratory session; (b) envelopes of each of the 15 tasks after normalisation to RMS EMG of Task 15 (maximum clench), rectification and low-pass filtering with amplitude threshold (r) shown in dashed lines; (c) square waves of each of the 15 tasks where values of 0 and 1 correspond to signals with envelopes smaller and larger, respectively, than the threshold. Modified from reference [382]

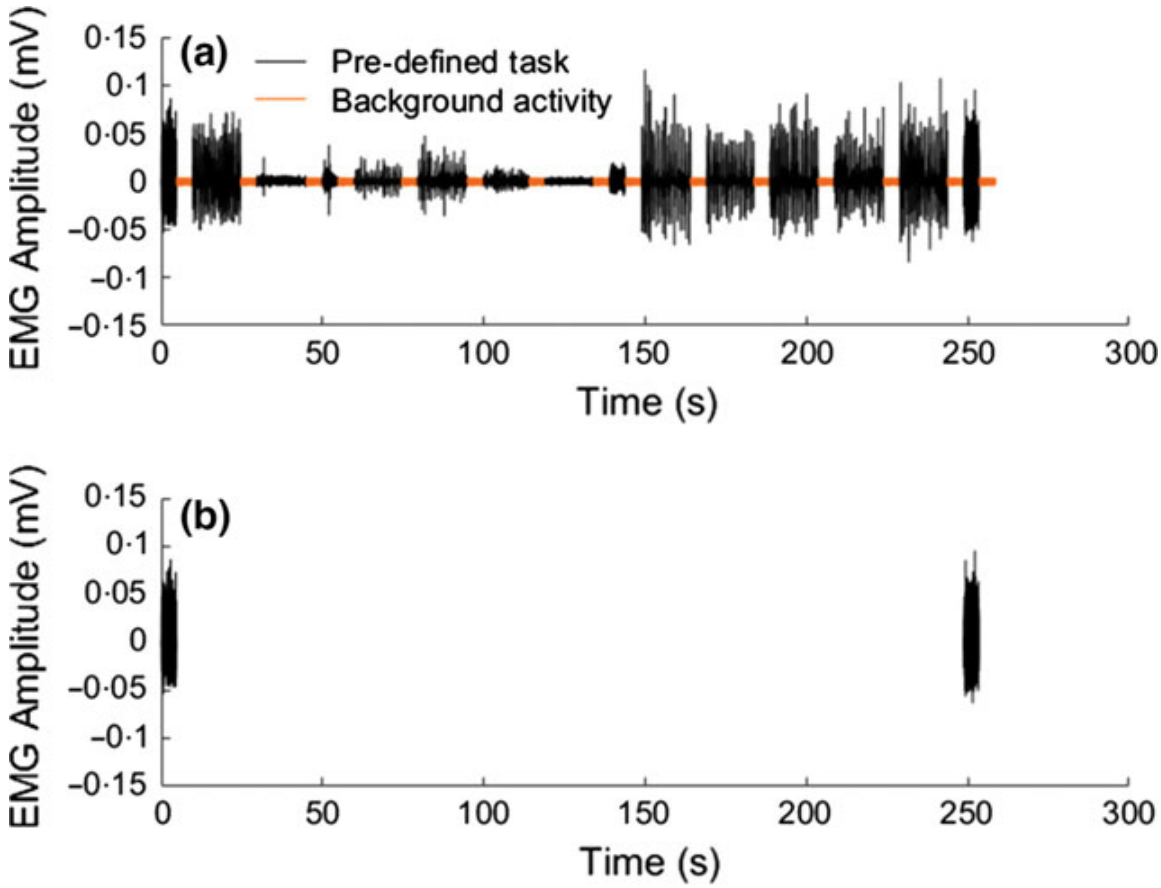

Figure 14. An event list data file.
(a) The event list data file was constructed by concatenating the EMG recordings of 15 tasks (black) and background activity (orange). (b) Two detected clench events were identified. Modified from reference [382]

Data analysis

The EMG data set for each subject consisted of two laboratory recordings and three night-time self-recordings. To validate the clench-detection algorithm, the algorithm was applied to the EMG event list data file from each OTC laboratory session to determine if all the arrhythmic (sustained) clench episodes could be recognized without referring to the corresponding laboratory log (Table 8) and to calculate the sensitivity, specificity, and accuracy of the detection algorithm. The number of detected sustained clench episodes (E1) and the number of tasks other than sustained clenching (E0) were used for the validation calculations. In each EMG event list data file, the first and last tasks were sustained clenches. Therefore, sensitivity was defined as number of correctly detected sustained clenches (E1) divided by two. Specificity was defined as number of correctly detected other oral tasks (E0) divided by 13. Accuracy was defined as the total number of correctly detected tasks (E1+E0) divided by 15.

The clench-detection algorithm was then applied via the customized computer program to analyze the night-time recordings of the temporalis muscle to determine the nocturnal clenching behavior of each subject. The parameters measured from each night-time recording were: the number of clench episodes, number of clench episodes per hour, mean clench duration, mean clench bite-force, and clench-related temporalis muscle duty factor. The clench-related temporalis muscle duty factor (%) was calculated as the sum of the clench episode durations divided by total recording time for a given night-time recording. Means and standard deviations of all parameters derived from the 3 nights of recording for each subject were determined.

Independent two-tailed homoscedastic t-tests with Bonferroni post-hoc corrections were used to determine differences between diagnostic groups (+DD+P vs -DD-P) for (i) number of clench episodes, (ii) number of clench episodes per hour, (iii) mean clench duration, (iv) mean clench bite-force, and (v) clench-related temporalis muscle duty factor. The average number of clench episodes were further analyzed with respect to duration (s) and bite-force (N). A Linear Mixed Effects Model was used to determine differences between diagnostic groups, restricted to levels including 95% of the data, for night-time average episode duration (s) and average episode force (N). Analyses were performed using commercially available software (SPSS, IBM SPSS Statistics, Version 23.0, IBM Corp., Armonk, NY; and Stata, StataCor LP. Stata Statistical Software: Release 14, 2015, College Station, TX).

Results

Twenty-four subjects met the inclusion criteria, with 12 women in each diagnostic group. The mean age (±standard deviation) of the +DD+P group was 37.4 (±14.9) years with a range of 21 to 62 years whereas, the mean age (±standard deviation) of the -DD-P group was 31.1(±8.7) years with a range of 24 to 56 years. The mean self-recording periods per night for +DD+P and –DD-P groups were 7.3 and 7.8 hours, respectively.

The two prescribed clenches were reliably recognized in the laboratory EMG event list data file by the clench-detection algorithm (Figure 14b, Table 9) with excellent averaged sensitivity (97%), specificity (96%) and accuracy (97%) over the two laboratory sessions. Recognition rates did not vary significantly between laboratory sessions.

Table 9. Clench-detection algorithm validation.
Sensitivity, specificity and accuracy values from laboratory sessions in two groups of women with/without (+/) both bilateral TMJ disc displacement (DD) and pain (P). Modified from reference [382]

Subject	Sensitivity (%)	Specificity (%)	Accuracy (%)
+DD+P1	100	100	100
+DD+P2	100	100	100
+DD+P3	100	92	93
+DD+P4	100	100	100
+DD+P5	100	100	100
+DD+P6	100	100	100
+DD+P7	100	100	100
+DD+P8	100	100	100
+DD+P9	100	100	100
+DD+P10	100	100	100
+DD+P11	50	100	93
+DD+P12	100	100	100
-DD-P1	100	92	93
-DD-P2	100	100	100
-DD-P3	100	92	93
-DD-P4	100	92	93
-DD-P5	100	100	100
-DD-P6	100	92	93
-DD-P7	100	100	100
-DD-P8	100	100	100
-DD-P9	100	85	87
-DD-P10	100	100	100
-DD-P11	100	92	93
-DD-P12	100	92	93
Mean	97	96	97

The +DD+P group compared to -DD-P group showed (Table 10) significantly longer mean clench durations (1.9±0.8 s compared to 1.4±0.4 s; p=0.042) and higher clench-associated temporalis muscle duty factors (0.47±0.34% compared to 0.26±0.22%; p=0.042). There were no significant differences between diagnostic groups with respect to number of clench episodes per night (67.5±41.3 compared to 47.5±37.1), number of clench episodes per hour (9.1±5.5 compar0ed to 6.3±5.2), or mean clench bite-force (6.9±6.0 N compared to 5.0±2.9 N).

Analysis of the distribution of clench episodes by duration (Figure 15a) and force (Figure 15b) indicated than in both diagnostic groups, greater than 50% of detected clenches lasted for less than 1 s and were associated with jaw loads lower than 4 N. The majority (95%) of clenches lasted for less than 4 s and were associated with jaw loads lower than 10 N. Differences between diagnostic groups analyzed for episode duration at each level and episode force at each level (Figure 15) were not significant but night-time clenching where loads were maintained between 1-2 s and at 4-5 N were 1.5-fold and 1.9-fold, respectively, more prevalent in +DD+P than in - DD-P subjects. Power analyses of these pilot data using a Hedge's g medium effect size (1-2 s duration = 0.532, 4-5 N load = 0.482) determined that 69 subjects per diagnostic group would be required to demonstrate between-group differences in night-time clenching durations and loads.

Table 10. Descriptive statistics for the detected clenches in nocturnal recordings. Descriptive statistics for the detected clenches during three nights in two groups of women with/without (+/-) both bilateral TMJ disc displacement (DD) and pain (P). Independent two-tailed homoscedastic t-tests with Bonferroni post hoc corrections were used to determine differences between diagnostic groups (-DD-P against +DD+P). Bold values indicate $P < 0.05$. Modified from reference [382]

Parameter	Mean ± SD	Bonferroni adjusted p-value
Number of clenches per night		0.112
+DD+P	67.5±41.3	
-DD-P	47.5±37.1	
Number of clenches per hour		0.106
+DD+P	9.1±5.5	
-DD-P	6.3±5.2	
Clench duration (second)		**0.042**
+DD+P	1.9±0.8	
-DD-P	1.4±0.4	
Mean clench bite force (N)		0.166
+DD+P	6.9±6.0	
-DD-P	5.0±2.9	
Duty factor (%clench time per total recording time)		**0.041**
+DD+P	0.47±0.34	
-DD-P	0.26±0.22	

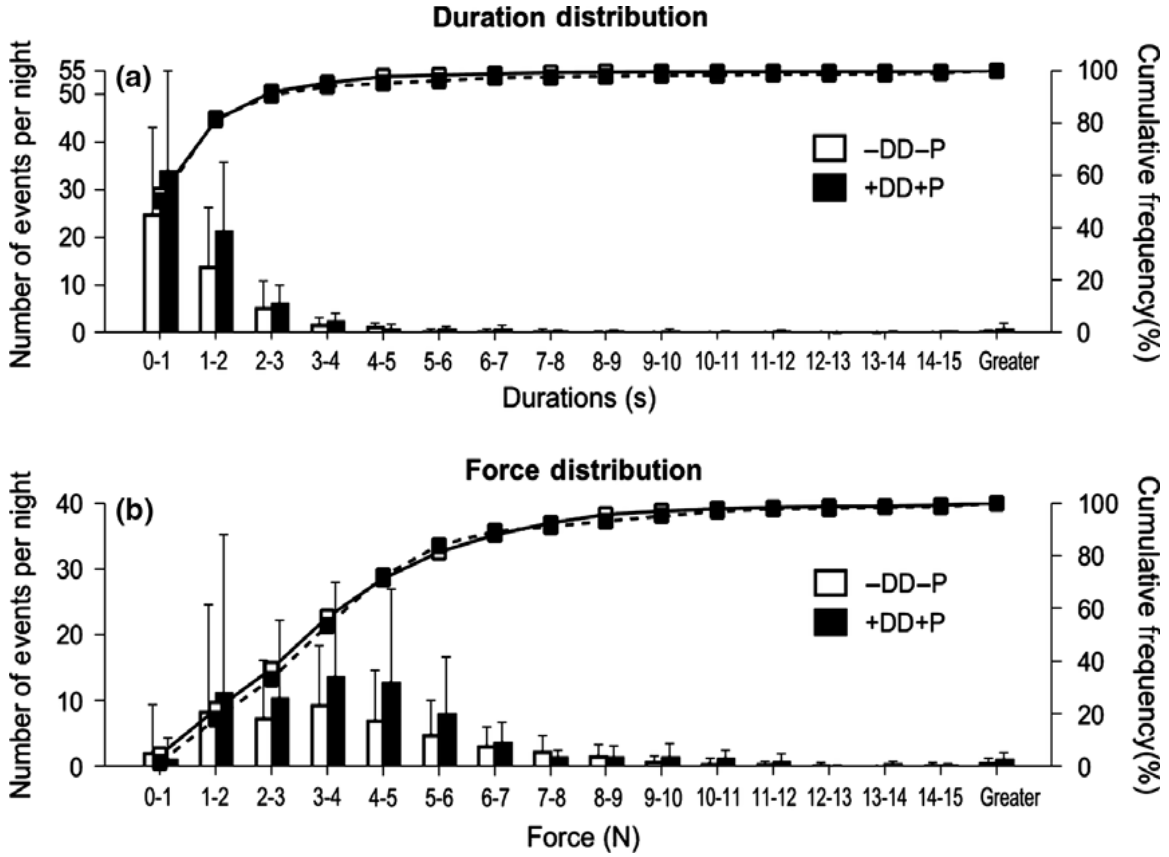

Figure 15. Distribution of number of clench episodes per night.
(a) duration time and (b) bite force. Modified from reference [382]

Discussion

This pilot study developed and validated an automated clench-detection algorithm to investigate if sustained night-time clenching behavior was more prevalent in +DD+P subjects compared to control (-DD-P) subjects. The validated computer algorithm facilitated the detection and characterization of a wide range of sustained clenching behaviors from EMG signals of the anterior temporalis muscle. In all subjects, 95% of the temporalis muscle related clenches had durations less than 4 s, and were associated with bite-forces lower than 10 N. At night, durations of clenching were 1.4-fold longer and temporalis muscle duty factors were 1.8-fold higher in the +DD+P compared to -DD-P group.

The duration of night recording periods of the participating subjects was similar to other reports [188, 196, 199, 201, 202]. The numbers of clenches per night in each diagnostic group were similar to previous reports for bruxer and non-bruxer groups [201]. Mean durations of clenching behavior in the current study was similar to some previously reported data [208] but shorter compared to other reports [188, 196, 199]. The latter differences may be attributed to different EMG amplitude threshold criteria used to define onset and duration of clenching. The results suggested that all subjects generally activated their temporalis muscles at low magnitudes at night, but average duration of activation was longer in +DD+P than -DD-P subjects.

Parafunctional loading of the mandible has been considered to have clinical relevance with respect to development of TMD-related myofascial pain [186]. Until recently, the focus has been on the management of sleep bruxism [383]. However, the

current results are consistent with previous reports [183, 185, 202], which suggested that sleep bruxism is an infrequent phenomenon compared to the predominant activities which were associated with low intensity jaw loading. That is, in the current study, 95% of night-time temporalis activities lasted less than 4 s and were associated with less than 10 N of bite-force. Similarly, a previous study has shown that low intensity jaw loading activities also predominate during awake-state ambulatory EMG recordings of the masticatory muscles, and furthermore, subjects with chronic TMD pain were found to engage more prevalently in these low intensity jaw loading activities compared to control subjects [185].

Sustained clenches of low intensity have been posited to contribute to jaw muscle fatigue and the development myofascial pain [186, 384]. Alternatively, frequent low intensity muscle activity may be a sign of homeostatic dysregulation. This has been demonstrated recently by data from animal models showing that increased activity of the sympathetic nervous system resulted in increased trigeminal motor neuron excitability [385] and glial cell-mediated neuroplasticity of trigeminal ganglia primary afferents [386] and subnucleus caudalis interneurons [387], and showing associations between stress, autonomic nervous system (ANS) dysregulation, and masticatory muscle activity [388]. In humans, increased masticatory muscle activities at low levels during sleep in subjects with self-reported anxiety and somatization compared to control subjects have been reported [36]. These findings support an alternative hypothesis where the relatively frequent low intensity muscle activity shown by the +DD+P subjects may be a sign of ANS dysregulation that promotes central and peripheral neuroplastic changes leading to pain

responses to non-noxious stimuli. Further research is required to address if homeostatic dysregulation is the basis of TMD-related chronic pain, rather than muscle activity per se.

A power analyses of these pilot data determined that 69 subjects per diagnostic group would be required to demonstrate a medium effect size for between-group differences in night-time clenching durations of 1-2 s and 4-5 N of load.

With respect to TMJ disc displacement, frequent and prolonged low intensity jaw loading may have contributed to mechanical fatigue failure of the TMJ disc cartilage. Whether or not this is due to a classical mechanical fatigue mechanism or a combined mechanism which includes compromised disc cell nutrition [86] due to duration of loading, remains to be determined.

From a technical perspective, a challenge remains to detect automatically and characterize fully clenching behaviors solely based on ambulatory EMG recordings. The computer-based algorithm had excellent sensitivity, specificity, and accuracy with very low variation to detect clenching episodes. However, the protocol required the additional calibration steps of determining subject-specific muscle activity per bite force (μV/N) from laboratory EMG recordings to facilitate characterization of the wide range of jaw loads associated with clenching. Other limitations of the current work include the small number of subjects and the lack of inclusion of men. As well, since TMD-related myofascial pain is not limited to the temporalis muscle, an analysis of masseter and lateral pterygoid activities during both day-time and night-time periods would be beneficial in future. It should also be noted that there were no recordings of EMG activities from subjects in the +DD-P and -DD+P diagnostic groups.

In conclusion, temporalis EMG was recorded from two diagnostic groups of women in the laboratory and natural settings and used to develop a computing recognition algorithm, based on statistical amplitude thresholds that automatically and reliably detected sustained teeth clenching behaviors. At night, subjects in both diagnostic groups predominantly used their temporalis muscles for durations less than 4 s and at magnitudes lower than 10 N. Nocturnal temporalis muscle activities detected by the validated algorithm were significantly longer per clench by 1.8-fold and recording time by 1.4-fold in +DD+P compared to -DD-P women.

CHAPTER FOUR: CASE STUDY OF HUMAN TMJ KINEMATICS - NORMAL OPEN-CLOSE MOVEMENT

Introduction

Human TMJ kinematics has the clinical role in evaluating TMJ function, planning pre-surgery treatment sequence and arranging the type of treatments [33], determining the posttreatment results [29, 31] and assessing the facial profile esthetics.

Previously, it has been quantitatively demonstrated that the motion parameters varied between pathological and nonpathological population [18, 213]. Two types of rigid body motion descriptors were widely discussed in literature: the range of motion (ROM) analysis focusing on one or multiple points attached to the rigid body and the axis of rotation (AoR) analysis targeting at the whole rigid body motion. AoR included the helical axis and the instantaneous center of rotation.

The incisor movement range of motion analysis has been adopted in the latest version of diagnostic criteria for TMJ [1]. The AoR is also defined as the transverse horizontal axis around which the mandible rotates in the prosthodontic terms. The profound consequence of erroneous center of rotation axis on the orthognathic surgery was assessed [32, 33, 276-280]. It was demonstrated, through mathematical model simulation, that there was discrepancy in the predicted result and the postoperative outcome if the AoR was incorrectly determined [278].

Biomechanically, the ROM analysis provides information for the dynamics and the contact mechanics study. For instance, the length change of the action line connecting the muscle insertion and the muscle origin will provide the critical information for the muscle modeling in dynamics. Also, The AoR analysis provides information for the correct role

determination of TMJ muscles and ligaments. For instance, incorrect determination of AoR can result in apparently fallacious conclusion over the muscular roles. The AoR has been used for the calculation of muscle moments by determining the lever arm and functional assessment of masticatory muscles. The joint muscle moments of two methods were compared : one was from the stationary hinge axis by connecting the condylar lateral pole and the condylar medial pole while the other method was from the instantaneous AoR from the Reuleaux technique [284]. An increase of the muscle contribution of the masseter muscle and the medial pterygoid muscle was found from the rest potion to the opening position when the stationary hinge axis was employed, contradicting the known function of these masticatory muscles. Therefore, to obtain correct analysis results, it was recommended to use the instantaneous AoR.

The finite helical axis (FHA) method gains its popularity in determining the AoR because it is more accurate than the geometric fitting method [287]. However, one problem with the FHA method is that it is quite sensitive to the noise in the collected data. In the previous study of determining the helical axis during maximum open-close movement [18, 301], two assumptions exist, the minimum angle interval of 1 ˚ and the minimum time interval of 14 ms, to make sure the rotation happens during the specified time interval. The first assumption was investigated and reported that the angle limit was better at 0.7˚ [303]. The second assumption was also noted in a study of the normal open-close movement but the sample size was limited [289].

Indeed, the FHA determined for the max open-close movement (sagittal rotation angle > 20˚) with those two interval variables would be appropriate enough since the

rotation angle is notable for the specified time interval. However, there is a paucity of information on determining the FHA for the habitual open-close movement.

The normal open-close with sagittal rotation angle around 20˚ is also quite important for the TMJ kinematics study since it happens much more frequently during our daily life than the excessive open-close movement. Moreover, it was observed from our EMG analysis that most parafunctional activities, such as bruxism, happened at a very low motion magnitude. So far, only one research article focusing on determination of the helical axis in normal open-close movement has been reported but the sample was limited to only the normal group [289]. Moreover, the individual time interval set in this study makes it impossible to compare the FHA parameters of the patients with those of the controls. Therefore, it is hard to detect the FHA change in patient kinematics during the habitual open-close movement.

The objectives of this study were to determine the kinematics variables for the normal open-close mandibular movement, and to identify the difference of the kinematics for a group of subjects with diagnostic results.

Materials and Methods

Subjects

This study was approved by the Institutional Review Boards of the University at Buffalo and University of Missouri-Kansas City. All participants volunteered for this pilot study. Subjects were recruited at the University at Buffalo School of Dental Medicine and gave informed consent before enrolling.

Cone beam computed tomography (CBCT) and magnetic resonance (MR) images were used with Research Diagnostic Criteria for TMD by calibrated examiners to categorize subjects. Subjects were excluded from participation if they reported a history of rheumatic diseases, presented with CBCT evidence of degenerative joint disease of the TMJ, had multiple missing teeth or large dental restorations, were pregnant, or were unable to perform the variety of tasks in the study protocol. This pilot investigation focused on approximate numbers of age-matched women and men in three diagnostic groups: a nDDnPF group containing 19 healthy female subjects (mean age of 30.96 ± 9.26-year-old, from 23.42 to 55.75), a nDDnPM group containing 18 healthy male subjects (mean age of 29.50 ± 11.14-year-old, from 19.75 to 59.92) and a wDDwPF group containing 16 female subjects with disc displacement or chronic pain (mean age of 33.42 ± 13.27-year-old, from 20.83 to 61.17).

Both sagittal and oblique axial MRI scans were obtained. MRI scans of these discs with higher contrast were used for segmentation and 3D model reconstruction. The voxel size is 0.25 x 0.25 mm. The slice thickness is 2 mm.

The motion trajectories of TMJ mandible were recorded with an optoelectronic jaw tracking system JAWS-3D with a set of active markers at sampling rage of 200 Hz. The method has been described in detail elsewhere [256]. The movement of the left side TMJs and the right TMJs were recorded separately. The subjects were asked to perform a list of 10 times normal open-close movement at their habitual speed. The motion trajectories of one left TMJ from nDDnPF and two right TMJs from wDDwPF subjects were not provided by our collaborators until the time of this manuscript.

Data analysis

The mandibular motion trajectories were transformed into the head coordinate system by a group of sequential transformation: ${}^{H}P(t) = {}^{H}T_{M}(t) * {}^{M}P(t)$.

The condylar lateral pole, the condylar medial pole and the condyle summit were picked up in reconstructed 3D model. These three points were provided as the reference markers in the motion trajectory models and the three-dimensional reconstructed model.

As the proximal segment was used as reference and its motion effect on the distal segment mandibular movement was removed, the joint coordinate system used in this study was the coordinate system built on the fossa bone. The Euler angles, including the flexion-extension, the adduction-abduction, and the axial rotation around the local coordinate system, were determined and plotted visually from the markers motion trajectories at each step. The next step involved separate storage of the data for the opening and closing movements, based on the angle of rotation: the separation of the ten open phases and the ten close cycles for each subject was determined after the rotation in the sagittal plane was extracted.

The range of motion analyzed the translation and rotation displacement of the lateral pole at each time step. The range of motion variables included the maximum rotation in the coronal or frontal plane $\varphi_{frontal\text{-}max}$, the maximum rotation in the horizontal plane $\varphi_{horizontal\text{-}max}$, the maximum rotation angle in the sagittal plane $\varphi_{saggital\text{-}max}$, the rotation magnitude Φ, the maximum translation component along three coordinate axes T_{ap}, T_{si}, and $T_{lateral}$, and T.

The finite helical axis parameters were calculated according the method in [389].To simplify the data analysis, the coordinate system (Figure 11) and the FHA parameters from a previous study [18] were used. The finite helical axis parameters were determined at the time interval of 14 ms and the angle interval of 1˚ for all subjects. For the calculated FHA location at time t_i, the $d_{cp}(t_i)$ was defined as the distance from the condyle lateral pole to the FHA axis. The angles between FHA axis and the x-axis, y-axis, and z-axis at time t_i were defined as θ_x, θ_y, and θ_z. The vibration or smoothness of the FHA axes at time t_i was defined as:

$$\theta_e(t_i) = \sqrt{[\theta_x\,(t_i) - \overline{\theta_x}]^2 + [\theta_y\,(t_i) - \overline{\theta_y}]^2 + [\theta_z\,(t_i) - \overline{\theta_z}]^2}$$

The finite helical axis parameters included the maximum total rotation around the finite helical axis θ_{max}, the maximum translation along the finite helical axis t_{max}, the maximum 3D spatial distance of the finite helical axis to the condylar lateral pole $d_{cp\text{-}max}$, the average orientation angle of the finite helical axis to the coordinate system $\overline{\theta_x}$, $\overline{\theta_y}$, and $\overline{\theta_z}$ and the mean fluctuation of the finite helical axis to the coordinate system $\overline{\theta_e}$.

The ROM and FHA parameters of the left TMJs were compared with those of the right TMJs using paired t-test.

The ROM and FHA parameters of the nDDnPF TMJs were compared with those of the nDDnPM TMJs to see the gender difference. The ROM and FHA parameters of the nDDnPF TMJs were also compared with those of the wDDwPF TMJs to see the difference between the patients and the controls. Both comparisons were performed using independent t-tests.

All the statistics were performed using two-tailed t-test. All differences were considered significant at the level of less than 5%. Analyses were performed using commercially available software (SPSS, IBM SPSS Statistics, Version 23.0, IBM Corp., Armonk, NY; and Stata, StataCor LP. Stata Statistical Software: Release 14, 2015, College Station, TX).

Results

A total of 103 TMJs, including 37 nDDnPF TMJs (19 right and 18 left TMJs), 36 nDDnPM TMJs (18 right and 18 left TMJs), and 30 wDDwPF TMJs (16 right and 14 left TMJs) motion data were analyzed. For the side comparison, 18 subjects from nDDnPF, 18 subjects from nDDnPM and 14 subjects from wDDwPF were selected.

The change of the rotation in three orthogonal anatomy planes and the condyle translation along the three coordinate system axes with respect to the recording time was shown in Figure 16 and Figure 17.

No significant difference of the ROM parameters was found between the left nDDnPF TMJs and the right nDDnPF TMJs. Therefore, the left nDDnPF TMJs and right side nDDnPF TMJs were combined.

No side difference of the ROM parameters was found in nDDnPM. Therefore, the left nDDnPM TMJs and right side nDDnPM TMJs were combined.

No side difference of the ROM parameters was found in wDDwPF. Therefore, the left wDDwPF TMJs and right side wDDwPF TMJs were combined.

The range of motion analysis between healthy female TMJs and healthy male TMJs was listed in Table 11. No significant difference was found in all of the ROM parameters

between female and male healthy subjects. The ROM analysis between female patients and controls was listed in Table 12. The female patients had greater rotation than the controls.

The change of the rotation around the finite helical axis and the translation along the finite helical axis with respect to the time is shown in Figure 18.

No significant difference was found between left and right TMJs in all the FHA parameters for nDDnPFs and nDDnPMs. However, for wDDwPFs, the FHA translation of left TMJ was significantly larger than the right TMJ. The finite helical axis analysis between healthy females and healthy males was listed in Table 13. No significant difference was found among these helical axis parameters.

The finite helical axis analysis between female patients and controls was listed in the Table 14. The rotation angle of 21.81˚ for the patient was significantly larger than the rotation angle of 18.99 ˚ for the controls. The variation of the helical axis orientation of the patient group was significant greater than that of the control group.

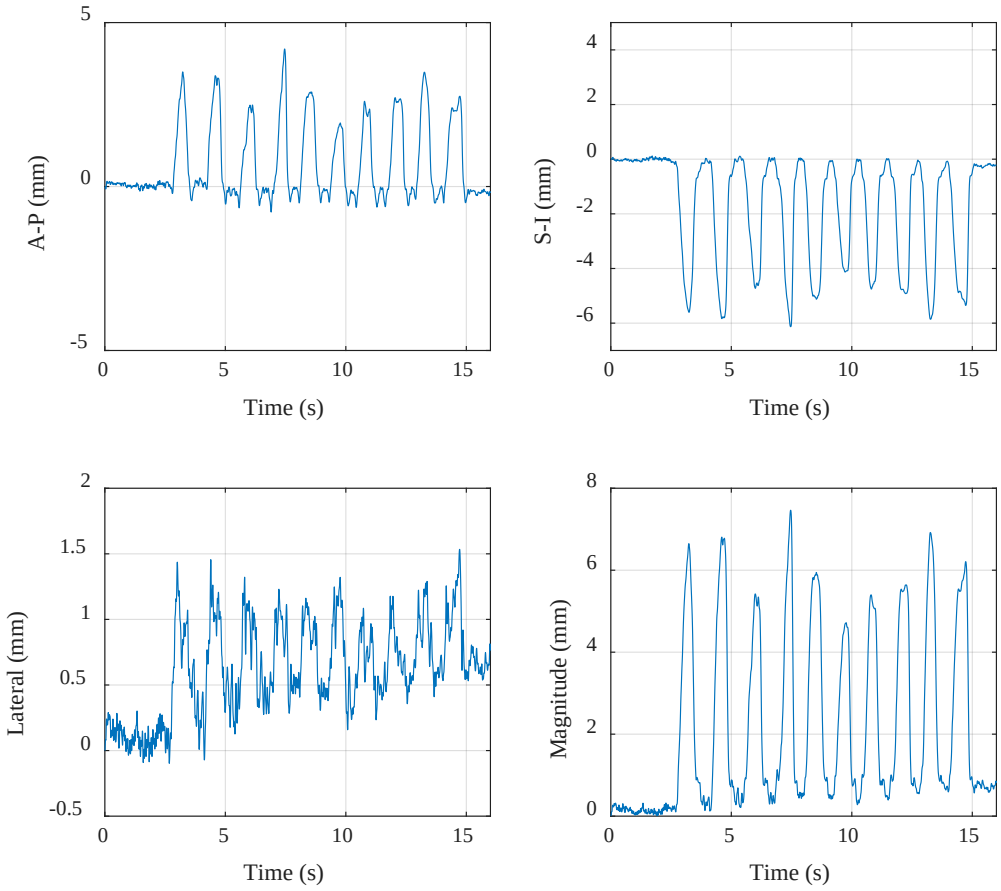

Figure 16. ROM translation of the condyle lateral pole.
The A-P translation is the translation along the anteroposterior direction. The S-I translation is the translation along the superior-inferior direction. The lateral translation is the translation along the left-right direction. The magnitude is the magnitude of the translation vector.

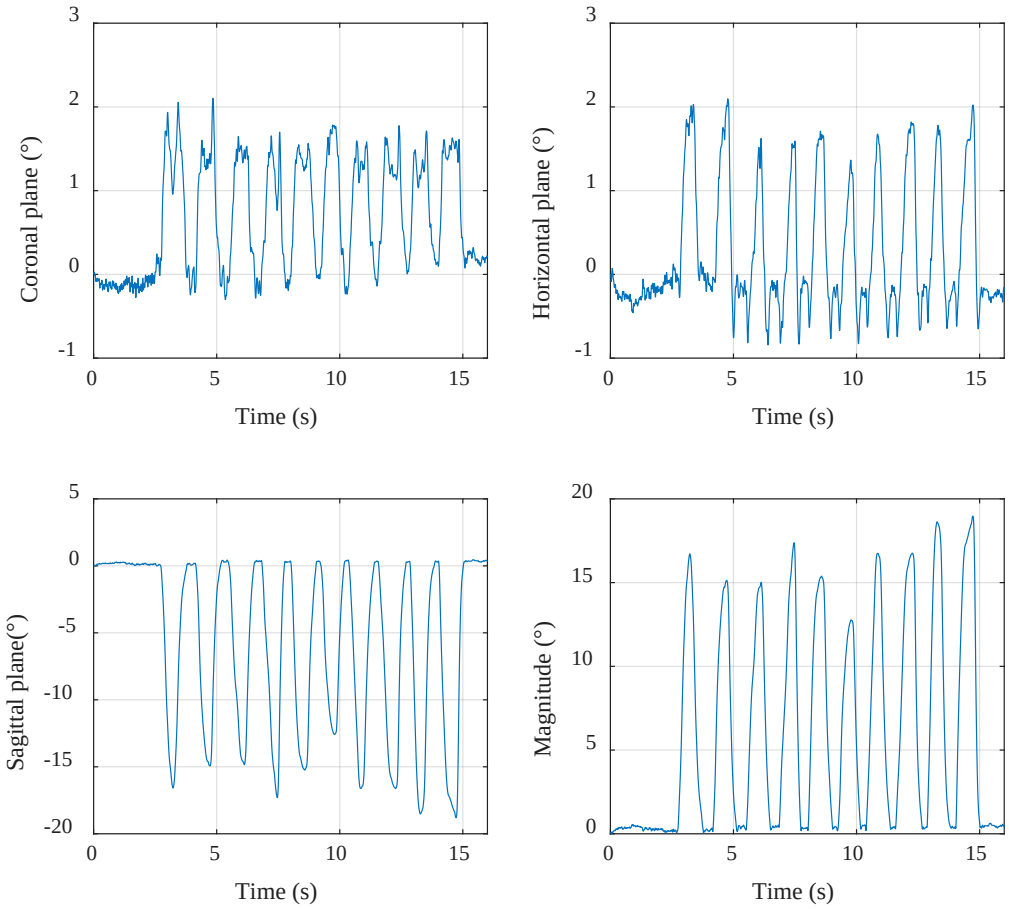

Figure 17. ROM rotation in three anatomical reference planes.
The magnitude is the magnitude of the rotation angle.

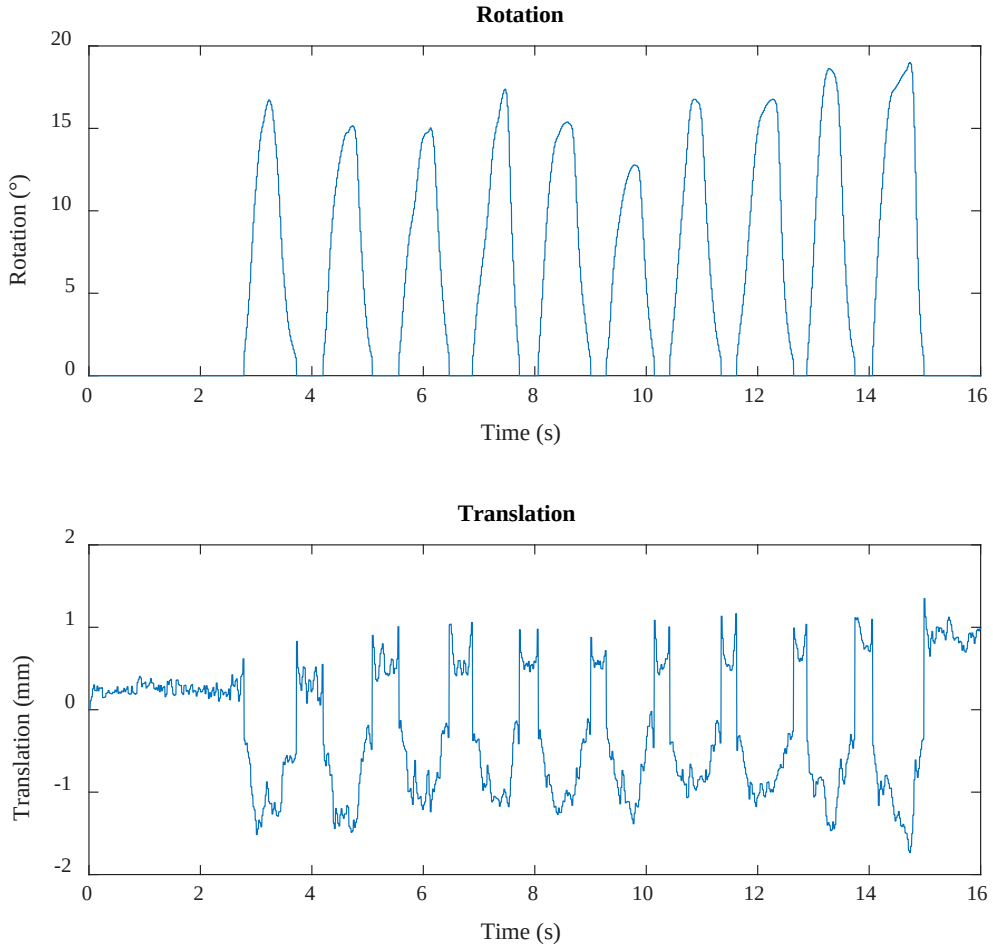

Figure 18. The mandibular translation along and rotation around the finite helical axis during the 10 cycles of normal mouth open-close.

Table 11. ROM parameters between nDDnPF and nDDnPM.
Φ is the rotation amount of the Euler angle. T is the translation.

ROM Parameters	nDDnPF (n = 37)	nDDnPM (n = 36)	p
$\varphi_{frontal\text{-}max}$ (˚)	1.73±0.92	1.78±0.72	0.80
$\varphi_{horizontal\text{-}max}$ (˚)	2.09±1.49	2.26±1.16	0.58
$\varphi_{saggital\text{-}max}$ (˚)	18.88±5.42	18.69±5.54	0.88
Φ (˚)	19.03±5.44	18.82±5.57	0.88
T_{ap} (mm)	7.17±4.12	8.16±4.05	0.30
T_{si} (mm)	7.40±2.81	7.80±2.25	0.50
$T_{lateral}$ (mm)	1.33±0.58	1.43±0.58	0.47
T (mm)	10.60±4.22	11.44±4.10	0.39

Table 12. ROM parameters between nDDnPF and wDDwPF.
Φ is the rotation amount of the Euler angle. T is the translation.

ROM Parameters	nDDnPF (n = 37)	wDDwPF (n = 30)	p
$\varphi_{frontal\text{-}max}$ (˚)	1.73±0.92	2.21±0.92	**0.04**
$\varphi_{horizontal\text{-}max}$ (˚)	2.09±1.49	2.07±0.96	0.96
$\varphi_{saggital\text{-}max}$ (˚)	18.88±5.42	21.62±5.94	**0.05**
Φ (˚)	19.03±5.44	21.82±5.90	**0.05**
T_{ap} (mm)	7.17±4.12	8.01±3.74	0.39
T_{si} (mm)	7.40±2.81	9.57±3.90	**0.01**
$T_{lateral}$ (mm)	1.33±0.58	1.57±0.52	0.08
T (mm)	10.60±4.22	12.82±4.26	**0.04**

Table 13. FHA parameters between nDDnPF and nDDnPM.
θ is the rotation around the helical axis. T is the translation along the helical axis. d_{cp} is the distance between the helical axis and the condyle reference point or the condyle lateral pole. θ_x is the angle between the helical axis and x-axis the coordinate system XYZ. θ_y is the angle between the helical axis and y-axis the coordinate system XYZ. θ_z is the angle between the helical axis and z-axis the coordinate system XYZ. θ_e is the global smoothness of the HA spatial orientation. Please refer to Figure 11 for the coordinate system.

FHA Parameters	nDDnPF(n = 37)	nDDnPM(n = 36)	p
θ_{max} (˚)	18.99±5.48	18.82±5.56	0.89
t_{max} (mm)	1.52±0.56	1.70±0.61	0.19
$d_{cp\text{-}max}$ (mm)	57.0±18.73	61.74±20.11	0.30
$\overline{\theta_x}$ (˚)	84.68±2.92	84.75±2.06	0.90
$\overline{\theta_y}$ (˚)	8.90±4.39	9.02±3.45	0.90
$\overline{\theta_z}$ (˚)	84.09±3.96	83.71±2.98	0.65
$\overline{\theta_e}$ (˚)	3.91±1.74	4.64±1.63	0.07

Table 14. FHA parameters between nDDnPF and wDDwPF.
θ is the rotation around the helical axis. T is the translation along the helical axis. d_{cp} is the distance between the helical axis and the condyle reference point or the condyle lateral pole. θ_x is the angle between the helical axis and x-axis the coordinate system XYZ. θ_y is the angle between the helical axis and y-axis the coordinate system XYZ. θ_z is the angle between the helical axis and z-axis the coordinate system XYZ. θ_e is the global fluctuation of the HA spatial orientation. Please refer to Figure 11 for the coordinate system.

FHA Parameters	nDDnPF(n = 37)	wDDwPF(n = 30)	p
θ_{max} (˚)	18.99±5.48	21.81±5.90	**0.05**
t_{max} (mm)	1.52±0.56	1.52±0.60	0.95
$d_{cp\text{-}max}$ (mm)	57.0±18.73	63.47±18.72	0.16
$\overline{\theta_x}$ (˚)	84.68±2.92	83.64±2.54	0.13
$\overline{\theta_y}$ (˚)	8.90±4.39	10.29±4.10	0.19
$\overline{\theta_z}$ (˚)	84.09±3.96	83.34±3.40	0.42
$\overline{\theta_e}$ (˚)	3.91±1.74	4.75±1.69	**0.05**

Discussion

The most frequent oral behavior during our normal daily life is normal open-close related activities. The functional assessment of this type of activities is of necessity for the orthognathic surgery and orthodontics surgery to evaluate the mandibular function after the surgery.

In biomechanics field, the ROM analysis for a point could provide the spatial position information for dynamics study. The length change of two points with respect to the mandibular movement provides crucial information for the dynamics. For instance, the length change of the muscle insertion and the muscle origin is one of the vital parameter for the muscle modeling. The determination of AoR is important for the identifying the role for each masticatory muscle from the computation of the moment during the mastication and other types of oral activities.

This study compared the TMJ ROM and FHA parameters for a total of 103 TMJs from three types of diagnostic groups. ROM analysis provides motion description for one or several points, which is necessary for the dynamics study and diagnosis. However, the single point motion analysis is severely affected by the choice of the reference landmark and the choice of the anatomical coordinate system. The FHA method has no such restriction, but it is hard to interpret for clinicians and its application must relate to the anatomical reference point such as the condyle lateral pole in this study.

No significant differences of the ROM parameters were found between the left TMJs and the right TMJs of any the three diagnostic groups. The comparison of the ROM parameters between the group nDDnPF and the group nDDnPM did not show any

significant gender difference. The comparison of ROM parameters between nDDnPFs and wDDwPFs demonstrated that the rotation was significantly different between the patients and the controls. The patients had more rotation than the controls. The major difference came from the frontal planar rotation as well as the sagittal rotation. The translation also differed between the patients and the controls: the patients had larger displacement of the lateral pole. The major difference came from the superior-inferior movement.

No significant differences of the FHA parameters were found between the left TMJs and the right TMJs for the group nDDnPF and the group nDDnPM. However, significant difference was found between the left TMJs and the right TMJs in patient group. This unbalanced motion pattern between the left and the right TMJs cannot be detected using the ROM analysis. The possible explanation is that the FHA analysis examines the motion of the mandibular as a whole rigid body while the ROM analysis depends on the choice of the selected reference point. Lower diagnostic results would be possible depending on the selection of the ROM reference point on TMJ [313-315].

The comparison of the FHA parameters between the nDDnPF group and the nDDnPM group did not show any significant gender difference, either. The female rotation of axis vibrated less than the male group. The wDDwPF group rotated with greater angle than the nDDnPF group. The motion path of the patients was significantly more irregular than the controls since the vibration was significantly larger in patients. It was found [18] that the patients with clicking joint had significantly larger rotation angle and much more fluctuation with respect to the anatomical coordinate system. The center of axis calculated from FHA provides quantitative parameters over the stability evaluation of the mandibular

motion. It is therefore concluded that the patients have less motion stability than the asymptotic subjects and that the patients have larger spatial motion.

The significant difference in ROM translation between the nDDnPF and the wDDwPF group was not observed in FHA translation. Since the ROM translation analysis severely depends on the selection of reference point and lower diagnostic results would be possible depending on the selection of the reference point on TMJ [313-315], it is preferable to use the FHA translation for diagnosis.

Compared to the maximum open-close mouth movement, the kinematics study of the habitual open-close mouth movement has its advantage since it happens more frequently during our daily life. However, the maximum open-close mouth movement provides the extent to which most of the joints with TMJ disorders could not come up. Another advantage of the maximum open-close mouth movement is that it has high repeatability for the same person although exercise will change this limit. Thus, it is preferred to use the maximum open-close oral activities for the TMJ kinematics study.

In the current study, large variation was observed in different cycles of the same motion recording for the same participant. Variation also was found between different subjects in a group. These variations reduced the diagnosis capability of most kinematics parameters. The oral task of the habitual open-close mouth movement partly explained the difference since each subject has their own understanding about the extent to which the mouth should open during the habitual open-close mouth movement.

CHAPTER FIVE: CASE STUDY OF HUMAN TMJ KINEMATICS - A CUSTOMIZED MOTION-EMG-BITEFORCE SIMUTANEOUS DATA COLLECTION SYSTE

Introduction

The functional assessment of the mandibular movement and muscle activities the clinical role in evaluating TMJ function, planning pre-surgery treatment sequence and arranging the type of treatments [33], determining the posttreatment results [29, 31] and assessing the facial profile esthetics.

In the past, the continuous development in advanced mechanical, electronic and optical high-technologies have facilitated the development of the scientific and objective diagnosis. Several data recording systems, for both the research purpose and the industrial use, have been reported for the kinematics evaluation. The commonly used systems include the mechanical devices, the photographic methods, the stereographic, roentgenographic methods, the electronic and telemetric methods, the magnetometry method (e.g., kinesiograph and sirognathograph), and the optoelectrical methods. Of these devices, the magnetometry method-based and optoelectrical method-based devices are promising since they meet the basic clinical requirements for a tracking device: reproducible, non-invasive, no interference or non-obstructive to the natural jaw movement, free head movement without fixation during the whole recording, simplified design, ability to perform distinct types of oral tasks including empty motion and mastication tasks, ability to integrate with other data collection system and best user experience.

Previously, the distinction of the kinematics variables has been identified between the patients with TMJ disorders and the controls. It was demonstrated that the motion

pattern of patients with TMJ disorders differed from controls in the rotation around and the translation along the FHA [18]. In addition, joint function was found to be more symmetric after the skeletal malocclusion surgery by using a kinematics assessment tool [213]. It was found that the patients with disc displacement with reduction produced less synchronized translation pattern compared to the controls and that the patients had grater asymmetric lateral movement.

However, their optoelectrical motion tracking devices either are designed with too much complexity for the necessity of the image-tracking markers registration (Figure 6) or do not consider imaging markers (Figure 8). The imaging consideration is of necessity if the motion of any mandibular point is required. Unfortunately, the complex and heavy design will inevitably interfere the natural mouth movement. Their device is complex because they used two separate sets of markers: one is set for imaging and the other is set for motion tracking. Furthermore, their tracking system's usage of active marker required the electricity cables.

To study the intra-articular space in "CHAPTER SIX: CASE STUDY OF HUMAN TMJ CONTACT AREA in TMJ INTRA-ARTICULAR SPACE" and the glucose diffusion in the TMJ disc, we will have to obtain image to reconstruct 3D model. In this study, therefore, we will improve the previous design by applying concentric mate to these two independent sets of markers. In addition, we will synchronize the EMG and motion tracking data collation systems by creating a customized mouse.

Upon completing the design of this device, we will have our customized data recording device for the clinical diagnosis system development. The collected

synchronized data will also provide critical information for the following dynamics and nutrition study.

Materials and Methods

Subjects

This study was approved by the Institutional Review Boards of the Medical University of South Carolina (MUSC). All participants volunteered for all aspects of this pilot study. Subjects were recruited at the Medical University of South Carolina School of Dental Medicine and gave informed consent before enrolling. The inclusion criteria included: the study participants have a symmetric occlusion determined by bilateral positions of the dentition and muscles of mastication, assessed by faculty in the Department of Oral and Maxillofacial Surgery at MUSC in accordance with the DC/TMD [1]. The study participants must have all canine teeth, first molars, and lateral and central incisors. The study participants must be 18 years or older. The exclusion criteria included: subjects with dental medical history outside of routine dental procedures; subjects with heavily restored first molars, canines, or incisors which may be affected by biting force and motion of custom frameworks during the experiment; subjects with any medical history including musculoskeletal disease (e.g. fibromyalgia, muscular dystrophy), evidence of degenerative osseous changes, or trauma to the TMJ or associated structures; women who are pregnant; subjects who have illiteracy or inability to speak the English language, or inability to follow auditory and visual commands; subjects with anatomic parameters placing the subject beyond the physical limits of the research devices and/or materials; subjects with previous contact hypersensitivity to alginate; subjects with any self-reported jaw clicking, popping

or pain. All collected data will be de-identified. Five male subjects with mean age of 30-year-old participated in this study.

Precision of the tracking system

An optoelectrical commercial tracking system (Figure 19h) with 3 cameras (s250e; NaturalPoint Inc., Corvallis, OR, USA Figure 19b) and a computerized control software was used to monitor the movement of two rigid marker frames: one marker frame headset is attached to upper teeth to record the head movement and the other marker frame is attached to lower teeth to record the mandibular movement. Each marker frame has four markers: at least three markers are required to build a rigid body in the tracking system, while more than 4 markers will cause interference in CBCT image since the space for placing the marker is relatively crowded for more than 4 makers. Three rings of 96 LEDs with 850 nm infrared light were placed around the lens and illuminated the field of view. Retroreflective material on the eight markers of the two marker frames will reflect the infrared light back to the lens (Figure 19g) so that the two-dimensional coordinate of each marker in each camera could be determined. Other objects in the field of view have no such strong reflective property as those markers. The camera field of view is 1.27 m x 1.27 m. The camera resolution is 0.7 MP and accuracy is sub-millimeter. During the processing of recording, capturing frame rate is 200 fps. The parameters of the camera exposure, the frame rate, the resolution, the image processing mode, and the LED intensity could be interactively adjusted in the computer software. An 8-port gigabit poE switch was used to transfer the data from camera to a computer-controlled software and synchronize the three cameras.

To determine the spatial relative positions and orientations of the three cameras, a calibration process has to be performed. A plastic bar with three retroreflective markers of which the relative positions are well measured ahead using calipers is utilized for the camera calibration. The plastic bar moved in a volume where the tracking target will happen. After the calibration, the global coordinate system will be built.

Before the experiment, we evaluated the noise level or the accuracy of our tracking system. We used a coordinate measuring device for the static measurement test in which the measurement was taken after the marker was moved to the targeted position. The hemispherical reflective marker of 3 mm was adopted for the test. A right triangle frame with three markers located at each vertex was constructed for the test: one leg length was 40 mm and the other leg length was 80 mm. The global coordinate system was set using the constructed triangle frame. Then the triangle frame was to well-defined positions: static at t = 0.0 s, a translation of 30 mm along one direction and 30 mm along another direction at t = 39.23 s and a translation of -20 mm along one direction and -20 mm along another direction t = 110.36 s. We then read the spatial coordinates of those markers in camera system and calculated the deviation from their desired coordinates. The distance from between the three cameras and the coordinate measuring device was set as 2000 mm. The distance between two cameras was 500 mm.

Experiment design

The whole motion-EMG-BF data collection system (Figure 19h) is consisted of (i) CBCT imaging device (Planmeca ProMax 3D Max; Planmeca USA, Roselle, IL, USA. Figure 19a), (ii) 3-camera motion tracking system (s250e; NaturalPoint Inc., Corvallis, OR,

USA. Figure 19b), (iii) EMG data acquisition system (DLK900 DataLINK; Biometrics Ltd., Newport, UK. Figure 19c), (iv)bite force measurement system (Flexforce; Tekscan Inc., Boston, MA, USA. Figure 20), (v)a customized mouse (Figure 19f), and (vi)their corresponding software.

All subjects follow the three-step experiment procedure: the clinical examination, the CBCT imaging, and the laboratory visit.

During the clinical examination step, the written informed consent and the Health Insurance and Portability and Accountability Act form will be signed from each subject. Cone beam computed tomography (CBCT) and magnetic resonance (MR) images will be used with Research Diagnostic Criteria for TMD by calibrated examiners to determine the TMJ health condition. Maxillary and Mandibular dental impressions will be obtained by licensed personnel. To determine the position of the CBCT imaging markers in the motion tracking system and to ensure that the position of these markers keeps the same among different experiment sessions, it is necessary to find a reference position on the joint or the teeth rigidly connected to the TMJ joint. An impression model is made by the dentist and the invisaligns for the lower and upper teeth were designed to faithfully fit the teeth.

For the CBCT imaging visit, the CBCT image of the participants with invisaligns will be performed by a clinician.

For the laboratory visit, the incisor range of motion will be measured using a ruler. The measurement items include the maximum inter-incisal opening capacity, the left-right lateral movement capacity, and the protrusion-retrusion capacity.

The left and right temporalis and masseter muscle activities during a series of oral tasks for five subjects will be collected using four channels of an eight-channel surface EMG device DLK900 with active probe SX230-1000 wired sensor from Biometrics Ltd. Up to 24 channels will be created if required.

We will use the recommended EMG settings: 3v dc channel sensitivity, 1000 Hz sampling rate, 4950 mV excitation output, and full scale of 3mV (DLK900 DataLINK; Biometrics Ltd., Newport, UK). The EMG sensor parameters are: 1000 gain, bandwidth 20-460 Hz, Noise < 5 μV, the common-mode rejection ratio >96 dB, input impedance > 1015 ohms and weight 5g (SX230-1000; Biometrics Ltd., Newport, UK). We will use sampling rate of 1000 Hz because the EMG signal will not be gained at a higher sampling rate.

This EMG device is portable and allows long term recording of more than 7 hours. In addition, this device permits programming of digital channels so that we can synchronize it with the motion tracking device on hardware level. Finally, this device also provides the DataLINK application interface functions capability to collect data using our own customized software so that we can synchronize it with the motion tracking device on software level.

The skin will be cleaned with isopropyl alcohol or water to reduce resistance and dried before attaching EMG electrodes. The centroids of the right and left masseter and anterior temporalis muscles will be determined by palpation, and then surface electrodes are affixed and pressed by hand. Similarly, a fifth single electrode is attached to the left or right wrist and wrapped by tape as a ground. The subjects are required to perform a list of

oral tasks including five maximum open-close, five protrusion and five retrusion, five lateral movement, five normal clench, and five normal open-close, at their own voluntary speed.

CBCT image of the whole head including mandible and temporal bone at maximum intercuspal position from five subjects with tracking and image markers will be obtained using Planmeca ProMax 3D Max at MUSC dental school (Figure 19a). The maximum field of view is ø230x260 mm and the voxel size is 0.4 x 0.4 x 0.4. Motion data will be collected using optiTrack tracking device and three S250e cameras (Figure 19b) from NaturalPoint Inc.. We will use this tracking system with passive marker because it reduces the disturbance to the user by discarding the wires required in active marker-based tracking system. Finally, bite force data will be collected using bite force sensor of Flexforce.

Before the data collection process, we will have to: 1) integrate the CBCT image markers with tracking markers so that we can determine their relative relationship without the assistance of the extra devices; and 2) synchronize the EMG and motion data collection system so that we could collect these two sets of data more efficiently.

(a) CBCT

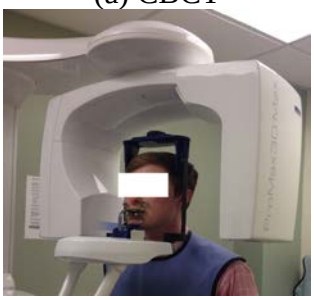

(b) Tracking camera

(c) EMG

(d) Customized concentric marker

(e) Data collection

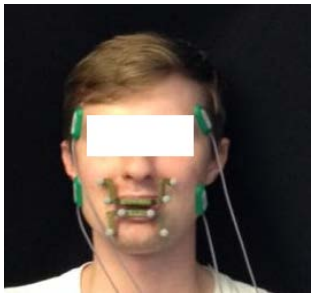

(f) Customized marker

(g) Marker frame

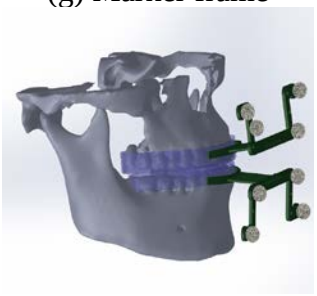

(h) Whole system

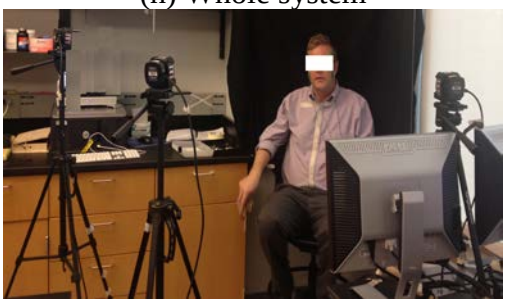

Figure 19. Data collection system of imaging, motion, EMG and bite force.
(a) Planmeca ProMax 3D Max. (b) S250e camera. (c) Biometrics EMG base unit and subject unit. (d) Section view of a customized concentric marker for both CBCT and Optitracking. (e) Data collection. (f) Mouse used for synchronization of EMG with motion. (g) Marker frame. (h) Overview of the whole data collection system.

Marker integration

A customized marker that serve as a landmark in both imaging system and motion tracking system was designed (Figure 19d). The method of determining the 3D relative space relationship between CBCT markers and tracking markers is to coin this special marker that has multiple purposes: begin with a plastic bead connected with a wooden stick, we will firstly roughen the surface of the plastic bead (the most inner layer in gray color) with sandpaper so as to increase its attachment capability, then we will uniformly coat this rough surface with about 0.5 mm barium sulfate emulsion layer (the middle layer in white color) which is visible in CBCT imaging and also allows the attachment of the retroreflective microspheres. After that, a 0.5 mm layer of retroreflective microspheres (the outmost layer in mixed color) for motion tracking device will be evenly sprayed on top of the barium sulfate emulsion layer. Then, the customized marker will be dried naturally and assembled on marker frame. Finally, the whole frame will be mounted to a self-made dental guard or splint (light blue part in Figure 19g) for both CBCT imaging and motion tracking usage.

Data synchronization

To synchronize motion tracking data collection device with EMG data collection device (Figure 19c), we will program one of the two available digital channels on the side of subject unit because it can be used as an event marker creator: a voltage input of +5V is equivalent to logic 1, and a voltage input of +0V is equivalent to logic 0. Therefore, to provide the digital input channel with a +5V triggering voltage, we will customize the control mouse (Figure 19f) of tracking system by adding a switch button, two power cables

and a diode indicator. In addition, the input pin and output pin of left button will be welded to the two power cables: one will be used for the electricity input and the other will be used for electricity output. The switch will control the on/off of mouse left button function. When the switch is turned off, the diode indicator will be turned off and it is a normal mouse: clicking left mouse has no extra function. When the switch is turned on, the diode indicator will be turned on and it is an armed mouse with the function to provide digital channel with a voltage of +5v when the left button is clicked.

Experiment tasks

The whole data collection and data analysis procedure is demonstrated in Figure 20. The subjects are seated upright approximately 1 m in front of camera in front of camera with the head unsupported to allow the freedom of head movement (Figure 19e and Figure 19h).

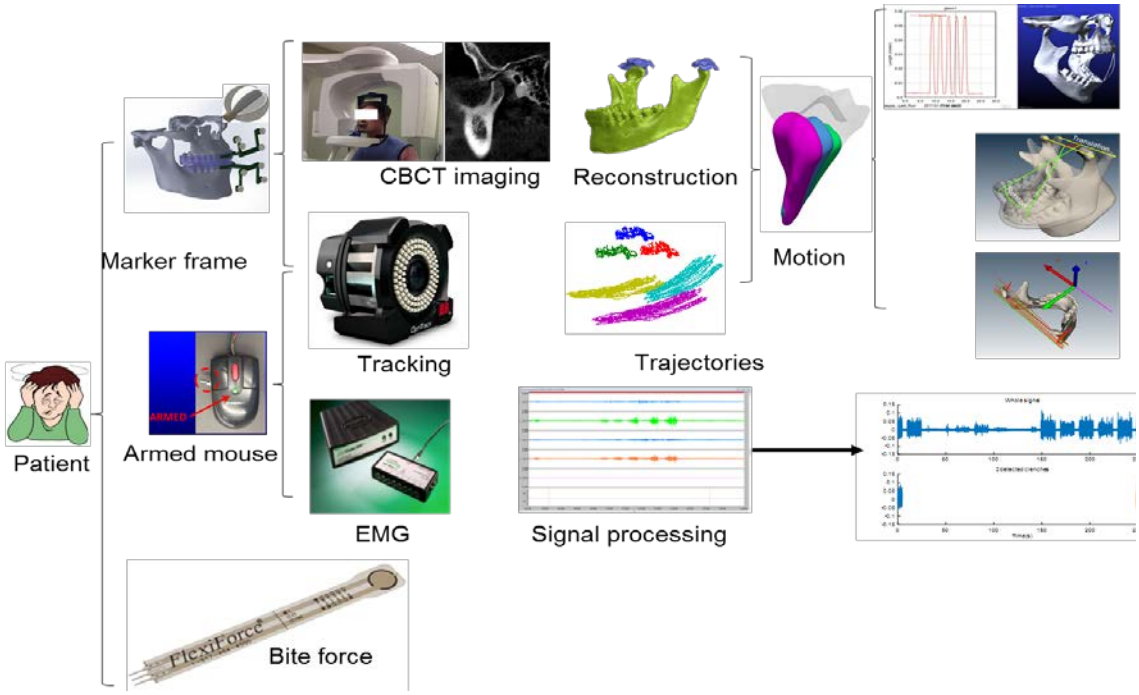

(a)

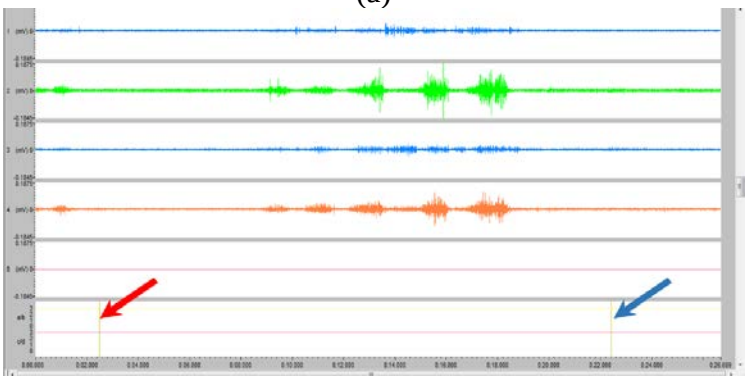

(b)

Figure 20. The data collection and analysis procedure of multiple data types.
(a) Four types of data, including image, tracking, EMG, and bite force data, are collected by the system. The image marker is integrated into the motion tracking marker by superimposing the tracking marker material on top of the CBCT marker material. Therefore, the marker is visible in both the tracking system and the imaging system. The self-designed mouse synchronizes the EMG data with the tracking data. (b) The EMG device is firstly turned on to record 4-channel muscle activities (the top four channels). With the clicking mouse in the tracking system, a current will be generated through the mouse and will be captured in the specific channel 8 of the EMG recording device. The red arrow stands for mouse clicking at the beginning of the motion tracking and the blue arrow stands for the mouse clicking at the end of the motion tracking.

The five pilot subjects follow the following Motion-EMG-BF fifteen-step experiment protocol: 1. Calibrate camera using self-made calibration tools to determine the 3D spatial pose relationship between the three cameras. 2. The global coordinate system for motion tracking system was then established. 3. Clean the lower and upper invisaligns with isopropyl alcohol and water. 4. Dry the invisaligns with abrasive paper and attach the invisaligns to lower and upper teeth tightly. 5. Allow the user to adjust the position of the two invisaligns to the closest position in CBCT. 6. Define the rigid body 'mandible' for lower invisalign and rigid body 'Fossa' for upper invisalgin when the teeth are in maximum intercuspal position. 7. Clean the subjects' skin surface with isopropyl alcohol or water to reduce resistance and dry it with abrasive paper before attaching EMG electrodes. 8. Locate the centroids of the right and left masseter and anterior temporalis muscles by palpation, and then affix and press surface electrodes by hand: electrode with label 1 will be attached and aligned to left anterior temporalis fiber, electrode with label 2 will be attached and aligned to left anterior masseter fiber, electrode 3 will be attached and aligned to right anterior temporalis fiber, and electrode 4 will be attached and aligned to right anterior masseter fiber. Do not attach the other end of these four electrodes to EMG subject unit. These four sets of electrodes are bipolar surface disc electrodes. The margin of these four sets of electrodes was secured with double-sided gel bought from the manufacturer. 9. Similarly, a fifth electrode with a single surface disc will be attached to the left or right wrist and wrapped by tape as a ground. 10. The wrapping around wrist using tape prevents electrode detachment from the wrist and ensures the continues tight contact during the experiment. 11. Attach the fifth electrode to the EMG subject unit. Set up biometrics EMG

software interface parameters: 1000 Hz. 12. Insert the four electrodes for muscles into subject unit. Test EMG device to make sure the sound connection. The raw EMG signals will be amplified and passed to a computer software for live recording and offline analysis. 13. The user will be required to perform a list of oral tasks at the voluntary speed: five times consecutive max open-close, 5 times consecutive protrusion and retrusion, 5 times consecutive lateral movements, 5 times consecutive rhythmic clench, 5 times normal consecutive habitual open close, bite soft rubber, bite peanut, force sensor calibration, 5 times bite on the force sensor as hard as possible using right molar, 5 times bite on the force sensor as hard as possible using left molar, 5 times bite on skittle using right molar, and 5 times bite on skittle using left molar. 14. Record the start and end time for each oral task. 15. EMG and motion data will be saved and exported.

The five subjects' data of five times max open-close, 5 times protrusion and retrusion, 5 times lateral movements, 5 times rhythmic clench and 5 times normal open close will be extracted and analyzed. The motion data will be superimposed on 3D model reconstructed from CBCT image. The interincisal and mandibular ROM will be computed. The finite helical axis and its parameters with respect to movement will be calculated.

Motion data analysis

Motion data trajectory smoothing methods: data was smoothed using a second order Butterworth filter with cut off frequency of 8 hz.

The mandibular range of motion analysis included the maximum incisor point distance (IP) during the maximum open-close (maximum o-c IP or IP MMO), the protrusion (protrusion IP), and the lateral movement (lateral IP). The IP components along

three orthogonal axes were also reported (IP caudal, IP dorsal, and IP lateral). In addition, the mandibular rotation angle and its three components in three orthogonal planes were calculated (sagittal angle, frontal angle, and horizontal angle). The displacement of the left condyle lateral pole (lCRP caudal, lCRP dorsal, and lCRP lateral) and the right condyle lateral pole (rCRP caudal, rCRP dorsal, and rCRP lateral) was also reported. The incisal distance was calculated with respect to the movement period. The boundaries of each maximum open-close cycle were determined after the interincisal distance was calculated. The individual opening-closing cycle was separated into 10 incremental parts at 10% increments of the 3D incisal distance to evaluate the mandibular rotation change with respect to the percentage of the incisor distance.

To evaluate the condyle translation, a middle point of the two condyle lateral points was selected as a reference landmark. The motion trajectory of the condyle middle point was calculated. The mandibular length in the sagittal plane is the distance from the condyle middle point to the mandibular incisor. By defining the translation of the condyle middle point (T, unit: mm), mandibular length (L, unit: mm) and the sagittal rotation of the whole mandible (R, unit: radian), the contribution of rotation during the whole mandibular maximum open-close process was defined (Figure 21) and reported for all subjects.

$$Percentage\ of\ rotation = \frac{R * L}{T + R * L}$$

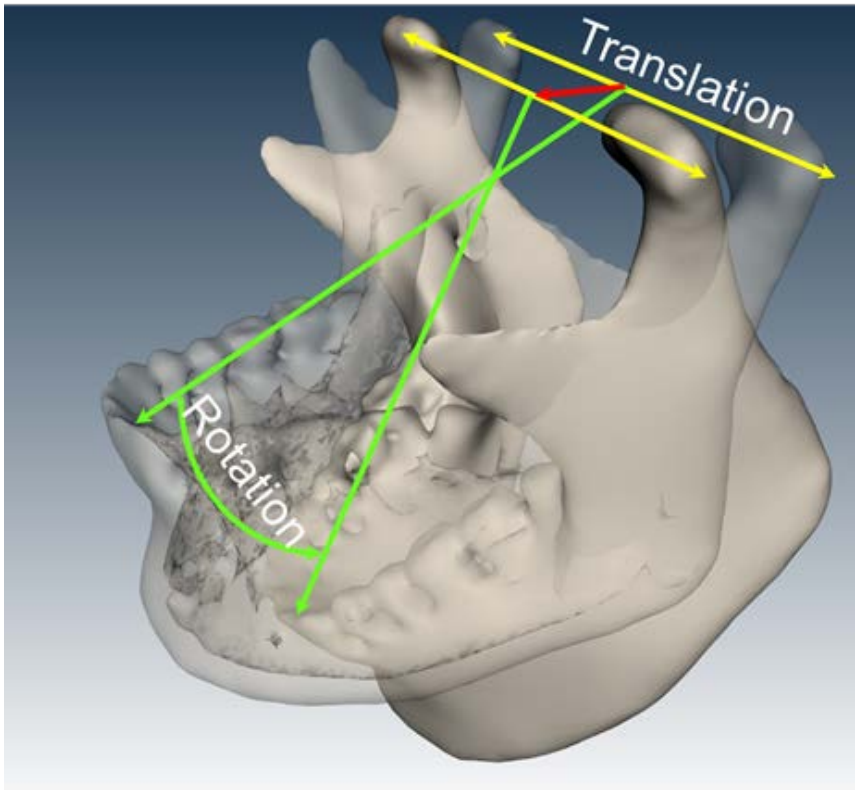

Figure 21. ROM analysis definition.
The condylar middle point is determined as the middle point of the two condyle lateral poles. Translation is defined as the displacement of the middle point. The mandibular length in the sagittal plane is the distance from the condyle middle point to the mandibular incisor. By defining the translation of the condyle middle point (T, unit: mm), mandibular length (L, unit: mm) and the sagittal rotation of the whole mandible (R, unit: radian), the contribution of rotation during the whole mandibular maximum open-close process was defined as (R*L)/(T+R*L).

The mandibular axis of rotation was calculated using the finite helical axis method. The finite helical axis parameters were determined at the time interval of 14 ms and the angle interval of 1˚ for all subjects. The finite helical axis parameters included the maximum total rotation around the finite helical axis θ_{max}, the maximum translation along the finite helical axis T_{max}, the maximum 3D spatial distance of the finite helical axis to the condylar lateral pole $d_{CP\text{-}max}$, the average orientation angle of the finite helical axis to the coordinate system $\overline{\theta_x}$, $\overline{\theta_y}$, and $\overline{\theta_z}$and the fluctuation of the finite helical axis to the coordinate system θ_e.

Software development

A software to compute and demonstrate the motion and the rotation of axis was developed. It also had the function to calculate and display the contact area for "CHAPTER SIX: CASE STUDY OF HUMAN TMJ CONTACT AREA in TMJ INTRA-ARTICULAR SPACE" with the mandibular motion. The results of the computation were validated in the commercially available software (Solidworks, Version 2017-2018, Dassault Systèmes SolidWorks Corp., Waltham, MA; and Adams, Version 2017, MSC software Corp., Newport Beach, CA) and academic opensource software OpenSim.

Results

A data collection system was designed to gather muscle EMG signal, jaw motion tracking data, TMJ imaging data and the bite force data. A new type of markers for both the imaging system and the motion tracking system was invented. The procedure of the data collection system was shown in Figure 20. The precision of the tracking system was estimated by the manufacturer to be less than 1 mm and the angular accuracy was 0.16˚.

Our measurement showed that the edge length deviation was within the range of 1 mm with the distance of 2 m.

The range of motion analysis result for each subject was listed in Table 15. The interincisal point (IP) distance during the maximum opening was 51.9±6.0 mm, close to the measure that was obtained by caliper determinations. The IP distance during protrusion was 8.2±2.9 mm. The IP distance during lateral movement was 11.3±1.7 mm. The contribution of rotation to total displacement in maximum open-close activity was calculated and plotted in Figure 22.

The FHA was calculated and displayed in Figure 23 and Figure 24. The helical axes were parallel to each other during the mandibular movement. It was located at the posterior and inferior of the condyle hinge axis at the initial stage and moved forward together with the mandibular movement. The FHA parameters, including maximum rotation θ_{max}, maximum translation T_{max}, left and right distance from condylar reference points to finite helical axis $d_{CP\text{-}max}$, relative orientation of FHA to anatomical coordinate system $\overline{\theta_x}$, $\overline{\theta_y}$, and $\overline{\theta_z}$, and global fluctuation $\overline{\theta_e}$ of the spatial orientation of FHA during the maximum open-close movement were calculated for each subject (Table 16 and Figure 24). The averaged maximum rotation was 36.0 ± 5.4 degree. The maximum translation was 1.8 ± 0.12 mm. The FHA to left condylar reference point distance was 66.9 ± 48.8 mm. The FHA to right condylar reference point distance was 72.4 ± 26.2 mm. The large variations came from P004. The mandible oriented almost horizontally ($\overline{\theta_x}$ = 92.5 ± 2.8°, $\overline{\theta_y}$= 4.1 ± 1.3°, and $\overline{\theta_z}$= 89.9 ± 1.9°).

Table 15. ROM analysis of maximum open-close for five subjects.
IP is the interincisal point. L is the left side. R is the right side. MMO is the maximum mouth opening. CRP is the condyle reference point.

	P001	P002	P003	P004	P005	Mean ± std
Max o-c IP (mm)	54.2	57.4	56.3	48.8	42.9	51.9±6.0
Protrusion IP (mm)	10.2	10.9	8.9	7.3	3.7	8.2±2.9
Lateral IP (mm)	12.4	13.1	9.6	9.4	11.9	11.3±1.7
IP MMO (mm)	54.2	57.4	56.3	48.8	42.9	51.9±6.0
IP caudal (mm)	46.7	47.2	49.4	43.7	37.6	44.9±4.6
IP dorsal (mm)	27.5	32.5	27.4	21.9	20.6	26.0±4.8
IP lateral (mm)	1.0	3.6	3.7	3.2	2.3	2.8±1.1
Sagittal angle (˚)	39.5	40.9	38.8	31.9	28.7	36.0±5.4
Frontal angle (˚)	2.4	1.7	4.6	4.3	3.1	3.2±1.2
Horizontal angle (˚)	0.0	7.1	3.9	3.0	1.2	3.1±2.7
lCRP caudal (mm)	2.5	4.5	5.8	9.2	5.8	5.6±2.5
lCRP ventral (mm)	16.5	16.9	21.1	18.2	12.1	17.0±3.2
lCRP lateral (mm)	2.6	1.4	3.0	1.9	1.5	2.1±0.7
rCRP caudal (mm)	2.6	8.8	6.0	9.3	2.9	5.9±3.1
rCRP ventral (mm)	15.0	17.4	19.6	16.9	12.4	16.3±2.7
rCRP lateral (mm)	2.6	1.6	2.9	1.8	1.4	2.1±0.7

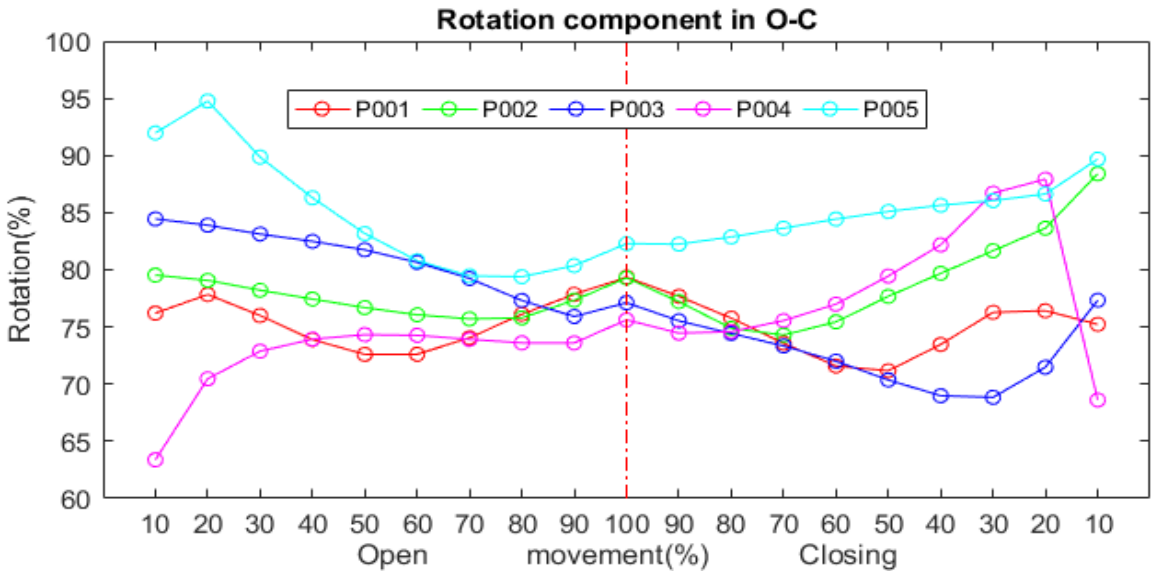

Figure 22. The contribution of rotation from five subjects.

Horizontal axis represents the percentage of maximum inter-incisor distance. Vertical axis represents the ratio of rotation to the sum of rotation and translation.

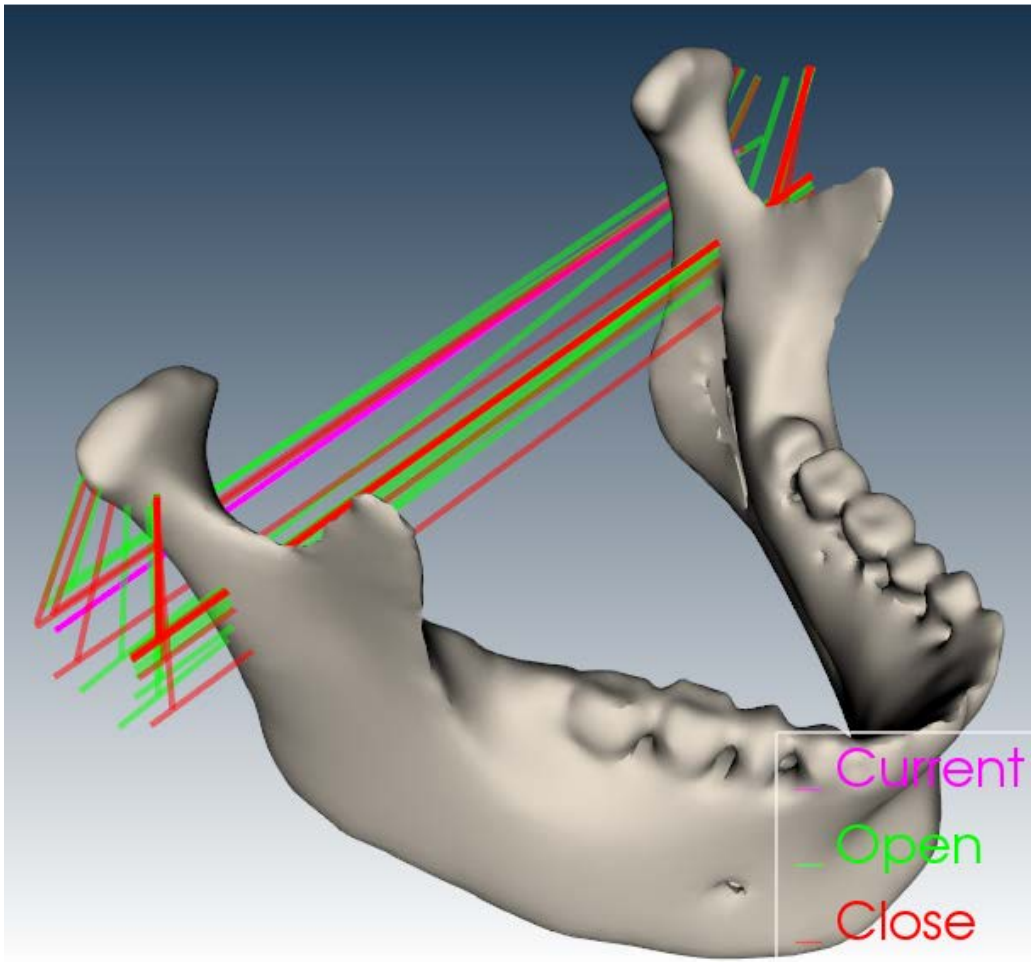

Figure 23. The axis of rotation calculated using the finite helical axis during one cycle of maximum open-close.
The green color lines are the FHA axes during the mouth opening. The red color lines are the FHA axes during the mouth closing. The magenta line is the FHA axis with a user-specific time. The opening cycle is separated into 10 steps according to the incisor distance. The closing cycle is separated into 10 steps according to the incisor distance.

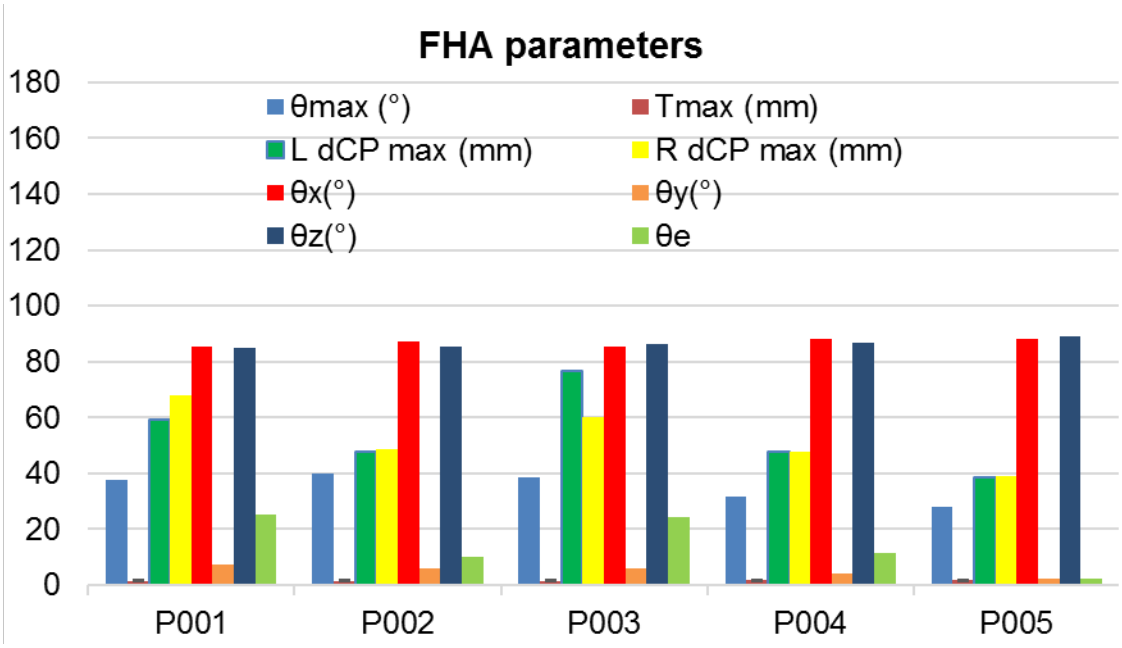

Figure 24. FHA parameters for five subjects.

θ_{max} is the rotation around FHA, T_{max} is the translation along the FHA, $d_{CP\text{-}max}$ is distance of FHA relative to lateral condylar pole, $\overline{\theta_x}$, $\overline{\theta_y}$, and $\overline{\theta_z}$ are orientation of FHA relative to global coordinate system, $\overline{\theta_e}$ is the fluctuation of the FHA orientation.

Table 16. The helical axis parameters during maximum jaw open/close in five subjects. θ is the rotation around the helical axis. T is the translation along the helical axis. d_{cp} is the distance between the helical axis and the condyle reference point or the condyle lateral pole. x_d is the anteroposterior component of the d_{cp}. z_d is the superior-inferior component of the d_{cp}. θ_x is the angle between the helical axis and x-axis the coordinate system XYZ. θ_y is the angle between the helical axis and y-axis the coordinate system XYZ. θ_z is the angle between the helical axis and z-axis the coordinate system XYZ. θ_e is the global fluctuation of the HA spatial orientation. L is the left side. R is the right side. Please refer to Figure 11 for the coordinate system.

	P01	P02	P03	P04	P05	Mean ± std
θ_{max} (°)	39.6	41.0	38.9	31.8	28.7	36.0±5.4
T_{max} (mm)	1.6	1.7	1.9	1.9	1.8	1.8±0.12
L $d_{CP\ max}$ (mm)	40.7	34.9	57.4	152.8	48.5	66.9±48.8
L x_{dmax} (mm)	22.1	18.3	38.0	93.1	37.7	41.9±30.0
L x_{dmin} (mm)	1.6	-13.3	6.4	19.9	-17.5	-0.6±15.2
L z_{dmax} (mm)	-0.7	-6.5	-11.5	48.5	42.5	14.5±28.7
L z_{dmin} (mm)	-40.5	-31.4	-45.8	-88.1	-30.0	-47.2±23.8
R $_{dCP\ max}$ (mm)	68.4	36.3	72.7	110.0	74.8	72.4±26.2
R x_{dmax} (mm)	31.9	24.4	55.3	102.2	64.3	55.6±30.8
R x_{dmin} (mm)	3.6	5.3	14.0	20.6	0.1	8.7±8.4
R z_{dmax} (mm)	-6.3	-8.0	-7.5	27.3	1.8	1.5±15.0
R z_{dmin} (mm)	-58.1	-29.0	-48.8	-62.6	-31.5	-46.0±15.2
$\overline{\theta_x}$ (˚)	95.9	91.9	93.8	88.3	92.8	92.5±2.8
$\overline{\theta_y}$ (˚)	6.2	3.0	4.7	3.6	3.2	4.1±1.3
$\overline{\theta_z}$ (˚)	90.8	87.9	88.1	92.2	90.3	89.9±1.9
$\overline{\theta_e}$ (˚)	7.1	3.8	37.9	50.4	12.6	22.3±20.6

Discussion

We have successfully used our motion-EMG-BF data collection system to collect patient-specific EMG, motion and bite force data for five subjects. Our system provides a practical, precise and clinically available solution for the integration data collection of motion, EMG and bite force signals. Also, our motion data analysis showed promising results: the system allows visually and sequentially determining of the condyle position relative to articular fossa and the detection of functional rotation axis. We are confident that the data collection system and the motion analysis methods can be applied.

Compared to previous studies, the use of the integrated image-motion maker for both the motion system and the imaging system reduced the inaccuracy of the mathematical transformation registration between the motion maker and CBCT marker since the two sets of markers were manually put at the co-centric position.

The current system design is harmless to human. The potential research risk for human comes from CBCT ultra-low patient dose of 215 μSv which is lower than 314 μSv of standard 2D panoramic imaging. The making of impression s of the teeth may cause discomfort if the subject is having difficulty breathing through the nose. Some subjects may experience a sensation of gagging while impressions are made. In rare cases the impression material may cause an allergic reaction. In addition, preparation of the skin for the surf ace electrodes requires the application of isopropyl alcohol and the rubbing of the skin, which may cause minor skin irritation. The data collection may take as lo ng as 1 hour total per session. The potential risks associated with jaw-tracking are minimal, however jaw muscle fatigue may occur.

From the ROM analysis, subject P05 had very limited protrusion range and the incisal distance during the maximum open-close was smaller than other subjects. From the figure, it was implied that the rotation took the major role during the initial opening stage and gradually decreased until the maximum opening. However, the translation happened together with the rotation during the whole process. For all five subjects, the rotation percentage during the whole motion always ranged from 60% to 95%. The rotation percentage of these five subjects converged to 75% at the maximum openning although the initial value at the start of opening varies among subjects. The subject P05 was more asymmetric than other subject during the open-close cycle.

The maximum FHA rotation values for P004 (31.8°) and P005 (28.7°) were less than the rest of the subjects. It is probably that these two subjects were TMJ disorders patients. Dispersion of FHA of P003 and P004 were larger than the rest of the subjects possibly because their motion trajectories were more irregular and their daily usage of TMJ had more magnitude than others.

Compared to large rotation proportion for one or two points in ROM analysis, the whole rigid body range of rotation of subject P005 was the lowest. This lowest rotation value met the real situation because the subject had limited max opening. Therefore, ROM and FHA analysis provided two perspectives to study the same motion problem. ROM analyzed the motion of one or more points on TMJ rigid body while FHA investigated the motion of the whole rigid body.

The potential improvement to data collection system, if exists, will be that: 1. We have learned in previous studies that the loss and flipping of the passive marker will be two

problems. To prevent missing marker, we will put four markers and create a rigid body so that we can still use the remaining markers on the rigid body if one of the marker is missing. In addition, we will develop our own software to detect missing marker and flipping moments in real time; 2. Currently, the subjects will perform the oral task at their voluntary speed. We will tell the subjects to follow a graphic oral task guide so that their data can be compared between subjects; 3. The current invisalign design might prevent the teeth contact and alter the mandibular resting position. This problem will also affect the precision of motion-image registration if the teeth position in motion tracking is not the same as it is in image. A retainer with exposed teeth used in previous experiment will replace current invisalign design if required; and 4. Current system is still quite complex for operator because it has four monitors, multiple device cables, and two control software on different computers. It is quite inconvenient for the software operator to move from one computer to another continuously. A self-designed software that controls both systems and incorporates video recording function may be one of the solution to apply this system into clinical settings since both EMG and tracking system provide hardware control C++ API. In this case, only one software is required for the control of EMG, tracking and real-time video recording and we can use our own software system without assistance of their software in clinics. The user does not have to move around to control each hardware. 5. The concentration of the barium sulfate emulsion cannot be too high to cause imaging interference between markers and cannot be too low to lose visibility in CBCT device. We have tried several concentrations and found the optimum concentration. 6. Preparation of the skin for the surface electrodes requires the application of isopropyl alcohol and the

rubbing of the skin, which may cause minor skin irritation. 7. The motion tracking will take about 1.5 hour and therefore muscle fatigue might happen. The introduction of relaxation periods between the end of one oral task and the beginning of the next oral task should solve such problem.

Realtime visualization is possible with our current hardware. It is possible to develop the software to complete all the functions required in real-time visualization for clinical evaluation in the future.

Thanks to the Nurbs and 3D printer of CAD-CAM field, it is possible to design and manufacture the digital intraoral impression model to cover larger areas up to full-arch impressions while keep the impression model tight enough. It is time saving and has high reproducibility. In addition, it owes high user experience since and it is not required to put material into the mouth of the participants. For designer, it is easier to modify the digital impression model. Thus, in the future, these advanced CAD-CAM techniques could be used to promote our TMJ data collection and analysis system. Furthermore, it is possible to apply the virtual reality techniques and thus provide the users with a friendly user-environment interaction, make our system more attractive and commercialize our product. Finally, with the help of virtual reality technologies, we should be able to create virtual articulators that precisely replicate the mandibular movement rather than to mimic the motion pattern for the current articulators.

CHAPTER SIX: CASE STUDY OF HUMAN TMJ CONTACT AREA IN TMJ INTRA-ARTICULAR SPACE

Introduction

The previous literature and the frequent clinical observations have demonstrated that the disc displacement is correlated with the change of the joint anatomy [16, 56, 123, 128, 129] and the intra-articular space [123, 390, 391]. However, the diagnostic value and the biomechanical meaning of the shape variation needs to be quantitatively clarified.

Biomechanically, the articular space analysis provides the quantitative and accurate geometrical description of the articular surface which is essential for the development of the accurate mathematical model analysis to understand the joint capability to distribute the applied loading and to investigate the underlying pathophysiology of TMJ disorders. For instance, with the reduced intra-articular joint space following the parafunctional activities, the intraarticular pressure will increase. The increasing intraarticular pressure above the capillary perfusion pressure leads to the hypoxia and the production of the reactive oxidative species. The uncontrolled reactive oxidative species can impede the biosynthesis of the hyaluronic acid and induce the hyaluronic acid degradation. The degradation of the hyaluronic acid imperils its capability of preventing the lysis of the surface-active phospholipid layer, the principal part of the boundary lubricant, by inhibiting the phospholipase A_2 [328-330]. It was also demonstrated that the contact area shape with decreasing congruency led to the stress concentration and caused the cartilage failure and the subsequent joint degeneration [114, 116]. Finally, it was indicated that the joint articular surface congruency was the dominant factor for the joint stability under the compressive loading [331].

The *in vivo* direct measurement of the human TMJ contact area without disrupting the function integrity has been proven extremely difficult due to its intricate anatomy in an extremely small region although there are *in vivo* experiment reports of intra-articular pressure by inserting needle into articular space of TMJ joint [328, 335, 336] and invasive *in vivo* strain and force data of Baboon [337], macaques [338, 339] and miniature pigs [340-342] using strain gauges and piezoelectric film. In addition, the introduce of prosthesis will cause harmful corrosion because of its different material properties of with the condyle bone.

It is hard to apply the contact theories of the hertz contact theory or the elastic foundation contact theory to model the TMJ. The elastic half-space perquisite of the hertz contact theory generally cannot be met in human joints. The cartilage thickness of TMJ fossa and condyle is relatively thin. The contact area of TMJ is comparable to the size of TMJ condyle and fossa. The curvature of TMJ articular surfaces is relatively large and non-uniformly distributed. Moreover, there is a deformable and moving soft TMJ disc between the articular bones. The TMJ disc is a biphasic viscoelastic material and cannot be simplified as a spring as in the elastic foundation contact theory. The deformation and motion of the TMJ disc also prevents the application of the elastic foundation contact theory which assumes no interaction between the elastic units.

Another way of the TMJ joint articular surface congruence estimation is through the examination of the distances between fossa and condyle surfaces or disc and condyle surfaces in intra-articular space. To evaluate the congruity of growing TMJs of 52 specimens, the frontal planar distances of 17 points distributed between lateral pole and

medial pole are graphed with respect to their positions [114, 344]. The articular surface congruency is normalized by subtracting the 2D mean distance from those 2D distances. The thickness of the soft tissues of the articular eminence and temporal fossa was uniformly set to 1.5 mm. In their later study, it was demonstrated that the cause of this surface incongruity was the shape of the growing articular eminence and that the consequence was the local stress concentration [116]. It was also found that the one of the disc function as the media to reduce the condyle-fossa articular surface incongruity was limited. The intraarticular space distance between the condyle and the fossa was also computed on 2D image [55, 123, 132-134, 390].

The studies of joint congruency and contact area in 3D space were possible with 3D intra articular space analysis [345, 346, 370]. The contact area or stress-field calculation was described as a statistical circle shape composed of 10 to 30 minimum distances *h* between the TMJ condyle and fossa. The radius of this circle *a* was the standard deviation around the centroid of the stress field. It was observed that the patients with clicking joints had a significant grater aspect ratio a/h than the controls [392].

However, it was shown in the study [346] that the shape of the contact area was more like an ellipsoid than a circle (Figure 12). Moreover, it is not clear whether there is sex dimorphism of the human TMJ contact area although it is well-known that the female condyle is much smaller in the mediolateral direction than that of the male. Therefore, the objective of this study was to determine morphometric and biomechanical findings with respect to gender to elucidate the background to sex difference regarding the clinical complains over TMJ disorders. Specifically, the aims of this research were: 1) to design an

improved method, the contact area descriptor II, with more accurate characterization of the contact area than the available statistical stress field method, or the contact area descriptor I, reported in literature [345, 346, 370]; 2) to investigate the diagnostic group gender difference between healthy females and healthy males to find out the mechanism on the notable dominance of women in TMJ disorders; and 3) to identify the risk factors for TMJ disorders.

Materials and Methods

Subjects

This study was approved by the Institutional Review Boards of the University at Buffalo and University of Missouri-Kansas City. All participants volunteered for this pilot study. Subjects were recruited at the University at Buffalo School of Dental Medicine and gave informed consent before enrolling.

Cone beam computed tomography (CBCT) and magnetic resonance (MR) images were used with Research Diagnostic Criteria for TMD by calibrated examiners to categorize subjects. Subjects were excluded from participation if they reported a history of rheumatic diseases, had signs of degenerative joint disease of the TMJ assessed by the CBCT mathod, had multiple missing teeth or large dental restorations, were pregnant, or were unable to perform the variety of tasks in the study protocol. This pilot investigation focused on equal numbers of age-matched and gender matched subjects in two diagnostic groups without TMJ disorders: a nDDnPF group containing asymptomatic female subjects without either bilateral TMJ disc displacement or chronic pain, and a nDDnPM group containing asymptomatic male subjects without either bilateral TMJ disc displacement or

chronic pain. A total of 18 females (mean age of 31.37 ± 9.35-year-old, from 23.42 to 55.75) and 18 males (mean age of 29.50 ± 11.14-year-old, from 19.75 to 59.92) were chosen from the original 110 subjects for the current research. All the left TMJs were selected for this study since the aim of this study was to investigate the gender difference.

The MRI images of the participants were obtained using the MRI parameters as described previously [139]. Briefly, MRI images were recorded by a 1.5 T MRI scanner. The mouth was biting in maximum intercuspation. The scanning procedure included an axial scan to locate the condylar long axis, followed by a sagittal scan of fourteen 2-mm images taken perpendicular to the condylar long axis. The field of view was 130 mm, 256 pixel × 256 pixel matrix, 35º flip angle, time repeat T_R = 500 ms, time echo T_E = 17 ms. The total scanning time was 3'50" per subject. Finally, an individualized oblique-axial scan of fourteen 2-mm images with the same scanning parameters with sagittal scanning was taken to the left and right side TMJs. Then all the images were interpolated to the pixel of 512 × 512.

Data analysis

The 3D CAD model was manually segmented and automatically reconstructed from a stack of MRI images for each subject. The voxel size of MRI was 0.25 x 0.25 mm and the slicing thickness was 2 mm. Base on reconstructed 3D CAD model from MRI images, the condyle anatomy was measured. The measurement of the condyle width was referred to an individualized cartesian coordinate system with one mediolateral axis aligned with the condylar long axis (the white double arrow axis and the green double arrow axis in Figure 25). The condylar head distance along anterior-posterior direction was measured

in the midplane perpendicular to the condylar long axis. To determine the gender difference, the anatomical condyle length along anteroposterior direction (the distance of the condylar lateral pole to the condylar medial pole, i.e., the white double arrow axis in Figure 25), condyle width along mediolateral direction (the green double arrow axis in Figure 25) and their ratio—defined as the anteroposterior length divided by the mediolateral length—were compared between the nDDnPF group and the nDDnPM group.

Two types of contact area methods, the contact area descriptor I and the contact area descriptor II, were adopted to characterize the contact area in the condyle-fossa intra-articular space. The difference was the distinct way of characterizing the contact area.

The contact area descriptor I was the stress field previously reported in [345] (Figure 12). In short, the stress field was a set of 30 minimum distances between the condyle and the fossa polygon vertices approximating the articular surfaces. The mean value of the set was defined as the minimum distance *h* between the condyle and the fossa. The centroid of the stress field was determined from the set. The standard deviation of the set of minimum distances around the centroid of the stress field was defined as the mean radius *a* of the circular stress field. Therefore, the condyle-fossa contact area was described using a circle with the radius *a*. The mean distance value *h* and the radius *a* of the contact area were compared between the nDDnPF group and the nDDnPM group. The sex dependent difference of the radius components in the x-axis and z-axis directions (Figure 25) were tested (radius equivalent components).

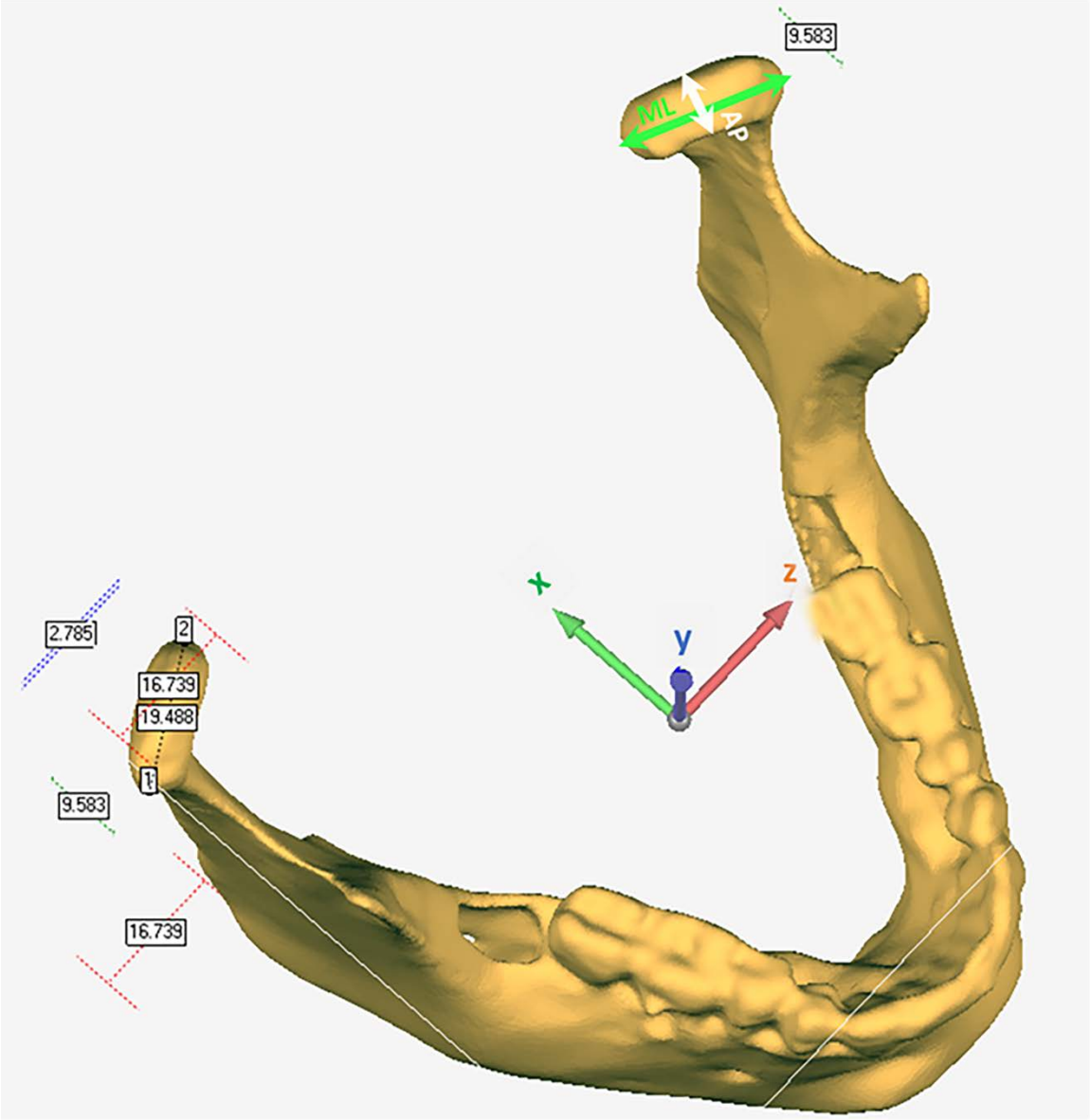

Figure 25. Measurement of the condyle anatomy.
The green double arrow line connecting the condyle lateral pole and the condyle medial pole is the condyle width along the mediolateral (ML) direction. The white double arrow line perpendicular to the green double arrow line is the condyle length along anteroposterior (AP) direction.The length ratio is the length of the white line divided by the length of the green line.

With the contact area descriptor II (Figure 26), the isosurface with a distance value below a certain distance threshold was extracted and then the contact area will be determined. Similar to the contact area descriptor I, all distances between the condyle and the fossa polygon vertices approximating the articular surfaces were computed. The distances between condyle and fossa vertices were assigned to the condyle vertices and interpolation was performed in the condyle facets connecting these condyle vertices (Figure 26a and Figure 26b). A set of 30 minimum distances was selected for determining the distance threshold. The mean value of the set was defined as the minimum distance *h* between the condyle and the fossa. Unlike the contact area descriptor I, the condyle-fossa contact area was described using an elliptical shape rather than a circle. The condyle isosurface with distance values below *h* was extracted on the condyle surface. The isoline with the highest distance value of the isosurface was fitted using an ellipse (Figure 26c). The length of the long axis direction and the length of the short axis of this elliptical contact area were compared between the nDDnPF group and the nDDnPM group (diameter equivalent components). The surface area of the extracted isosurface region was computed and compared between the two diagnostic groups.

Statistical analysis

The student two tailed t-test was performed to compare the difference of morphometric parameters and the contact area parmeters between the groups of nDDnPF and nDDnPM. All the statistics were performed in the SPSS software (SPSS 25, Inc., Chicago, IL). All differences were considered significant if $p < 0.05$.

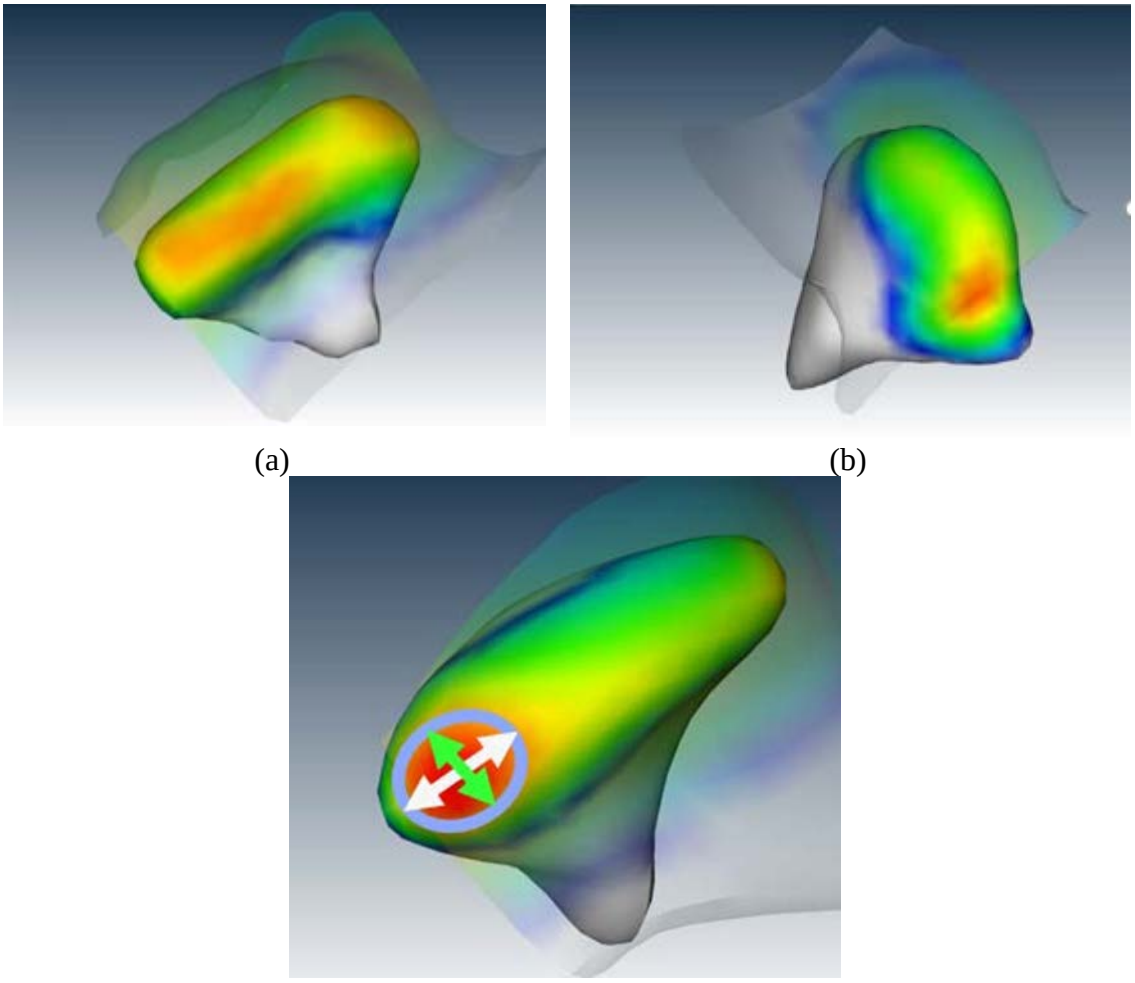

(a) (b)

(c)

Figure 26. The contact area descriptor II.
(a) The contact area of a male TMJ. (b) The contact area of a female TMJ. (c) The contact area is approximated using an elliptical curve with its long axis aligned with the mediolateral direction and its short axis aligned with the anteroposterior direction.

Results

The comparison of the anatomical lengths along mediolateral and anteroposterior directions were shown in Figure 27. The condylar length along anteroposterior direction was 9.1 ± 1.1 mm for the group nDDnPF and 8.7 ± 1.2 mm for the group nDDnPM (p = 0.4). The condylar length along mediolateral direction was 18.7 ± 2.0 mm for the group nDDnPF and 21.4 ± 1.7 mm for the group nDDnPM (**p < 0.001**). The length ratio was 0.5 ± 0.1 for the group nDDnPF and 0.4 ± 0.1 for the group nDDnPM (**p< 0.05**).

With the contact area descriptor I (Figure 28), the mean minimum distance value *h* of the contact area was 2.0 ± 0.7 mm for the group nDDnPF and 2.0 ± 0.5 mm for the group nDDnPM (p = 0.5). The radius *a* of the stress field was 5.2 ± 1.1 mm for the group nDDnPF and 6.0 ± 1.8 mm for the group nDDnPM (p = 0.1). The length of the x-axis component (radius equivalent components) of the contact area radius was 2.2 ± 0.9 mm for the group nDDnPF and 2.5 ± 1.1 mm for the group nDDnPM (p = 0.3). The length of the z-axis component (radius equivalent components) of the contact area radius was 4.3 ± 1.2 mm for the group nDDnPF and 5.2 ± 1.7 mm for the group nDDnPM (p = 0.1). The length ratio of the x-axis length divided by the z-axis length was 0.5 ± 0.3 for the group nDDnPF and 0.5 ± 0.2 mm for the group nDDnPM (p = 0.8).

With the contact area descriptor II (Figure 29), the length of the contact area along the anteroposterior direction (diameter equivalent components) was 4.8 ± 1.5 mm for the group nDDnPF and 4.1 ± 1.3 mm for the group nDDnPM (p = 0.2). The length of the contact area along the mediolateral direction was 5.7 ± 2.6 mm for the group nDDnPF and 11.5 ± 5.5 mm for the group nDDnPM (**p < 0.001**). The length ratio was 0.9 ± 0.2 mm for

the group nDDnPF and 0.4 ± 0.2 mm for the group nDDnPM (**p < 0.001**). The surface area of the contact area was 29.5 ± 23.8 mm^2 for the group nDDnPF and 37.7 ± 21.8 mm^2 for the group nDDnPM (p = 0.3).

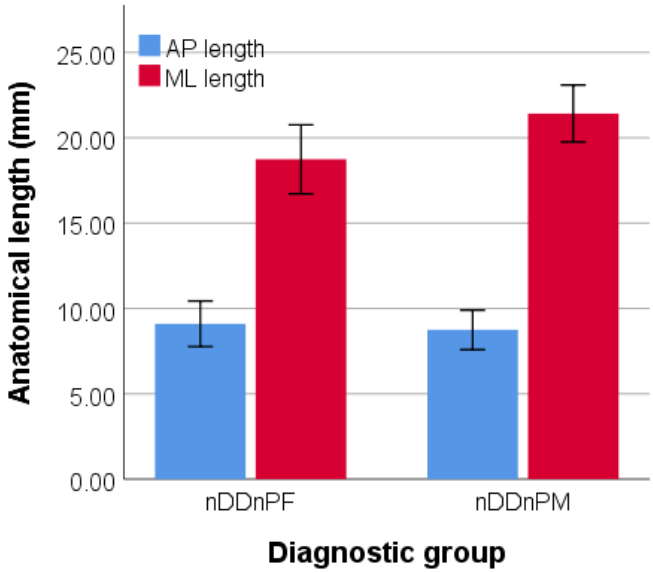

(a)

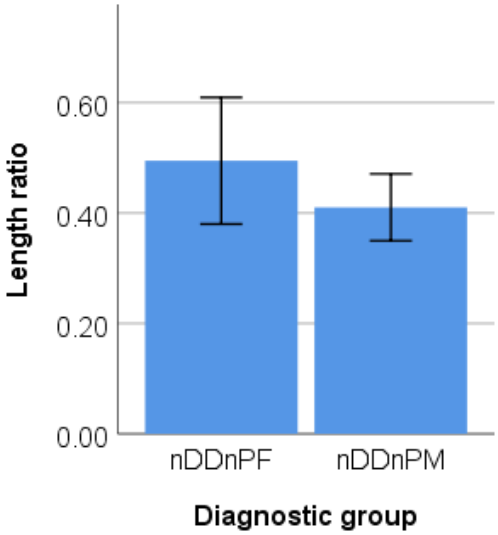

(b)

Figure 27. The anatomical length measurement of condyle.
(a) lengths along ML direction and AP direction. (b) the length ratio. The ML length is the length along the condylar mediolateral direction. The AP length is the length along the condylar anteroposterior direction. Length ratio is the value of the AP length divided by the ML length. Error bars: 95% confidence interval. Error bars: 1 SD.

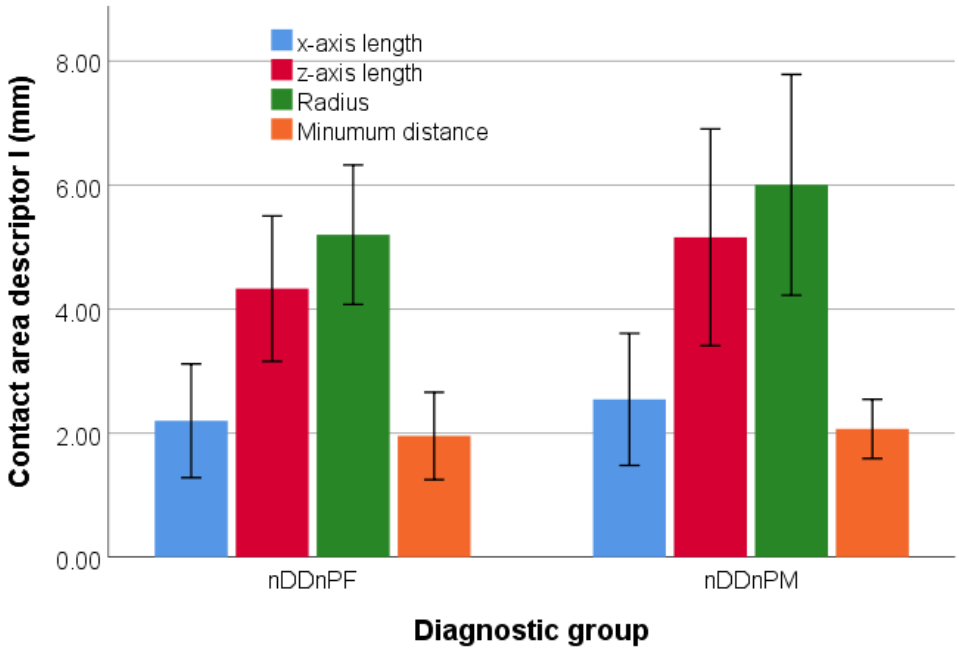

(a)

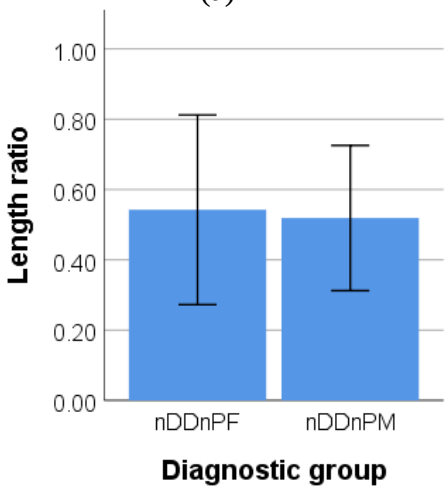

(b)

Figure 28. The parameters of the contact area descriptor I and the comparison between male and female.
(a) the x-axis length is the length of the contact area along the x-axis of the coordinate system. The z-axis length is the length of the contact area along the z-axis of the coordinate system. The minimum distance is the mean value of a set of 30 minimum distances between the condyle ad fossa surfaces. (b) the length ratio is the length ratio of the x-axis length divided by the z-axis length. Radius is the standard deviation of the set of minimum distances around the centroid of the stress field. Error bars: 95% confidence interval. Error bars: 1 SD.

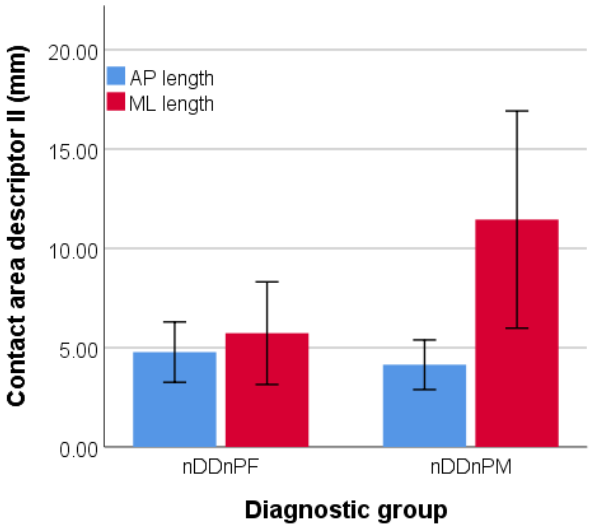

(a)

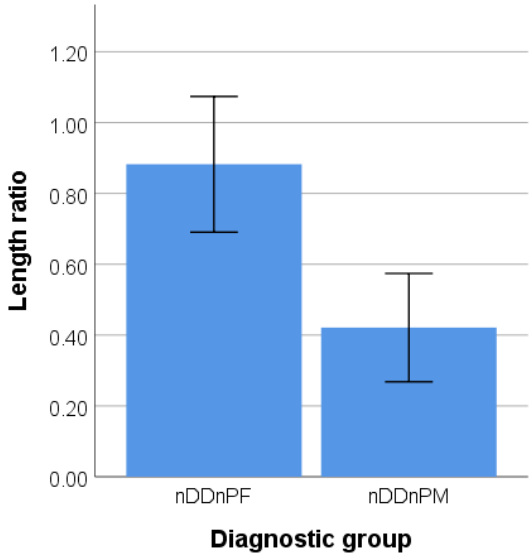

(b)

Figure 29. The parameters of the contact area descriptor II and the comparison between male and female.
(a) lengths along ML direction and AP direction. (b) the length ratio. The ML length is the length along the condylar mediolateral direction. The AP length is the length along the condylar anteroposterior direction. Length ratio is the value of the AP length divided by the ML length. Error bars: 95% confidence interval. Error bars: 1 SD.

Discussion

The intraarticular space analysis combines the anatomy of both the condyle bone and the fossa bone. Also, it is affected by the bone anatomy [114]. Therefore, the intraarticular space analysis provides much more powerful diagnostic information about the articular surface congruency than the anatomy measurement.

This study created a more accurate method of characterizing the contact area based on the distance between the condyle-fossa articular surfaces. It produced more meaningful results than the previous stress field method.

As to the condyle anatomy, the condyle mediolateral length of the male group was greater than that of the female group. No significant difference was found in the anteroposterior length. The length ratio was much greater in females.

With contact area descriptor I, the overall shape of the contact area is of circular shape. No significant sex difference was observed in the x-axis length, the z-axis length, the length ratio, the radius *a* of the stress field, or the minimum distance *h* of the articular surfaces.

With contact area descriptor II, the overall shape of the contact area is of oval shape, consistent with the anatomy of TMJ disc and TMJ condyle. The mediolateral length of contact area was significantly smaller in females than males. Thus, the congruency of the condyle-fossa articular surface along mediolateral direction was much greater in males. Hence, the female joints have more chance to suffer from the stress concentration and the female joint health is worse affected by the stress concentration [114]. The length ratio was significantly greater in females than that of the male group. As a result, the shape of the

contact area of females is substantially rounder than that of males. The anteroposterior length of contact was greater in females although no significant difference was found. The contact area surface area was larger in males and the sex difference was not statistically meaningful probably due to the large variations in the group. The large variation of the contact area was probably due to the improper determination of the distance threshold. A better distance threshold method should base on the precise patient-specific disc thickness and cartilage thickness, which were difficult to gather from the current available data due to its poor resolution. Another possible solution to the variation was to plot the relationship between a set of the distance thresholds and the corresponding set of surface areas of the extracted contact areas. Following that, the optimal distance threshold could be determined based on an assumption: the surface area of the extracted contact area increased with a slower speed when the extracted contact area was beyond the actual contact. This method was employed in the "Future Goals" of the Chapter Seven.

The gender difference in contact area found in the contact area descriptor II was consistent with the clinical anatomy sex difference previously reported in the condyle bone: the male condyle was greater than the female condyle in the mediolateral direction even after the adjust for the sex difference craniofacial size [393, 394]. However, this distinction was ignored by the statistical method as reported in the contact area descriptor I.

Indeed, the shape of the contact area was more like an ellipsoid than a circle as the first statistical contact area descriptor I. Consequently, the subsequent contact stress distribution, the work done to cartilage and energy density [85], might deviate from the previous reports due to the algorithm update of the contact area. For instance, the

ellipsoidal shaped contact data show that the loading area along mediolateral direction is longer than that of anteroposterior direction, which conforms to the condyle anatomical features and enables the major stress distribution along long mediolateral direction. However, should an idealized stress field circle be used to statistically depict the contact area and remove the eccentric property of the contact area originated from TMJ anatomy, the condyle and disc would have the same contact area along any direction and the contact stress would have more distribution along anteroposterior direction and less distribution along mediolateral direction, leading to the possible stress concentration in conflict with *in vivo* contact properties and contradicting the TMJ condyle anatomy. Moreover, the stress field is located out of the condylar anteroposterior anatomical boundary if the standard deviation is too large due to the elongated condylar shape in that direction, which is a common finding in the morphometrical measurement TMJ studies. In addition, the distance values and volume and surface area of the local loading zone will indicate the extent to which the stress concentrates and thus the progression of TMJ degeneration. The increase of the cartilage pressurization and the tissue fatigue due to localized compression and stress concentration can be estimated from the contact area descriptor II. Furthermore, the application analysis of glucose diffusion in TMJ disc may also be more accurate by improving the contact area calculation. Finally, this method of precise calculating the contact area with joint movement was already applied in the knee joint [348], the glenohumeral joint [349] and the CMC joint [350] as shown in Table 7.

In sum, we have successfully determined relative position of condyle to the articular fossa and the patient-specific contact area in the articulation space. In addition, the contact

area shape change with respect to mandibular movement has been demonstrated and uploaded on our lab website with link [395]. Future study will focus on how the mandibular movement during various types of oral behaviors affects the variation of the contact area and thus the stress distribution. Then it is possible to identify whether the anatomy or the mandibular motion has more influence on the surface congruency. Finally, the application of contact area descriptor II to the glucose diffusion in the TMJ disc tissue has been tested in healthy subjects from our collaborator at UMKC. Please see the “Future Goals” of the Chapter Seven for more details.

CHAPTER SEVEN: OVERALL CONCLUSIONS AND FUTURE DIRECTIONS

Conclusion

The purposes of this study were to 1) build a simplified, non-invasive, and light weighted motion-EMG-bite force data collection system; and 2) investigate the oral behavior, TMJ functional and TMJ shape properties to establish an objective, subject-specific, non-invasive TMJ disorders diagnosis and to understand TMJ disorders pathophysiology.

The TMJ muscle analysis, motion analysis and shape analysis are correlated. TMJ motion analysis aimed to determine the irregular motion path caused by the abnormal muscle activities and the aberrant TMJ anatomy. The complex TMJ movement is activated and maintained by the harmonious cooperation of a group of muscles mainly composed of temporalis muscle, masseter muscle, medial pterygoid muscle, lateral pterygoid muscle and digastric muscle. In addition, TMJ motion is affected by its anatomy. Aberrant muscle coordination will induce the abnormal TMJ motion pattern and affect the TMJ anatomy. The EMG signal pattern analysis was to identify the possible parafunctional activities impeding the nutrient supply and leading to TMJ disorders. Based on the intra-articular space analysis, joint stability, articulation surface friction, as well as contact stress distribution can be estimated. The parafunctional activities decrease the intra-articular space, leading to the lubricant breakdown, the cartilage degeneration, as well as joint dysfunction. The objective assessment of TMJ motion function, EMG muscle behavior, and shape contact area analysis provided clinicians with a quantitative and non-invasive tool for the TMJ disorders diagnosis and the evaluation over surgery results.

This study provided an effective and integrated data collection system to gather the EMG, motion, and bite force signals at the same time. The data collection system simplified the data collection procedure by improving the design and thus reduces the interference to the natural mandibular movement. The study brought the clinicians a non-invasive, subject-specific and objective method for diagnosis of TMJ disorders. The study provided the clinicians with an objective evaluation tool as to the functional assessment before and after the surgery. Finally, it also gave us insight on the nutrient concentration gradient in the TMJ disc tissue, leading to better understanding of the underlying pathophysiology of TMJ disorders.

TMJ EMG study

The EMG signal of the temporalis muscle was collected from patients and controls in both the laboratory and the natural settings. The data was used to develop a computing recognition algorithm, based on statistical amplitude thresholds, that automatically and reliably detected sustained teeth clenching behaviors. It was found in the temporalis long term recording EMG study that the sustained night-time clench behavior occurred at higher frequency in patients. In all subjects, 95% of the temporalis muscle related clenches had duration less than 4 s, and were associated with bite-forces lower than 10 N. The patients had longer clench duration than the normal controls although the detected clenches had a short duration. It was observed that all subjects generally activated their temporalis muscles at low magnitudes at night, but average duration of activation was longer in +DD+P than -DD-P subjects.

It was implied in the current EMG study that sleep bruxism was an infrequent phenomenon compared to the predominant activities which were associated with low intensity jaw loading. Sustained clenches of low intensity have been posited to contribute to jaw muscle fatigue and the development of myofascial pain [186, 384]. Alternatively, frequent low intensity muscle activity may be a sign of homeostatic dysregulation. The current study supports the hypothesis that relatively frequent low intensity muscle activity shown by the +DD+P subjects may be a sign of autonomic nervous system dysregulation that promotes the central and peripheral neuroplastic changes and thus leads to pain response to the no-noxious stimuli.

TMJ motion of normal open-close

For the TMJ motion analysis of the normal open-close mouth movement, three diagnostic groups—the healthy men group of nDDnPM, the healthy women group of nDDnPF, and the women patient group wDDwPF—were recruited. The current study did not include male patient data because the sample size is rather small (N = 5).

Two types of kinematics descriptors were employed to characterize the motion features. ROM analysis provides motion description for one or several points, which is necessary for the dynamics study and diagnosis. FHA analysis examines the motion of the mandibular rigid body.

The gender difference between the nDDnPM group and the nDDnPF group was compared. The difference between the nDDnPF group and the wDDwPF group was also determined. Finally, the side difference was reported for each group using these two kinematics characterization descriptors.

For ROM analysis, no side difference was found for all the three groups. Also, no difference was found between the nDDnPM group and the nDDnPF group. However, difference was found between the nDDnPF group and the wDDwPF group. The rotation and translation were significantly larger in patients.

For FHA analysis, no side difference was found in the nDDnPM group and the nDDnPF group. However, the left TMJs were significantly different from the right TMJs in the wDDwPF group. Thus, FHA is more sensitive to the irregular motion path or the motion asymmetry than ROM. No difference was found between the nDDnPM group and the nDDnPF group. However, difference was found between the nDDnPF group and the wDDwPF group. The rotation was significantly larger in patients. Moreover, the rotation axis of the patients had greater fluctuation during the movement. However, compared to ROM translation analysis, the FHA translation along the helical axis of the nDDnPF group was similar to that of the wDDwPF group. The explanation is that the ROM translation analysis mainly depends on the selection of reference point and that lower diagnostic results would be possible depending on the selection of the reference point on TMJ [313-315]. It is therefore preferable to use the FHA translation for diagnosis.

TMJ motion of a new customized device

A data collection system was designed to gather muscle EMG signal, jaw motion tracking data, TMJ imaging data and the bite force data. A new type of markers for both the imaging system and the motion tracking system was invented to simplify data collection procedure and increase the data processing accuracy. Five subjects were recruited, and their

data were collected for the kinematics study. A motion analysis software was created and validated using available software.

TMJ shape analysis

Surface congruency was proved to affect the stress distribution and contributed to the stress concentration, resulting in the cartilage failure and the subsequent joint degeneration [114, 116]. Intra-articular space analysis also contributed to the determination of lubrication failure [328-330].

The overall shape of the contact area is of circular shape for the contact area descriptor I. No gender difference was detected. By introducing a more accurate contact area descriptor II, the overall shape of the contact area is of oval shape, consistent with the anatomy of TMJ disc and TMJ condyle. The mediolateral length of contact area was significantly smaller in females than that in males. Thus, the congruency of the condyle-fossa articular surface along mediolateral direction was much greater in males, indicating more suffer from stress concentration in female TMJs than male TMJs.

Future Goals

Multibody dynamics study

TMJ kinematics only considers the mandibular movement without considering its causal effect: the modeling of masticatory muscles and ligaments. The dynamics study is concerned with forces and torques of muscles as well as ligaments. The inverse dynamics allows us to determine the forces responsible for mandibular movement. The inverse dynamics is required since it is hard to obtain direct in-vivo measurement without breaking the joint integrity.

The kinematics study provides the 3D coordinates and thus velocity/acceleration of individual segment. The muscle force vectors estimated from EMG study provide input to the dynamics study. The anatomy study of bone, disc and other soft tissues is crucial for building the mathematical model. Then the reaction force will be estimated through the dynamics of the motion. Optimization is required since many unknown variables and non-subject-specific items exist in the dynamics model. For instance, it is impossible to know the exact morphometric properties of live human muscles and ligaments without surgery.

TMJ disc nutrition simulation

The objectives of this pilot study were to: (1) determine the difference of the condyle-disc contact area between male and female asymptomatic subjects; (2) determine the effect of parafunctional activities, e.g. bruxism, on glucose diffusion; and (3) determine the difference of nutrient environment between male and female subjects without TMJ disorders. Specifically, the bruxism will be simulated by applying the contact area to the disc. The glucose diffusion simulation results before and after the application of contact area were compared.

This study was approved by the Institutional Review Boards of the University at Buffalo and University of Missouri-Kansas City. All participants volunteered for this pilot study. Subjects were recruited at the University at Buffalo School of Dental Medicine and gave informed consent before enrolling.

Cone beam computed tomography (CBCT) and magnetic resonance (MR) images were used with Research Diagnostic Criteria for TMD by calibrated examiners to categorize subjects. Subjects were excluded from participation if they reported a history of

rheumatic diseases, presented with CBCT evidence of degenerative joint disease of the TMJ, had multiple missing teeth or large dental restorations, were pregnant, or were unable to perform the variety of tasks in the study protocol. This pilot investigation focused on equal numbers of age-matched and gender matched subjects in two diagnostic groups without TMJ disorders: a nDDnPF group containing healthy female subjects, and a nDDnPM group containing healthy male subjects. A total of 12 females (mean age of 34.25 ± 10.85-year-old) and 12 males (mean age of 31.33 ± 9.43-year-old) were chosen from the original 110 subjects for the current research. All the left TMJs were selected for this study.

The MRI images of the participants were obtained using the parameters as described previously [139], Briefly, MRI images were recorded by a 1.5 T scanner. The mouth was biting in maximum intercuspation. The scanning procedure was: firstly, an axial scan was used to locate the condylar long axis. Then, a sagittal scan of 14 2-mm images was taken perpendicular to the condylar long axis. The field of view was 130 mm, 256 pixel × 256 pixel matrix, 35º flip angle, time repeat T_R = 500 ms, time echo T_E = 17 ms. The total scanning time is 3'50" per subject. Finally, an individualized oblique-axial scan of 14 2-mm images with the same scanning parameters with sagittal scanning was taken to the left and right TMJs. Then all the images were interpolated to the pixel of 512 × 512.

The contact area of the condyle-disc articular surface was calculated between condyle and TMJ disc using a new method. The distance between condyle and disc was calculated. Then the disc iso-surfaces at different thresholds were extracted (Figure 30). The surface area changes with respect to the different distance thresholds were plotted in Figure 31. It was demonstrated that the surface area increases slowly from the distance of

0.1 to the distance of 0.3. Then the surface area increased dramatically until the reach of the distance of 0.7 mm. Therefore, the distance of 0.7 mm was used as the threshold for contact area determination. The underlying assumption was the observation that the surface area of the extracted contact area increased with a slower speed when the extracted contact area was beyond the actual contact.

The contact area was compared between females and males using t-Test (Table 17). It was found that the male group had significantly greater mediolateral length, length ratio, and the surface area. No gender difference was observed in the anteroposterior length of the contact area. No gender difference was found in the distance threshold.

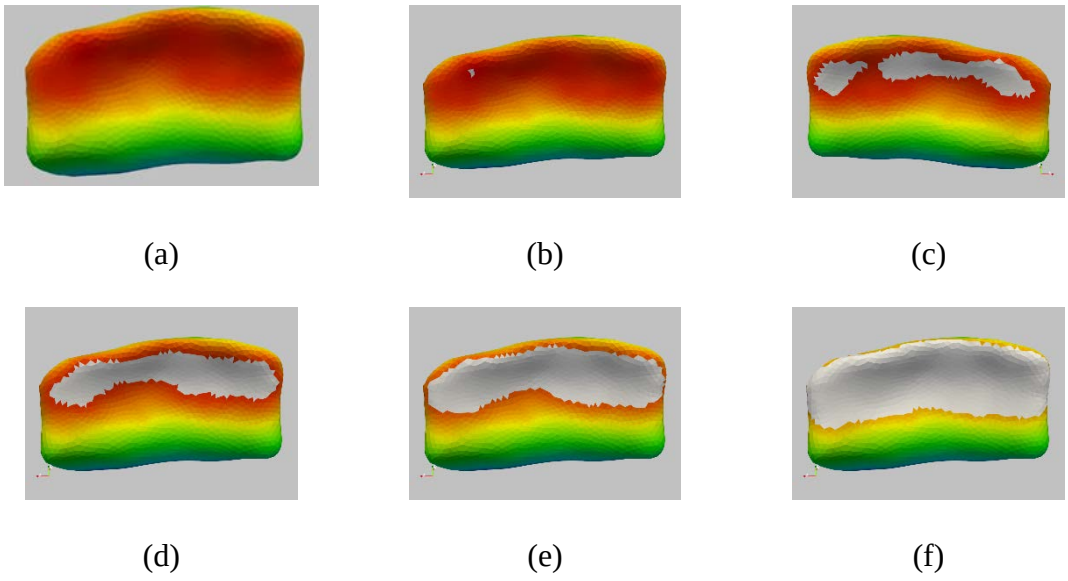

Figure 30. Isosurface of contact area with different distance thresholds.
The change of the contact area with the distance D increment between condyle and disc. (a) D = 0 mm. (b) D = 0.1 mm. (c) D = 0.4 mm. (d) D = 0.5 mm. (e) D = 1.0 mm. (f) D = 1.6 mm.

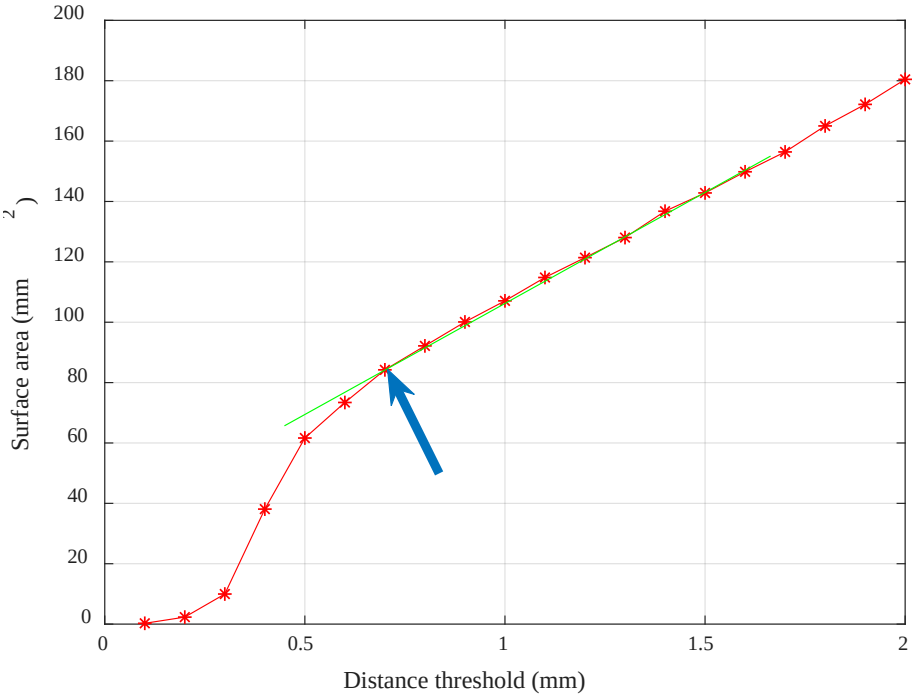

Figure 31. Surface area change of the contact area with distance of condyle-disc
The red line is the surface area change of the contact area with the distance variation of the condyle-disc complex. The green line is the slope at the distance of 0.7 mm. The blue arrow points to the final distance threshold for the termination of contact area.

Table 17. Contact area of condyle-disc surfaces.

	nDDnPF (n=12)	nDDnPM (n =12)	p
Anteroposterior length (mm)	5.70±1.02	5.45±0.56	0.47
Mediolateral length (mm)	15.54±1.82	19.87±2.41	**<0.001**
Length ratio	0.37±0.09	0.28±0.03	**0.001**
Surface area (mm^2)	76.00±16.37	100.49±26.04	**0.01**
Distance threshold (mm)	1.01±0.25	0.94±0.20	0.48

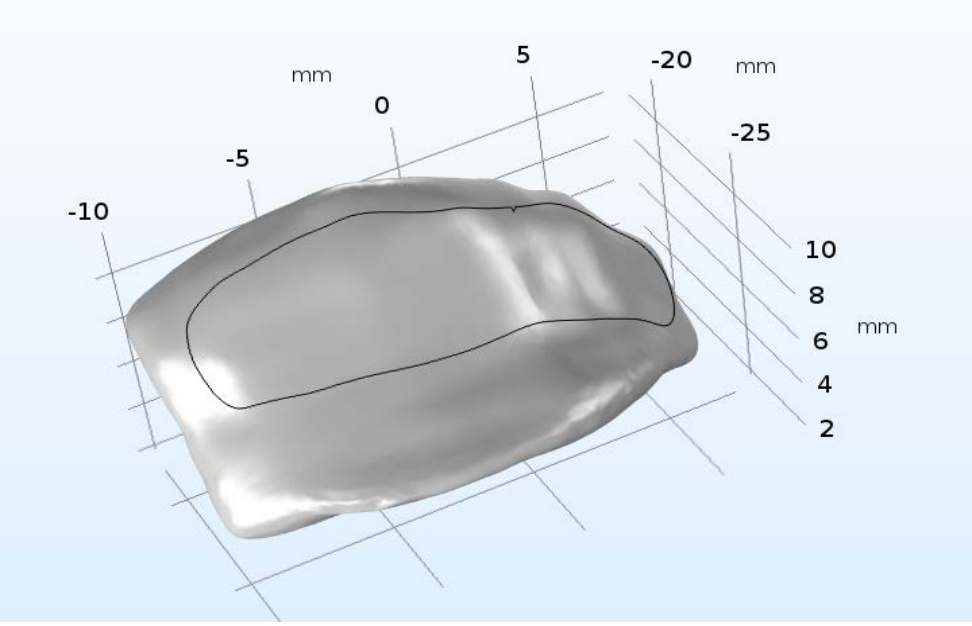
mm
-10
-5
0
5
-20
mm
-25
10
8
6
4
2
mm

(a)

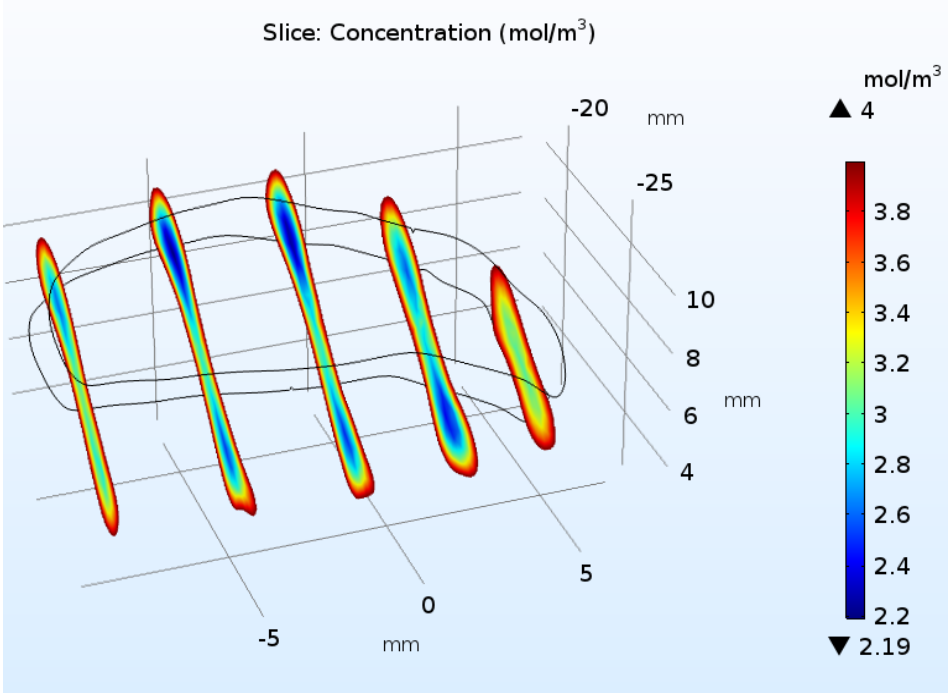
Slice: Concentration (mol/m3)
mol/m3
▲ 4
3.8
3.6
3.4
3.2
3
2.8
2.6
2.4
2.2
▼ 2.19
-20
mm
-25
10
8
6
4
mm
5
0
-5
mm

(b)

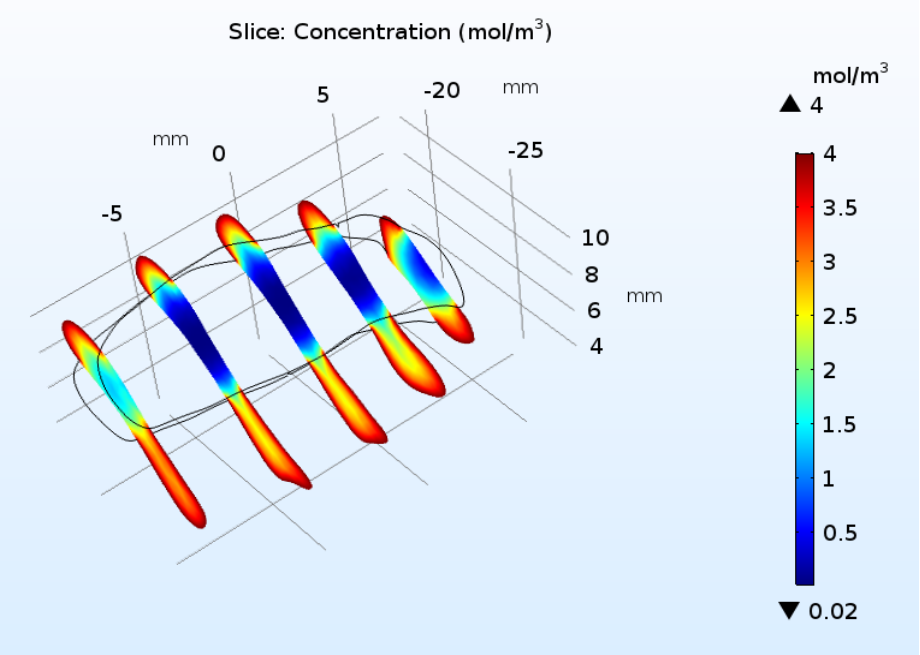

(c)

Figure 32. Glucose diffusion under parafunctional activity.
Glucose diffusion with and without contact. The contact situation is simulating the parafunctional activity. (a) Contact area. (b) Glucose diffusion without contact. (c) Glucose diffusion with contact.

Notably, using the new condyle-disc contact area determination method, the surface area variations in both the female group and the male group were smaller than the contact area method reported in Chapter Six.

The glucose diffusion was then compared between disc without contact and disc with contact (simulating the bruxism). The TMJ anatomy of condyle and disc was obtained from human MRI data. The diffusion property diffusivity $D_{glucose} = 4.93 \pm 1.74 \times 10^{-11}$ m^2/s was from our previous experiment study [396]. The diffusion equation of the Fick's second law was:

$$\frac{\partial c_i}{\partial t} = D \frac{\partial^2 c_i}{\partial x^2}$$

The simulation result was shown in Figure 32. The lowest glucose concentration was 2.19 mol/m^3 before the application of contact area. After the application of the contact, the lowest glucose concentration was 0.02 mol/m^3, which was below the cellular viability nutrient level of 0.5 mM [397]. It was suggested that the TMJ disc cells could not survive and the cell number would decrease when the nutrient was blocked due to the pathological parafunctional activities.

To determine the difference between female healthy group and male healthy group. The critical zone was defined as the area where the glucose concentration was below the cellular viability nutrient level of 0.5 mM. No gender difference was found in the surface area of the critical zone when contact area was applied. The experimental validation of the simulation results is still under process and will be published in future.

REFERENCE

1. Schiffman, E., et al., *Diagnostic Criteria for Temporomandibular Disorders (DC/TMD) for Clinical and Research Applications: recommendations of the International RDC/TMD Consortium Network* and Orofacial Pain Special Interest Groupdagger*. J Oral Facial Pain Headache, 2014. **28**(1): p. 6-27.
2. Scrivani, S.J., D.A. Keith, and L.B. Kaban, *Temporomandibular disorders.* N Engl J Med, 2008. **359**(25): p. 2693-705.
3. Palla, S., *Anatomy and Pathophysiology of the Temporomandibular Joint*, in *Functional Occlusion in Restorative Dentistry and Prosthodontics*, S.E. Eckert, Editor. 2016, Mosby. p. 67-85.
4. Cisewski, S.E., et al., *The effects of oxygen level and glucose concentration on the metabolism of porcine TMJ disc cells.* Osteoarthritis Cartilage, 2015. **23**(10): p. 1790-6.
5. Durham, J., et al., *Oro-facial pain and nutrition: a forgotten relationship?* J Oral Rehabil, 2015. **42**(1): p. 75-80.
6. Zhang, Y.L., et al., *Morphologic Analysis of the Temporomandibular Joint Between Patients With Facial Asymmetry and Asymptomatic Subjects by 2D and 3D Evaluation: A Preliminary Study.* Medicine (Baltimore), 2016. **95**(13): p. e3052.
7. Linss, W. and K. Moller, *Remarks on the morphology of the human temporomandibular joint in the fetal period.* Ann Anat, 2007. **189**(4): p. 418-22.
8. Tasaki, M.M. and P.L. Westesson, *Temporomandibular joint: diagnostic accuracy with sagittal and coronal MR imaging.* Radiology, 1993. **186**(3): p. 723-9.
9. NIDCR. *TMJ Disorders*. 2018 [cited 2018 2/20]; Available from: https://www.nidcr.nih.gov/health-info/tmj/tmj-disorders.
10. Chisnoiu, A.M., et al., *Factors involved in the etiology of temporomandibular disorders - a literature review.* Clujul Med, 2015. **88**(4): p. 473-8.
11. Sessle, B.J., *The Societal, political, educatinal, scientific and clinical context of orofacial pain*, in *Orofacial Pain: Recent Advances in Assessment, Management, and Understanding of Mechanisms*, B.J. Sessle, Editor. 2014, International Association for the Study of Pain: Washington, DC. p. 1-15.
12. Ohrbach, R. and S.F. Dworkin, *The Evolution of TMD Diagnosis: Past, Present, Future.* J Dent Res, 2016.
13. List, T. and R.H. Jensen, *Temporomandibular disorders: Old ideas and new concepts.* Cephalalgia, 2017: p. 333102416686302.
14. Tasaki, M.M., et al., *Classification and prevalence of temporomandibular joint disk displacement in patients and symptom-free volunteers.* Am J Orthod Dentofacial Orthop, 1996. **109**(3): p. 249-62.
15. Naeije, M., et al., *Disc displacement within the human temporomandibular joint: a systematic review of a 'noisy annoyance'.* J Oral Rehabil, 2013. **40**(2): p. 139-58.

16. Muller-Leisse, C., et al., *[Temporomandibular joint morphology and morphometric findings in relation to degree of disk displacement. Comparative magnetic resonance tomography studies]*. Radiologe, 1997. **37**(2): p. 152-8.
17. Jonsson, G., O. Eckerdal, and A. Isberg, *Thickness of the articular soft tissue of the temporal component in temporomandibular joints with and without disk displacement.* Oral Surg Oral Med Oral Pathol Oral Radiol Endod, 1999. **87**(1): p. 20-6.
18. Gallo, L.M., et al., *Relevance of mandibular helical axis analysis in functional and dysfunctional TMJs.* J Biomech, 2006. **39**(9): p. 1716-25.
19. Hattori-Hara, E., et al., *The influence of unilateral disc displacement on stress in the contralateral joint with a normally positioned disc in a human temporomandibular joint: An analytic approach using the finite element method.* J Craniomaxillofac Surg, 2014. **42**(8): p. 2018-24.
20. Roh, H.S., et al., *Relationships between disk displacement, joint effusion, and degenerative changes of the TMJ in TMD patients based on MRI findings.* J Craniomaxillofac Surg, 2012. **40**(3): p. 283-6.
21. Isberg, A. and P.L. Westesson, *Steepness of articular eminence and movement of the condyle and disk in asymptomatic temporomandibular joints.* Oral Surg Oral Med Oral Pathol Oral Radiol Endod, 1998. **86**(2): p. 152-7.
22. Wilkes, C.H., *Internal derangements of the temporomandibular joint. Pathological variations.* Arch Otolaryngol Head Neck Surg, 1989. **115**(4): p. 469-77.
23. Poveda Roda, R., et al., *Review of temporomandibular joint pathology. Part I: classification, epidemiology and risk factors.* Med Oral Patol Oral Cir Bucal, 2007. **12**(4): p. E292-8.
24. Wang, X.D., et al., *Current understanding of pathogenesis and treatment of TMJ osteoarthritis.* J Dent Res, 2015. **94**(5): p. 666-73.
25. Stegenga, B., L.G. de Bont, and G. Boering, *Osteoarthrosis as the cause of craniomandibular pain and dysfunction: a unifying concept.* J Oral Maxillofac Surg, 1989. **47**(3): p. 249-56.
26. Owen, A.H., 3rd, *Orthodontic/orthopedic treatment of craniomandibular pain dysfunction. Part 2: posterior condylar displacement.* J Craniomandibular Pract, 1984. **2**(4): p. 333-49.
27. Wang, M.Q., et al., *A preliminary anatomical study on the association of condylar and occlusal asymmetry.* Cranio, 2011. **29**(2): p. 111-6.
28. Yashiro, K., S. Miyawaki, and K. Takada, *Stabilization of jaw-closing movements during chewing after correction of incisor crossbite.* J Oral Rehabil, 2004. **31**(10): p. 949-56.
29. Fish, L.C. and B.N. Epker, *Surgical-orthodontic cephalometric prediction tracing.* J Clin Orthod, 1980. **14**(1): p. 36-52.
30. Bryan, D.C., *An investigation into the accuracy and validity of three points used in the assessment of autorotation in orthognathic surgery.* Br J Oral Maxillofac Surg, 1994. **32**(6): p. 363-72.

31. Schendel, S.A., et al., *Superior repositioning of the maxilla: stability and soft tissue osseous relations.* Am J Orthod, 1976. **70**(6): p. 663-74.
32. Wang, Y.C., et al., *The inter-relationship between mandibular autorotation and maxillary LeFort I impaction osteotomies.* J Craniofac Surg, 2006. **17**(5): p. 898-904.
33. Lindauer, S.J., et al., *Condylar movement and mandibular rotation during jaw opening.* Am J Orthod Dentofacial Orthop, 1995. **107**(6): p. 573-7.
34. Worms, F.W., et al., *Posttreatment stability and esthetics of orthognathic surgery.* Angle Orthod, 1980. **50**(4): p. 251-73.
35. Hobo, S., H.T. Shillingburg, Jr., and L.D. Whitsett, *Articulator selection for restorative dentistry.* J Prosthet Dent, 1976. **36**(1): p. 35-43.
36. Khawaja, S.N., et al., *Association between waking-state oral parafunctional behaviours and bio-psychosocial characteristics.* J Oral Rehabil, 2015. **42**(9): p. 651-6.
37. Michelotti, A., et al., *Oral parafunctions as risk factors for diagnostic TMD subgroups.* J Oral Rehabil, 2010. **37**(3): p. 157-62.
38. Hirose, M., et al., *Three-dimensional finite-element model of the human temporomandibular joint disc during prolonged clenching.* Eur J Oral Sci, 2006. **114**(5): p. 441-8.
39. eMedicineHealth. *Temporomandibular Joint (TMJ) Syndrome - Symptoms*. 2018 [cited 2018 26 Feb 2018]; Available from: http://www.emedicinehealth.com/temporomandibular_joint_tmj_syndrome/viewer-comments_em-78.htm.
40. Murphy, M.K., et al., *Temporomandibular disorders: a review of etiology, clinical management, and tissue engineering strategies.* Int J Oral Maxillofac Implants, 2013. **28**(6): p. e393-414.
41. Melis, M. and M.D. Giosia, *The role of genetic factors in the etiology of temporomandibular disorders: a review.* Cranio, 2014: p. 2151090314Y0000000027.
42. Oral, K., et al., *Etiology of temporomandibular disorder pain.* Agri, 2009. **21**(3): p. 89-94.
43. Grace, E.G. and A.F. North, *Temporomandibular joint dysfunction and orofacial pain caused by parotid gland malignancy: report of case.* J Am Dent Assoc, 1988. **116**(3): p. 348-50.
44. Bavitz, J.B. and L.C. Chewning, *Malignant disease as temporomandibular joint dysfunction: review of the literature and report of case.* J Am Dent Assoc, 1990. **120**(2): p. 163-6.
45. Huntley, T.A. and D. Wiesenfeld, *Delayed diagnosis of the cause of facial pain in patients with neoplastic disease: a report of eight cases.* J Oral Maxillofac Surg, 1994. **52**(1): p. 81-5.
46. Sharav, Y. and M. Feinsod, *Nasopharyngeal tumor initially manifested as myofascial pain dysfunction syndrome.* Oral Surg Oral Med Oral Pathol, 1977. **44**(1): p. 54-7.

47. Heo, M.S., et al., *Use of advanced imaging modalities for the differential diagnosis of pathoses mimicking temporomandibular disorders.* Oral Surg Oral Med Oral Pathol Oral Radiol Endod, 2003. **96**(5): p. 630-8.
48. Singh, S., B. Desai, and D. Laskin, *Metastatic melanoma misdiagnosed as a temporomandibular disorder: a case report and review of the literature.* J Am Dent Assoc, 2014. **145**(10): p. 1052-7.
49. Emanuelsson, J., et al., *Osteoblastoma of the temporal articular tubercle misdiagnosed as a temporomandibular joint disorder.* Int J Oral Maxillofac Surg, 2017. **46**(5): p. 610-613.
50. Gauer, R.L. and M.J. Semidey, *Diagnosis and treatment of temporomandibular disorders.* Am Fam Physician, 2015. **91**(6): p. 378-86.
51. Al-Jamali, J.M., et al., *Malignant tumors could be misinterpreted as temporomandibular joint disorders.* Oral Surg Oral Med Oral Pathol Oral Radiol, 2013. **116**(5): p. e362-7.
52. Dworkin, S.F. and L. LeResche, *Research diagnostic criteria for temporomandibular disorders: review, criteria, examinations and specifications, critique.* J Craniomandib Disord, 1992. **6**(4): p. 301-55.
53. Giraudeau, A., et al., *Disc displacement without reduction: a retrospective study of a clinical diagnostic sign.* Cranio, 2017. **35**(2): p. 86-93.
54. Rao, V.M., A. Farole, and D. Karasick, *Temporomandibular joint dysfunction: correlation of MR imaging, arthrography, and arthroscopy.* Radiology, 1990. **174**(3 Pt 1): p. 663-7.
55. Fernandez Sanroman, J., J.M. Gomez Gonzalez, and J.A. del Hoyo, *Relationship between condylar position, dentofacial deformity and temporomandibular joint dysfunction: an MRI and CT prospective study.* J Craniomaxillofac Surg, 1998. **26**(1): p. 35-42.
56. Augthun, M., et al., *Anterior disk displacement of the temporomandibular joint. Significance of clinical signs and symptoms in the diagnosis.* J Orofac Orthop, 1998. **59**(1): p. 39-46.
57. Gallo, L.M., K. Fushima, and S. Palla, *Mandibular helical axis pathways during mastication.* J Dent Res, 2000. **79**(8): p. 1566-72.
58. Gomes, L.R., et al., *Cone beam computed tomography-based models versus multislice spiral computed tomography-based models for assessing condylar morphology.* Oral Surg Oral Med Oral Pathol Oral Radiol, 2016. **121**(1): p. 96-105.
59. Zhang, Y., X. Xu, and Z. Liu, *Comparison of Morphologic Parameters of Temporomandibular Joint for Asymptomatic Subjects Using the Two-Dimensional and Three-Dimensional Measuring Methods.* J Healthc Eng, 2017. **2017**: p. 5680708.
60. Caruso, S., et al., *Temporomandibular Joint Anatomy Assessed by CBCT Images.* Biomed Res Int, 2017. **2017**: p. 2916953.
61. Hintze, H., M. Wiese, and A. Wenzel, *Cone beam CT and conventional tomography for the detection of morphological temporomandibular joint changes.* Dentomaxillofac Radiol, 2007. **36**(4): p. 192-7.

62. Yang, C., et al., *Magnetic resonance arthrography applied to the diagnosis of intraarticular adhesions of the temporomandibular joint.* Int J Oral Maxillofac Surg, 2005. **34**(7): p. 733-8.
63. Yen, P., et al., *Dynamic MR imaging of the temporomandibular joint using a balanced steady-state free precession sequence at 3T.* AJNR Am J Neuroradiol, 2013. **34**(3): p. E24-6.
64. Wang, E.Y., et al., *Dynamic sagittal half-Fourier acquired single-shot turbo spin-echo MR imaging of the temporomandibular joint: initial experience and comparison with sagittal oblique proton-attenuation images.* AJNR Am J Neuroradiol, 2007. **28**(6): p. 1126-32.
65. Krohn, S., et al., *Real-time MRI of the temporomandibular joint at 15 frames per second-A feasibility study.* Eur J Radiol, 2016. **85**(12): p. 2225-2230.
66. Chen, Y.J., et al., *Dynamic magnetic resonance imaging technique for the study of the temporomandibular joint.* J Orofac Pain, 2000. **14**(1): p. 65-73.
67. Brooks, S.L. and P.L. Westesson, *Temporomandibular joint: value of coronal MR images.* Radiology, 1993. **188**(2): p. 317-21.
68. Farina, D., et al., *TMJ disorders and pain: assessment by contrast-enhanced MRI.* Eur J Radiol, 2009. **70**(1): p. 25-30.
69. Kottke, R., et al., *Contrast-enhanced MRI of the temporomandibular joint: findings in children without juvenile idiopathic arthritis.* Acta Radiol, 2015. **56**(9): p. 1145-52.
70. Al-Saleh, M.A.Q., et al., *Usefulness of MRI-CBCT image registration in the evaluation of temporomandibular joint internal derangement by novice examiners.* Oral Surg Oral Med Oral Pathol Oral Radiol, 2017. **123**(2): p. 249-256.
71. Al-Saleh, M.A., et al., *Assessing the reliability of MRI-CBCT image registration to visualize temporomandibular joints.* Dentomaxillofac Radiol, 2015. **44**(6): p. 20140244.
72. Lin, Y.L., et al., *[Three-dimensional reconstruction of temporomandibular joint with CT and MRI medical image fusion technology]*. Hua Xi Kou Qiang Yi Xue Za Zhi, 2008. **26**(2): p. 140-3.
73. Dai, J., Y. Dong, and S.G. Shen, *Merging the computed tomography and magnetic resonance imaging images for the visualization of temporomandibular joint disk.* J Craniofac Surg, 2012. **23**(6): p. e647-8.
74. Shaffer, S.M., et al., *Temporomandibular disorders. Part 2: conservative management.* J Man Manip Ther, 2014. **22**(1): p. 13-23.
75. Okeson, J.P., *Management of Temporomandibular Disorders and Occlusion*. 7th ed. ed. 2012, St Louis, UNITED STATES: Elsevier Health Sciences. 500.
76. Gonzalez-Garcia, R., J.L. Gil-Diez Usandizaga, and F.J. Rodriguez-Campo, *Arthroscopic anatomy and lysis and lavage of the temporomandibular joint.* Atlas Oral Maxillofac Surg Clin North Am, 2011. **19**(2): p. 131-44.
77. Stark, T.R., C.V. Perez, and J.P. Okeson, *Recurrent TMJ Dislocation Managed with Botulinum Toxin Type A Injections in a Pediatric Patient.* Pediatr Dent, 2015. **37**(1): p. 65-9.

78. Roth, S.H., *Coming to terms with nonsteroidal anti-inflammatory drug gastropathy.* Drugs, 2012. **72**(7): p. 873-9.
79. Hawkey, C.J., *Nonsteroidal anti-inflammatory drug gastropathy.* Gastroenterology, 2000. **119**(2): p. 521-35.
80. FDA, U. *COX-2 Selective (includes Bextra, Celebrex, and Vioxx) and Non-Selective Non-Steroidal Anti-Inflammatory Drugs (NSAIDs).* 2005 [cited 2018 26 Feb 2018]; Available from: https://www.fda.gov/Drugs/DrugSafety/PostmarketDrugSafetyInformationforPatientsandProviders/ucm429364.htm.
81. Wolff, J., *Concept of the Law of Bone Remodelling*, in *The Law of Bone Remodelling*. 1986, Springer Berlin Heidelberg: Berlin, Heidelberg. p. 1-1.
82. Ikeda, M., et al., *Association between 3-dimensional mandibular morphology and condylar movement in subjects with mandibular asymmetry.* Am J Orthod Dentofacial Orthop, 2017. **151**(2): p. 324-334.
83. Kuroda, S., et al., *Biomechanical and biochemical characteristics of the mandibular condylar cartilage.* Osteoarthritis Cartilage, 2009. **17**(11): p. 1408-15.
84. Wang, Y., et al., *Tissue interaction is required for glenoid fossa development during temporomandibular joint formation.* Dev Dyn, 2011. **240**(11): p. 2466-73.
85. Iwasaki, L.R., et al., *TMJ energy densities in healthy men and women.* Osteoarthritis Cartilage, 2017.
86. Wright, G.J., et al., *Effect of mechanical strain on solute diffusion in human TMJ discs: an electrical conductivity study.* Ann Biomed Eng, 2013. **41**(11): p. 2349-57.
87. Stankovic, S., et al., *Morphological and biomechanical features of the temporomandibular joint disc: an overview of recent findings.* Arch Oral Biol, 2013. **58**(10): p. 1475-82.
88. Iwasaki, L.R., et al., *Human temporomandibular joint eminence shape and load minimization.* J Dent Res, 2010. **89**(7): p. 722-7.
89. Markova, M. and L.M. Gallo, *The influence of the human TMJ eminence inclination on predicted masticatory muscle forces.* Hum Mov Sci, 2016. **49**: p. 132-140.
90. Iwasaki, L.R., et al., *Neuromuscular objectives of the human masticatory apparatus during static biting.* Arch Oral Biol, 2003. **48**(11): p. 767-77.
91. Hansson, T., et al., *Thickness of the soft tissue layers and the articular disk in the temporomandibular joint.* Acta Odontol Scand, 1977. **35**(2): p. 77-83.
92. Singh, M. and M.S. Detamore, *Biomechanical properties of the mandibular condylar cartilage and their relevance to the TMJ disc.* J Biomech, 2009. **42**(4): p. 405-17.
93. Fang, W., et al., *Expression of chondromodulin-1 in the temporomandibular joint condylar cartilage and disc.* J Oral Pathol Med, 2010. **39**(4): p. 356-60.
94. Wang, L., M. Lazebnik, and M.S. Detamore, *Hyaline cartilage cells outperform mandibular condylar cartilage cells in a TMJ fibrocartilage tissue engineering application.* Osteoarthritis Cartilage, 2009. **17**(3): p. 346-53.

95. Almarza, A.J. and K.A. Athanasiou, *Design characteristics for the tissue engineering of cartilaginous tissues.* Ann Biomed Eng, 2004. **32**(1): p. 2-17.
96. Tanaka, E., et al., *The effect of experimental cartilage damage and impairment and restoration of synovial lubrication on friction in the temporomandibular joint.* J Orofac Pain, 2005. **19**(4): p. 331-6.
97. Tanaka, E., et al., *Dynamic compressive properties of the mandibular condylar cartilage.* J Dent Res, 2006. **85**(6): p. 571-5.
98. Singh, M. and M.S. Detamore, *Tensile properties of the mandibular condylar cartilage.* J Biomech Eng, 2008. **130**(1): p. 011009.
99. Singh, M. and M.S. Detamore, *Stress relaxation behavior of mandibular condylar cartilage under high-strain compression.* J Biomech Eng, 2009. **131**(6): p. 061008.
100. Hansson, T. and B. Nordstrom, *Thickness of the soft tissue layers and articular disk in temporomandibular joints with deviations in form.* Acta Odontol Scand, 1977. **35**(6): p. 281-8.
101. Ateshian, G.A., L.J. Soslowsky, and V.C. Mow, *Quantitation of articular surface topography and cartilage thickness in knee joints using stereophotogrammetry.* J Biomech, 1991. **24**(8): p. 761-76.
102. Eckstein, F., D. Burstein, and T.M. Link, *Quantitative MRI of cartilage and bone: degenerative changes in osteoarthritis.* NMR Biomed, 2006. **19**(7): p. 822-54.
103. Jurvelin, J.S., et al., *Comparison of optical, needle probe and ultrasonic techniques for the measurement of articular cartilage thickness.* J Biomech, 1995. **28**(2): p. 231-5.
104. Swann, A.C. and B.B. Seedhom, *Improved techniques for measuring the indentation and thickness of articular cartilage.* Proc Inst Mech Eng H, 1989. **203**(3): p. 143-50.
105. Alomar, X., et al., *Anatomy of the temporomandibular joint.* Semin Ultrasound CT MR, 2007. **28**(3): p. 170-83.
106. Wright, G.J., et al., *Tensile biomechanical properties of human temporomandibular joint disc: Effects of direction, region and sex.* J Biomech, 2016. **49**(16): p. 3762-3769.
107. Detamore, M.S. and K.A. Athanasiou, *Motivation, characterization, and strategy for tissue engineering the temporomandibular joint disc.* Tissue Eng, 2003. **9**(6): p. 1065-87.
108. Dolwick, M.F., et al., *Sagittal anatomy of the human temporomandibular joint spaces: normal and abnormal findings.* J Oral Maxillofac Surg, 1983. **41**(2): p. 86-8.
109. Tanaka, E., et al., *Lubrication of the temporomandibular joint.* Ann Biomed Eng, 2008. **36**(1): p. 14-29.
110. Wu, Y., et al., *Viscoelastic shear properties of porcine temporomandibular joint disc.* Orthod Craniofac Res, 2015. **18 Suppl 1**: p. 156-63.
111. Coombs, M.C., et al., *Structure-Function Relationships of Temporomandibular Retrodiscal Tissue.* J Dent Res, 2017. **96**(6): p. 647-653.

112. Makris, E.A., P. Hadidi, and K.A. Athanasiou, *The knee meniscus: structure-function, pathophysiology, current repair techniques, and prospects for regeneration.* Biomaterials, 2011. **32**(30): p. 7411-31.
113. Bird, M.D. and M.B. Sweet, *A system of canals in semilunar menisci.* Ann Rheum Dis, 1987. **46**(9): p. 670-3.
114. Nickel, J.C. and K.R. McLachlan, *An analysis of surface congruity in the growing human temporomandibular joint.* Arch Oral Biol, 1994. **39**(4): p. 315-21.
115. Fujikawa, K., B.B. Seedhom, and V. Wright, *Biomechanics of the patello-femoral joint. Part I: A study of the contact and the congruity of the patello-femoral compartment and movement of the patella.* Eng Med, 1983. **12**(1): p. 3-11.
116. Nickel, J.C. and K.R. McLachlan, *In vitro measurement of the stress-distribution properties of the pig temporomandibular joint disc.* Arch Oral Biol, 1994. **39**(5): p. 439-48.
117. Stohler, C., Y. Yamada, and M.M. Ash, Jr., *Antagonistic muscle stiffness and associated reflex behaviour in the pain-dysfunctional state.* Schweiz Monatsschr Zahnmed (1984), 1985. **95**(8): p. 719-26.
118. van Eijden, T.M., J.H. Koolstra, and P. Brugman, *Three-dimensional structure of the human temporalis muscle.* Anat Rec, 1996. **246**(4): p. 565-72.
119. Westesson, P.L., S.L. Bronstein, and J. Liedberg, *Internal derangement of the temporomandibular joint: morphologic description with correlation to joint function.* Oral Surg Oral Med Oral Pathol, 1985. **59**(4): p. 323-31.
120. de Farias, J.F., et al., *Correlation between temporomandibular joint morphology and disc displacement by MRI.* Dentomaxillofac Radiol, 2015. **44**(7): p. 20150023.
121. Murakami, S., et al., *Magnetic resonance evaluation of the temporomandibular joint disc position and configuration.* Dentomaxillofac Radiol, 1993. **22**(4): p. 205-7.
122. Taskaya-Yilmaz, N. and M. Ogutcen-Toller, *Magnetic resonance imaging evaluation of temporomandibular joint disc deformities in relation to type of disc displacement.* J Oral Maxillofac Surg, 2001. **59**(8): p. 860-5; discussion 865-6.
123. Vieira-Queiroz, I., et al., *Biometric parameters of the temporomandibular joint and association with disc displacement and pain: a magnetic resonance imaging study.* Int J Oral Maxillofac Surg, 2013. **42**(6): p. 765-70.
124. Sulun, T., et al., *Axial condyle morphology and horizontal condylar angle in patients with internal derangement compared to asymptomatic volunteers.* Cranio, 2001. **19**(4): p. 237-45.
125. Oberg, T., G.E. Carlsson, and C.M. Fajers, *The temporomandibular joint. A morphologic study on a human autopsy material.* Acta Odontol Scand, 1971. **29**(3): p. 349-84.
126. Stratmann, U., K. Schaarschmidt, and P. Santamaria, *Morphometric investigation of condylar cartilage and disc thickness in the human temporomandibular joint: significance for the definition of ostearthrotic changes.* J Oral Pathol Med, 1996. **25**(5): p. 200-5.

127. Kurita, K., et al., *Histologic features of the temporomandibular joint disk and posterior disk attachment: comparison of symptom-free persons with normally positioned disks and patients with internal derangement.* Oral Surg Oral Med Oral Pathol, 1989. **67**(6): p. 635-43.
128. Lemke, A.J., et al., *[Morphometric analysis of the temporomandibular joint with MRI in 320 joints]*. Rofo, 2005. **177**(2): p. 217-28.
129. Peroz, I., et al., *MRI of the TMJ: morphometric comparison of asymptomatic volunteers and symptomatic patients.* Quintessence Int, 2011. **42**(8): p. 659-67.
130. Wang, M.Q., et al., *The effect of physiological nonbalanced occlusion on the thickness of the temporomandibular joint disc: a pilot autopsy study.* J Prosthet Dent, 2008. **99**(2): p. 148-52.
131. Orhan, K., et al., *Comparison of altered signal intensity, position, and morphology of the TMJ disc in MR images corrected for variations in surface coil sensitivity.* Oral Surg Oral Med Oral Pathol Oral Radiol Endod, 2006. **101**(4): p. 515-22.
132. Yang, Z.J., et al., *Magnetic resonance imaging of temporomandibular joint: morphometric study of asymptomatic volunteers.* J Craniofac Surg, 2015. **26**(2): p. 425-9.
133. Fernandez Sanroman, J., et al., *Morphometric and morphological changes in the temporomandibular joint after orthognathic surgery: a magnetic resonance imaging and computed tomography prospective study.* J Craniomaxillofac Surg, 1997. **25**(3): p. 139-48.
134. Pullinger, A.G. and D.A. Seligman, *Multifactorial analysis of differences in temporomandibular joint hard tissue anatomic relationships between disk displacement with and without reduction in women.* J Prosthet Dent, 2001. **86**(4): p. 407-19.
135. Pullinger, A.G., et al., *Multifactorial comparison of disk displacement with and without reduction to normals according to temporomandibular joint hard tissue anatomic relationships.* J Prosthet Dent, 2002. **87**(3): p. 298-310.
136. Pedulla, E., et al., *Morphometric evaluation of the temporomandibular joint and the masticatory spaces: the role of high-definition MRI.* Minerva Stomatol, 2009. **58**(4): p. 127-43.
137. Torres, M.G., et al., *Morphometric features of the mandibular condyle and association with disk abnormalities.* Oral Surg Oral Med Oral Pathol Oral Radiol, 2016. **121**(5): p. 566-72.
138. Coogan, J.S., et al., *Determination of sex differences of human cadaveric mandibular condyles using statistical shape and trait modeling.* Bone, 2018. **106**: p. 35-41.
139. Chen, Y.J., et al., *Individualized oblique-axial magnetic resonance imaging for improved visualization of mediolateral TMJ disc displacement.* J Orofac Pain, 2000. **14**(2): p. 128-39.
140. Chen, Y.J., L.M. Gallo, and S. Palla, *The mediolateral temporomandibular joint disc position: an in vivo quantitative study.* J Orofac Pain, 2002. **16**(1): p. 29-38.

141. Wang, M., et al., *Magnetic resonance imaging on TMJ disc thickness in TMD patients: a pilot study*. J Prosthet Dent, 2009. **102**(2): p. 89-93.
142. Almasan, O.C., et al., *Disk and joint morphology variations on coronal and sagittal MRI in temporomandibular joint disorders.* Clin Oral Investig, 2013. **17**(4): p. 1243-50.
143. Hilgers, M.L., et al., *Accuracy of linear temporomandibular joint measurements with cone beam computed tomography and digital cephalometric radiography.* Am J Orthod Dentofacial Orthop, 2005. **128**(6): p. 803-11.
144. Schilling, J., et al., *Regional 3D superimposition to assess temporomandibular joint condylar morphology*. Dentomaxillofac Radiol, 2014. **43**(1): p. 20130273.
145. Styner, M., et al., *Framework for the Statistical Shape Analysis of Brain Structures using SPHARM-PDM.* Insight J, 2006(1071): p. 242-250.
146. Alhadidi, A., et al., *3D quantification of mandibular asymmetry using the SPHARM-PDM tool box.* Int J Comput Assist Radiol Surg, 2012. **7**(2): p. 265-71.
147. Gomes, L.R., et al., *Diagnostic index of 3D osteoarthritic changes in TMJ condylar morphology.* Proc SPIE Int Soc Opt Eng, 2015. **9414**.
148. Carvalho Fde, A., et al., *Three-dimensional assessment of mandibular advancement 1 year after surgery*. Am J Orthod Dentofacial Orthop, 2010. **137**(4 Suppl): p. S53 e1-12; discussion S53-5.
149. Kurita, H., et al., *Is the morphology of the articular eminence of the temporomandibular joint a predisposing factor for disc displacement?* Dentomaxillofac Radiol, 2000. **29**(3): p. 159-62.
150. Corbett, N.E., et al., *The relation of the condylar path to the articular eminence in mandibular protrusion.* Angle Orthod, 1971. **41**(4): p. 286-92.
151. Kerstens, H.C., et al., *Inclination of the temporomandibular joint eminence and anterior disc displacement.* Int J Oral Maxillofac Surg, 1989. **18**(4): p. 228-32.
152. Kerstens, H.C., D.B. Tuinzing, and W.A. van der Kwast, *Eminectomy and discoplasty for correction of the displaced temporomandibular joint disc.* J Oral Maxillofac Surg, 1989. **47**(2): p. 150-4.
153. Ren, Y.F., A. Isberg, and P.L. Westesson, *Steepness of the articular eminence in the temporomandibular joint. Tomographic comparison between asymptomatic volunteers with normal disk position and patients with disk displacement.* Oral Surg Oral Med Oral Pathol Oral Radiol Endod, 1995. **80**(3): p. 258-66.
154. Ilguy, D., et al., *Articular eminence inclination, height, and condyle morphology on cone beam computed tomography.* ScientificWorldJournal, 2014. **2014**: p. 761714.
155. Panmekiate, S., A. Petersson, and S. Akerman, *Angulation and prominence of the posterior slope of the eminence of the temporomandibular joint in relation to disc position.* Dentomaxillofac Radiol, 1991. **20**(4): p. 205-8.
156. Rabelo, K.A., et al., *Condyle Excursion Angle, Articular Eminence Inclination, and Temporomandibular Joint Morphologic Relations With Disc Displacement.* J Oral Maxillofac Surg, 2017. **75**(5): p. 938 e1-938 e10.
157. Atkinson, W.B. and R.E. Bates, Jr., *The effects of the angle of the articular eminence on anterior disk displacement.* J Prosthet Dent, 1983. **49**(4): p. 554-5.

158. Gokalp, H., H. Turkkahraman, and N. Bzeizi, *Correlation between eminence steepness and condyle disc movements in temporomandibular joints with internal derangements on magnetic resonance imaging.* Eur J Orthod, 2001. **23**(5): p. 579-84.
159. Sulun, T., et al., *Morphology of the mandibular fossa and inclination of the articular eminence in patients with internal derangement and in symptom-free volunteers.* Oral Surg Oral Med Oral Pathol Oral Radiol Endod, 2001. **92**(1): p. 98-107.
160. Galante, G., et al., *Angle of the articular eminence in patients with temporomandibular joint dysfunction and asymptomatic volunteers.* Oral Surg Oral Med Oral Pathol Oral Radiol Endod, 1995. **80**(2): p. 242-9.
161. Seward, F.S., *Tooth attrition and the temporomandibular joint.* Angle Orthod, 1976. **46**(2): p. 162-70.
162. Standring, S., *Gray's anatomy : the anatomical basis of clinical practice*. 2016, Elsevier Limited: New York :.
163. Antonopoulou, M., et al., *Variations of the attachment of the superior head of human lateral pterygoid muscle.* J Craniomaxillofac Surg, 2013. **41**(6): p. e91-7.
164. Litko, M., et al., *Correlation between the lateral pterygoid muscle attachment type and temporomandibular joint disc position in magnetic resonance imaging.* Dentomaxillofac Radiol, 2016. **45**(8): p. 20160229.
165. Imanimoghaddam, M., A.S. Madani, and E.M. Hashemi, *The evaluation of lateral pterygoid muscle pathologic changes and insertion patterns in temporomandibular joints with or without disc displacement using magnetic resonance imaging.* Int J Oral Maxillofac Surg, 2013. **42**(9): p. 1116-20.
166. Hasegawa, H., et al., *Condylar shape in relation to anterior disk displacement in juvenile females.* Cranio, 2011. **29**(2): p. 100-10.
167. Rao, V.M., et al., *Altered condylar morphology associated with disc displacement in TMJ dysfunction: observations by MRI.* Magn Reson Imaging, 1990. **8**(3): p. 231-5.
168. Legrell, P.E., et al., *Temporomandibular joint condyle changes after surgically induced non-reducing disk displacement in rabbits: a macroscopic and microscopic study.* Acta Odontol Scand, 1999. **57**(5): p. 290-300.
169. Dupuy-Bonafe, I., et al., *Biometry of the temporomandibular joint using computerized tomography.* Surg Radiol Anat, 2014. **36**(9): p. 933-9.
170. Sumbullu, M.A., et al., *Radiological examination of the articular eminence morphology using cone beam CT.* Dentomaxillofac Radiol, 2012. **41**(3): p. 234-40.
171. Almarza, A.J., C.K. Hagandora, and S.E. Henderson, *Animal models of temporomandibular joint disorders: implications for tissue engineering approaches.* Ann Biomed Eng, 2011. **39**(10): p. 2479-90.
172. Shi, C., et al., *Relationship between anisotropic diffusion properties and tissue morphology in porcine TMJ disc.* Osteoarthritis Cartilage, 2013. **21**(4): p. 625-33.
173. Kalpakci, K.N., et al., *An interspecies comparison of the temporomandibular joint disc.* J Dent Res, 2011. **90**(2): p. 193-8.

174. Nickel, J., et al., *Static and dynamic mechanics of the temporomandibular joint: plowing forces, joint load and tissue stress.* Orthod Craniofac Res, 2009. **12**(3): p. 159-67.
175. Herring, S.W., *TMJ anatomy and animal models.* J Musculoskelet Neuronal Interact, 2003. **3**(4): p. 391-4; discussion 406-7.
176. Matuska, A.M., et al., *Biomechanical and biochemical outcomes of porcine temporomandibular joint disc deformation.* Arch Oral Biol, 2016. **64**: p. 72-9.
177. Orset, E., P. Chaffanjon, and G. Bettega, *Temporomandibular joint model: anatomic and radiologic comparison between rat and human.* Surg Radiol Anat, 2014. **36**(2): p. 163-6.
178. Stembirek, J., et al., *The pig as an experimental model for clinical craniofacial research.* Lab Anim, 2012. **46**(4): p. 269-79.
179. Herring, S.W., et al., *Temporomandibular joint in miniature pigs: anatomy, cell replication, and relation to loading.* Anat Rec, 2002. **266**(3): p. 152-66.
180. Nishi, S.E., R. Basri, and M.K. Alam, *Uses of electromyography in dentistry: An overview with meta-analysis.* Eur J Dent, 2016. **10**(3): p. 419-25.
181. Cifrek, M., et al., *Surface EMG based muscle fatigue evaluation in biomechanics.* Clin Biomech (Bristol, Avon), 2009. **24**(4): p. 327-40.
182. Blanco Aguilera, A., et al., *Relationship between self-reported sleep bruxism and pain in patients with temporomandibular disorders.* J Oral Rehabil, 2014. **41**(8): p. 564-72.
183. Raphael, K.G., et al., *Masticatory muscle sleep background electromyographic activity is elevated in myofascial temporomandibular disorder patients.* J Oral Rehabil, 2013. **40**(12): p. 883-91.
184. Nickel, J.C. and K.R. McLachlan, *In vitro measurement of the frictional properties of the temporomandibular joint disc.* Arch Oral Biol, 1994. **39**(4): p. 323-31.
185. Iwasaki, L.R., et al., *A pilot study of ambulatory masticatory muscle activities in temporomandibular joint disorders diagnostic groups.* Orthod Craniofac Res, 2015. **18 Suppl 1**: p. 146-55.
186. Glaros, A.G., K.N. Tabacchi, and E.G. Glass, *Effect of parafunctional clenching on TMD pain.* J Orofac Pain, 1998. **12**(2): p. 145-52.
187. Hodges, P.W. and B.H. Bui, *A comparison of computer-based methods for the determination of onset of muscle contraction using electromyography.* Electroencephalogr Clin Neurophysiol, 1996. **101**(6): p. 511-9.
188. Reding, G.R., et al., *Nocturnal teeth-grinding: all-night psychophysiologic studies.* J Dent Res, 1968. **47**(5): p. 786-97.
189. Rugh, J.D. and W.K. Solberg, *Electromyographic studies of bruxist behavior before and during treatment.* J Calif Dent Assoc, 1975. **3**(9): p. 56-9.
190. Wagner, M.T., *Controlling nocturnal bruxism through the use of aversive conditioning during sleep.* American Journal of Clinical Biofeedback, 1981. **4**(2): p. 87-92.
191. Piccione, A., et al., *Nocturnal biofeedback for nocturnal bruxism.* Biofeedback Self Regul, 1982. **7**(4): p. 405-19.

192. Stock, P. and N.G. Clarke, *Monitoring bruxism.* Med Biol Eng Comput, 1983. **21**(3): p. 295-300.
193. Ware, J.C. and J.D. Rugh, *Destructive bruxism: sleep stage relationship.* Sleep, 1988. **11**(2): p. 172-81.
194. Okeson, J.P., et al., *Nocturnal bruxing events in healthy geriatric subjects.* J Oral Rehabil, 1990. **17**(5): p. 411-8.
195. Okeson, J.P., et al., *Nocturnal bruxing events in subjects with sleep-disordered breathing and control subjects.* J Craniomandib Disord, 1991. **5**(4): p. 258-64.
196. Okeson, J.P., et al., *Nocturnal bruxing events: a report of normative data and cardiovascular response.* J Oral Rehabil, 1994. **21**(6): p. 623-30.
197. Velly-Miguel, A.M., et al., *Bruxism and other orofacial movements during sleep.* J Craniomandib Dis Fac Oral Pain, 1992. **6**(1): p. 71-81.
198. Kondo, K. and G. Clark, *A method for detecting a bruxism event.* J Dent Res, 1991. **70**: p. 512.
199. Gallo, L.M., S.S. Gross, and S. Palla, *Nocturnal masseter EMG activity of healthy subjects in a natural environment.* J Dent Res, 1999. **78**(8): p. 1436-44.
200. Nitschke, I., et al., *Nocturnal masseter electromyographic activity of complete denture wearers.* Gerodontology, 2012. **29**(2): p. e595-601.
201. Lavigne, G.J., P.H. Rompre, and J.Y. Montplaisir, *Sleep bruxism: validity of clinical research diagnostic criteria in a controlled polysomnographic study.* J Dent Res, 1996. **75**(1): p. 546-52.
202. Raphael, K.G., et al., *Sleep bruxism and myofascial temporomandibular disorders: a laboratory-based polysomnographic investigation.* J Am Dent Assoc, 2012. **143**(11): p. 1223-31.
203. Gohdo, Y. and M. Fujisawa, *Determination of Electromyogram Biofeedback Threshold for Patients with Clenching Behavior.* Prosthodontic Research & Practice, 2004. **3**(1): p. 46-54.
204. Fujisawa, M., et al., *Determination of daytime clenching events in subjects with and without self-reported clenching.* J Oral Rehabil, 2013. **40**(10): p. 731-6.
205. Camparis, C.M., et al., *Sleep bruxism and temporomandibular disorder: Clinical and polysomnographic evaluation.* Arch Oral Biol, 2006. **51**(9): p. 721-8.
206. Rossetti, L.M., et al., *Association between rhythmic masticatory muscle activity during sleep and masticatory myofascial pain: a polysomnographic study.* J Orofac Pain, 2008. **22**(3): p. 190-200.
207. Rossetti, L.M., et al., *Association between sleep bruxism and temporomandibular disorders: a polysomnographic pilot study.* Cranio, 2008. **26**(1): p. 16-24.
208. Schmitter, M., et al., *Sleep-associated aspects of myofascial pain in the orofacial area among Temporomandibular Disorder patients and controls.* Sleep Med, 2015. **16**(9): p. 1056-61.
209. Okeson, J.P., *Orthodontic therapy and the patient with temporomandibular disorder,* in *Orthodontics-E-Book: Current Principles and Techniques*, R.L.V. Lee W. Graber, Katherine W. L. Vig, Greg J. Huang, Editor. 2016, Mosby: St. Louis. p. 353-366.

210. Sun, Q., et al., *Dynamic MR imaging of temporomandibular joint: an initial assessment with fast imaging employing steady-state acquisition sequence.* Magn Reson Imaging, 2015. **33**(3): p. 270-5.
211. Krohn, S., et al., *Diagnosis of disk displacement using real-time MRI: Clinical report of two patients.* J Prosthet Dent, 2017.
212. Ugolini, A., et al., *Kinematic analysis of mandibular motion before and after orthognathic surgery for skeletal Class III malocclusion: A pilot study.* Cranio, 2017. **35**(2): p. 94-100.
213. Mapelli, A., et al., *Three-dimensional analysis of jaw kinematic alterations in patients with chronic TMD - disc displacement with reduction.* J Oral Rehabil, 2016. **43**(11): p. 824-832.
214. Takeda, H., et al., *Examination of masticatory movement and rhythm before and after surgical orthodontics in skeletal Class III patients with unilateral posterior cross-bite.* J Oral Maxillofac Surg, 2009. **67**(9): p. 1844-9.
215. D., T. and H. D., *Specialty imaging. temporomandibular joint.* 1st edition ed. 2016, Philadelphia, PA: Elsevier.
216. Sinn, D.P., E.A. de Assis, and G.S. Throckmorton, *Mandibular excursions and maximum bite forces in patients with temporomandibular joint disorders.* J Oral Maxillofac Surg, 1996. **54**(6): p. 671-9.
217. Travers, K.H., et al., *Associations between incisor and mandibular condylar movements during maximum mouth opening in humans.* Arch Oral Biol, 2000. **45**(4): p. 267-75.
218. Buschang, P.H., et al., *Incisor and mandibular condylar movements of young adult females during maximum protrusion and lateratrusion of the jaw.* Arch Oral Biol, 2001. **46**(1): p. 39-48.
219. Salaorni, C. and S. Palla, *Condylar rotation and anterior translation in healthy human temporomandibular joints.* Schweiz Monatsschr Zahnmed, 1994. **104**(4): p. 415-22.
220. Agerberg, G., *Maximal mandibular movements in young men and women.* Sven Tandlak Tidskr, 1974. **67**(2): p. 81-100.
221. Reicheneder, C., et al., *Comparison of maximum mouth-opening capacity and condylar path length in adults and children during the growth period.* Ann Anat, 2008. **190**(4): p. 344-50.
222. Larheim, T.A. and F. Floystrand, *Temporomandibular joint abnormalities and bite force in a group of adults with rheumatoid arthritis.* J Oral Rehabil, 1985. **12**(6): p. 477-82.
223. Szentpetery, A., *Clinical utility of mandibular movement ranges.* J Orofac Pain, 1993. **7**(2): p. 163-8.
224. Theusner, J., et al., *Axiographic tracings of temporomandibular joint movements.* J Prosthet Dent, 1993. **69**(2): p. 209-15.
225. Lewis, R.P., P.H. Buschang, and G.S. Throckmorton, *Sex differences in mandibular movements during opening and closing.* Am J Orthod Dentofacial Orthop, 2001. **120**(3): p. 294-303.

226. Mohl, N.D., et al., *Devices for the diagnosis and treatment of temporomandibular disorders. Part I: Introduction, scientific evidence, and jaw tracking.* J Prosthet Dent, 1990. **63**(2): p. 198-201.
227. Soboleva, U., L. Laurina, and A. Slaidina, *Jaw tracking devices--historical review of methods development. Part I.* Stomatologija, 2005. **7**(3): p. 67-71.
228. Soboleva, U., L. Laurina, and A. Slaidina, *Jaw tracking devices--historical review of methods development. Part II.* Stomatologija, 2005. **7**(3): p. 72-6.
229. Balch, J.H., *Verification of the Accuracy of Electronic Mandibular Movement Recording Devices: : An in vitro investigation*, in *Prosthodontics*. 2012, The University of Tennessee Health Science Center.
230. Posselt, U., *Terminal hinge movement of the mandible. 1957.* J Prosthet Dent, 2001. **86**(1): p. 2-9.
231. Celar, A.G. and K. Tamaki, *Accuracy of recording horizontal condylar inclination and Bennett angle with the Cadiax compact.* J Oral Rehabil, 2002. **29**(11): p. 1076-81.
232. Hanssen, N., S. Ruge, and B. Kordass, *SICAT function: anatomical real-dynamic articulation by merging cone beam computed tomography and jaw motion tracking data.* Int J Comput Dent, 2014. **17**(1): p. 65-74.
233. Kordass, B. and S. Ruge, *On the analysis of condylar path versus real motion of the temporomandibular joint: application for Sicat Function.* Int J Comput Dent, 2015. **18**(3): p. 225-35.
234. He, S., et al., *The use of a dynamic real-time jaw tracking device and cone beam computed tomography simulation.* Ann Maxillofac Surg, 2016. **6**(1): p. 113-9.
235. He, S. and C.H. Kau, *Dynamic Motion Capture of the Mandible*, in *Digital Planning and Custom Orthodontic Treatment*. 2017, John Wiley & Sons, Inc. p. 15-26.
236. Aslanidou, K., et al., *The fabrication of a customized occlusal splint based on the merging of dynamic jaw tracking records, cone beam computed tomography, and CAD-CAM digital impression.* J Orthod Sci, 2017. **6**(3): p. 104-109.
237. Michler, L., M. Bakke, and E. Moller, *Graphic assessment of natural mandibular movements.* J Craniomandib Disord, 1987. **1**(2): p. 97-114.
238. Pinheiro, P.F., Jr., et al., *The use of electrognathography in jaw movement research: a literature review.* Cranio, 2012. **30**(4): p. 293-303.
239. Hamborg, R. and S. Karlsson, *Movement and signal analysis by means of a computer-assisted system.* J Oral Rehabil, 1996. **23**(2): p. 121-8.
240. Hannam, A.G., et al., *The kinesiographic measurement of jaw displacement.* J Prosthet Dent, 1980. **44**(1): p. 88-93.
241. Balkhi, K.M., et al., *Error analysis of a magnetic jaw-tracking device.* J Craniomandib Disord, 1991. **5**(1): p. 51-6.
242. Baltali, E., et al., *Accuracy and precision of a method to study kinematics of the temporomandibular joint: combination of motion data and CT imaging.* J Biomech, 2008. **41**(11): p. 2581-4.
243. Palla, S., L.M. Gallo, and D. Gossi, *Dynamic stereometry of the temporomandibular joint.* Orthod Craniofac Res, 2003. **6 Suppl 1**: p. 37-47.

244. Airoldi, R.L., L.M. Gallo, and S. Palla, *Precision of the jaw tracking system JAWS-3D.* J Orofac Pain, 1994. **8**(2): p. 155-64.
245. Naeije, M., J.J. Van der Weijden, and C.C. Megens, *OKAS-3D: optoelectronic jaw movement recording system with six degrees of freedom.* Med Biol Eng Comput, 1995. **33**(5): p. 683-8.
246. Fang, J.J. and T.H. Kuo, *Modelling of mandibular movement.* Comput Biol Med, 2008. **38**(11-12): p. 1152-62.
247. De Felicio, C.M., et al., *Mandibular kinematics and masticatory muscles EMG in patients with short lasting TMD of mild-moderate severity.* J Electromyogr Kinesiol, 2013. **23**(3): p. 627-33.
248. Mapelli, A., *Temporomandibular joint in health and disease: a 3d morphofunctional analysis*, in *Physiological and sports department of human morphology and biomedical sciences*. 2012, Università degli Studi di Milano.
249. Jankelson, B., et al., *Kinesiometric instrumentation: a new technology.* J Am Dent Assoc, 1975. **90**(4): p. 834-40.
250. Jemt, T. and B. Hedegard, *The relative movements of the chin and the mandible during chewing.* J Oral Rehabil, 1982. **9**(3): p. 253-8.
251. Sforza, C., et al., *Three-dimensional mandibular motion after closed and open reduction of unilateral mandibular condylar process fractures.* J Craniomaxillofac Surg, 2011. **39**(4): p. 249-55.
252. Hannam, A.G., J.D. Scott, and R.E. De Cou, *A computer-based system for the simultaneous measurement of muscle activity and jaw movement during mastication in man.* Arch Oral Biol, 1977. **22**(1): p. 17-23.
253. Mapelli, A., et al., *Translation and rotation movements of the mandible during mouth opening and closing.* Clin Anat, 2009. **22**(3): p. 311-8.
254. Markelj, P., et al., *A review of 3D/2D registration methods for image-guided interventions.* Med Image Anal, 2012. **16**(3): p. 642-61.
255. Maintz, J.B. and M.A. Viergever, *A survey of medical image registration.* Med Image Anal, 1998. **2**(1): p. 1-36.
256. Krebs, M., et al., *A new method for three-dimensional reconstruction and animation of the temporomandibular joint.* Ann Acad Med Singapore, 1995. **24**(1): p. 11-6.
257. Hamming, N.M., et al., *Automatic image-to-world registration based on x-ray projections in cone-beam CT-guided interventions.* Med Phys, 2009. **36**(5): p. 1800-12.
258. Bailey, J.O., Jr., W.D. McCall, Jr., and M.M. Ash, Jr., *Electromyographic silent periods and jaw motion parameters: quantitative measures of temporomandibular joint dysfunction.* J Dent Res, 1977. **56**(3): p. 249-53.
259. McCall, W.D., Jr., J.O. Bailey, Jr., and M.M. Ash, Jr., *A quantitative measure of mandibular joint dysfunction: phase plane modelling of jaw movement in man.* Arch Oral Biol, 1976. **21**(11): p. 685-9.
260. Howell, P.G., et al., *The recording and analysis of EMG and jaw tracking. I. The recording procedure.* J Oral Rehabil, 1992. **19**(6): p. 595-605.

261. Amemori, Y., et al., *Influence of nocturnal bruxism on the stomatognathic system. Part I: a new device for measuring mandibular movements during sleep.* J Oral Rehabil, 2001. **28**(10): p. 943-9.
262. Sforza, C., et al., *Mandibular movements at maximum mouth opening and EMG activity of masticatory and neck muscles in patients rehabilitated after a mandibular condyle fracture.* J Craniomaxillofac Surg, 2009. **37**(6): p. 327-33.
263. Shimada, A., L. Baad-Hansen, and P. Svensson, *Effect of experimental jaw muscle pain on dynamic bite force during mastication.* Arch Oral Biol, 2015. **60**(2): p. 256-66.
264. Shimada, A., et al., *Measurement of dynamic bite force during mastication.* J Oral Rehabil, 2012. **39**(5): p. 349-56.
265. Okura, K., et al., *Mandibular movement during sleep bruxism associated with current tooth attrition.* J Prosthodont Res, 2017. **61**(1): p. 87-95.
266. Merlini, L. and S. Palla, *The relationship between condylar rotation and anterior translation in healthy and clicking temporomandibular joints.* Schweiz Monatsschr Zahnmed, 1988. **98**(11): p. 1191-9.
267. Grood, E.S. and W.J. Suntay, *A joint coordinate system for the clinical description of three-dimensional motions: application to the knee.* J Biomech Eng, 1983. **105**(2): p. 136-44.
268. Cole, G.K., et al., *Application of the joint coordinate system to three-dimensional joint attitude and movement representation: a standardization proposal.* J Biomech Eng, 1993. **115**(4A): p. 344-9.
269. Wu, G., et al., *ISB recommendation on definitions of joint coordinate system of various joints for the reporting of human joint motion--part I: ankle, hip, and spine. International Society of Biomechanics.* J Biomech, 2002. **35**(4): p. 543-8.
270. Wu, G., et al., *ISB recommendation on definitions of joint coordinate systems of various joints for the reporting of human joint motion--Part II: shoulder, elbow, wrist and hand.* J Biomech, 2005. **38**(5): p. 981-992.
271. Baker, R., *ISB recommendation on definition of joint coordinate systems for the reporting of human joint motion-part I: ankle, hip and spine.* J Biomech, 2003. **36**(2): p. 300-2; author reply 303-4.
272. Dixon, P.C., et al., *biomechZoo: An open-source toolbox for the processing, analysis, and visualization of biomechanical movement data.* Comput Methods Programs Biomed, 2017. **140**: p. 1-10.
273. Leader, J.K., et al., *Mandibular kinematics represented by a non-orthogonal floating axis joint coordinate system.* J Biomech, 2003. **36**(2): p. 275-81.
274. Roth, R.H. and R.E. Williams, *Comment on condylar movement and mandibular rotation during jaw opening.* Am J Orthod Dentofacial Orthop, 1996. **110**(3): p. 21A-23A.
275. Rubenstein, L.K., et al., *Quantitation of rotational movements associated with surgical mandibular advancement.* Angle Orthod, 1991. **61**(3): p. 167-73; discussion 174.
276. Rekow, E.D., et al., *Treatment-induced errors in occlusion following orthognathic surgery.* Am J Orthod, 1985. **88**(5): p. 425-32.

277. Rekow, E.D., T.M. Speidel, and R.A. Koenig, *Location of the mandibular center of autorotation in maxillary impaction surgery.* Am J Orthod Dentofacial Orthop, 1993. **103**(6): p. 530-6.
278. Nattestad, A., P. Vedtofte, and E. Mosekilde, *The significance of an erroneous recording of the centre of mandibular rotation in orthognathic surgery.* J Craniomaxillofac Surg, 1991. **19**(6): p. 254-9.
279. Nattestad, A. and P. Vedtofte, *Mandibular autorotation in orthognathic surgery: a new method of locating the centre of mandibular rotation and determining its consequence in orthognathic surgery.* J Craniomaxillofac Surg, 1992. **20**(4): p. 163-70.
280. Sperry, T.P., M.J. Steinberg, and B.J. Gans, *Mandibular movement during autorotation as a result of maxillary impaction surgery.* Am J Orthod, 1982. **81**(2): p. 116-23.
281. Lupkiewicz, S.M., et al., *The instantaneous hinge axis - its reproducibility and use as an indicator for dysfunction.* J Dent Res, 1982. **61**(1): p. 2-7.
282. Thieme, K.M., et al., *The mandibularly fixed hinge axis--investigation of patients with sound and pathological jaws.* Ann Anat, 2007. **189**(4): p. 384-6.
283. Sadat-Khonsari, R., et al., *Mandibular instantaneous centers of rotation in patients with and without temporomandibular dysfunction.* J Orofac Orthop, 2003. **64**(4): p. 256-64.
284. Grant, P.G., *Biomechanical significance of the instantaneous center of rotation: the human temporomandibular joint.* J Biomech, 1973. **6**(2): p. 109-13.
285. Cappozzo, A., et al., *Position and orientation in space of bones during movement: experimental artefacts.* Clin Biomech (Bristol, Avon), 1996. **11**(2): p. 90-100.
286. Schwartz, M.H. and A. Rozumalski, *A new method for estimating joint parameters from motion data.* J Biomech, 2005. **38**(1): p. 107-16.
287. Ehrig, R.M., et al., *A survey of formal methods for determining functional joint axes.* J Biomech, 2007. **40**(10): p. 2150-7.
288. Ehrig, R.M., et al., *A survey of formal methods for determining the centre of rotation of ball joints.* J Biomech, 2006. **39**(15): p. 2798-809.
289. Sadat-Khonsari, R., et al., *The helical axis of the mandible during the opening and closing movement of the mouth.* J Orofac Orthop, 2003. **64**(3): p. 178-85.
290. Reuleaux, F., *Theoretische Kinematik: Grundzüge einer Theorie des Maschinenwesens*. Vol. 1. 1875: F. Vieweg und Sohn.
291. Panjabi, M.M., *Centers and angles of rotation of body joints: a study of errors and optimization.* J Biomech, 1979. **12**(12): p. 911-20.
292. Halvorsen, K., M. Lesser, and A. Lundberg, *A new method for estimating the axis of rotation and the center of rotation.* J Biomech, 1999. **32**(11): p. 1221-7.
293. Gamage, S.S. and J. Lasenby, *New least squares solutions for estimating the average centre of rotation and the axis of rotation.* J Biomech, 2002. **35**(1): p. 87-93.
294. MacWilliams, B.A., *A comparison of four functional methods to determine centers and axes of rotations.* Gait Posture, 2008. **28**(4): p. 673-9.

295. Monnet, T., et al., *Comparison of the SCoRE and HA methods for locating in vivo the glenohumeral joint centre.* J Biomech, 2007. **40**(15): p. 3487-92.
296. Colle, F., et al., *Comparison of three formal methods used to estimate the functional axis of rotation: an extensive in-vivo analysis performed on the knee joint.* Comput Methods Biomech Biomed Engin, 2016. **19**(5): p. 484-92.
297. Taylor, W.R., et al., *Repeatability and reproducibility of OSSCA, a functional approach for assessing the kinematics of the lower limb.* Gait Posture, 2010. **32**(2): p. 231-6.
298. Sangeux, M., H. Pillet, and W. Skalli, *Which method of hip joint centre localisation should be used in gait analysis?* Gait Posture, 2014. **40**(1): p. 20-5.
299. Sun, Z., Z.J. Liu, and S.W. Herring, *Movement of temporomandibular joint tissues during mastication and passive manipulation in miniature pigs.* Arch Oral Biol, 2002. **47**(4): p. 293-305.
300. Chen, X., *The instantaneous center of rotation during human jaw opening and its significance in interpreting the functional meaning of condylar translation.* Am J Phys Anthropol, 1998. **106**(1): p. 35-46.
301. Gallo, L.M., et al., *Description of mandibular finite helical axis pathways in asymptomatic subjects.* J Dent Res, 1997. **76**(2): p. 704-13.
302. Hayashi, K., et al., *A novel statistical model for mandibular helical axis analysis.* J Oral Rehabil, 2009. **36**(2): p. 102-9.
303. DeLong, R., et al., *Helical axis errors affect computer-generated occlusal contacts.* J Dent Res, 2002. **81**(5): p. 338-43.
304. Sadat-Khonsari, R., et al., *Dimeric link chain and instantaneous centers of rotation of the mandible.* Ann Anat, 2007. **189**(4): p. 390-2.
305. Ferrario, V.F., et al., *Open-close movements in the human temporomandibular joint: does a pure rotation around the intercondylar hinge axis exist?* J Oral Rehabil, 1996. **23**(6): p. 401-8.
306. Yatabe, M., et al., *The kinematic center: a reference for condylar movements.* J Dent Res, 1995. **74**(10): p. 1644-8.
307. Yatabe, M., et al., *Movements of the mandibular condyle kinematic center during jaw opening and closing.* J Dent Res, 1997. **76**(2): p. 714-9.
308. Gallo, L.M., et al., *Relationship between kinematic center and TMJ anatomy and function.* J Dent Res, 2008. **87**(8): p. 726-30.
309. Epker, B.N. and L.C. Fish, *Surgical superior repositioning of the maxilla: what to do with the mandible?* Am J Orthod, 1980. **78**(2): p. 164-91.
310. Lemoine, J.J., et al., *Geometry-based algorithm for the prediction of nonpathologic mandibular movement.* J Oral Maxillofac Surg, 2007. **65**(12): p. 2411-7.
311. Dai, J., et al., *A novel method to determine the potential rotational axis of the mandible during virtual three-dimensional orthognathic surgery.* J Craniofac Surg, 2013. **24**(6): p. 2014-7.
312. Marin, F., et al., *Correction of axis misalignment in the analysis of knee rotations.* Hum Mov Sci, 2003. **22**(3): p. 285-96.

313. Peck, C.C., et al., *The variability of condylar point pathways in open-close jaw movements.* J Prosthet Dent, 1997. **77**(4): p. 394-404.
314. Morneburg, T. and P.A. Proschel, *Differences between traces of adjacent condylar points and their impact on clinical evaluation of condyle motion.* Int J Prosthodont, 1998. **11**(4): p. 317-24.
315. Zwijnenburg, A., C.C. Megens, and M. Naeije, *Influence of choice of reference point on the condylar movement paths during mandibular movements.* J Oral Rehabil, 1996. **23**(12): p. 832-7.
316. Robertson, G.K., G.; Caldwell, G.; Hamill, J.; Whittlesey, S., *Research Methods in Biomechanics*. 2nd Edition ed. 2013: Human Kinetics.
317. Woltring, H.J., et al., *Instantaneous helical axis estimation from 3-D video data in neck kinematics for whiplash diagnostics.* J Biomech, 1994. **27**(12): p. 1415-32.
318. Willson, J.D. and I.S. Davis, *Utility of the frontal plane projection angle in females with patellofemoral pain.* J Orthop Sports Phys Ther, 2008. **38**(10): p. 606-15.
319. Hirsch, C., et al., *Mandibular jaw movement capacity in 10-17-yr-old children and adolescents: normative values and the influence of gender, age, and temporomandibular disorders.* Eur J Oral Sci, 2006. **114**(6): p. 465-70.
320. Pullinger, A.G., et al., *Differences between sexes in maximum jaw opening when corrected to body size.* J Oral Rehabil, 1987. **14**(3): p. 291-9.
321. Westling, L. and E. Helkimo, *Maximum jaw opening capacity in adolescents in relation to general joint mobility.* J Oral Rehabil, 1992. **19**(5): p. 485-94.
322. Matsumoto, A., et al., *An analysis of hinge axis translation and rotation during opening and closing in dentulous and edentulous subjects.* Cranio, 1995. **13**(4): p. 238-41.
323. Dijkstra, P.U., et al., *Temporomandibular joint mobility assessment: a comparison between four methods.* J Oral Rehabil, 1995. **22**(6): p. 439-44.
324. Iwasaki, L.R., et al., *Modeling of muscle forces in humans with and without temporomandibular joint disorders.* Orthod Craniofac Res, 2015. **18 Suppl 1**: p. 170-9.
325. Koolstra, J.H., *Dynamics of the human masticatory system.* Crit Rev Oral Biol Med, 2002. **13**(4): p. 366-76.
326. Nickel, J.C., et al., *The effect of disc thickness and trauma on disc surface friction in the porcine temporomandibular joint.* Arch Oral Biol, 2001. **46**(2): p. 155-62.
327. Conconi, M., et al., *Is early osteoarthritis associated with differences in joint congruence?* J Biomech, 2014. **47**(16): p. 3787-93.
328. Nitzan, D.W., Y. Mahler, and A. Simkin, *Intra-articular pressure measurements in patients with suddenly developing, severely limited mouth opening.* J Oral Maxillofac Surg, 1992. **50**(10): p. 1038-42; discussion 1043.
329. Nitzan, D.W., *The process of lubrication impairment and its involvement in temporomandibular joint disc displacement: a theoretical concept.* J Oral Maxillofac Surg, 2001. **59**(1): p. 36-45.

330. Nitzan, D.W., *'Friction and adhesive forces'--possible underlying causes for temporomandibular joint internal derangement.* Cells Tissues Organs, 2003. **174**(1-2): p. 6-16.
331. Hsieh, H.H. and P.S. Walker, *Stabilizing mechanisms of the loaded and unloaded knee joint.* J Bone Joint Surg Am, 1976. **58**(1): p. 87-93.
332. Zhang, J., et al., *The reproducibility of temporomandibular joint vibrations over time in the human.* J Oral Rehabil, 2014. **41**(3): p. 206-17.
333. Gupta, B., P. Thumati, and J. Radke, *Temporomandibular joint vibrations from totally asymptomatic subjects.* Cranio, 2016. **34**(3): p. 169-75.
334. Bullough, P.G., *The geometry of diarthrodial joints, its physiologic maintenance, and the possible significance of age-related changes in geometry-to-load distribution and the development of osteoarthritis.* Clin Orthop Relat Res, 1981(156): p. 61-6.
335. Casares, G., et al., *Influence of oral stabilization appliances in intra-articular pressure of the temporomandibular joint.* Cranio, 2014. **32**(3): p. 219-23.
336. Nitzan, D.W., *Intraarticular pressure in the functioning human temporomandibular joint and its alteration by uniform elevation of the occlusal plane.* J Oral Maxillofac Surg, 1994. **52**(7): p. 671-9; discussion 679-80.
337. Hohl, T.H. and W.H. Tucek, *Measurement of condylar loading forces by instrumented prosthesis in the baboon.* J Maxillofac Surg, 1982. **10**(1): p. 1-7.
338. Hylander, W.L., *Experimental analysis of temporomandibular joint reaction force in macaques.* Am J Phys Anthropol, 1979. **51**(3): p. 433-56.
339. Brehnan, K., et al., *Direct measurement of loads at the temporomandibular joint in Macaca arctoides.* J Dent Res, 1981. **60**(10): p. 1820-4.
340. Liu, Z.J. and S.W. Herring, *Masticatory strains on osseous and ligamentous components of the temporomandibular joint in miniature pigs.* J Orofac Pain, 2000. **14**(4): p. 265-78.
341. Liu, Z.J. and S.W. Herring, *Bone surface strains and internal bony pressures at the jaw joint of the miniature pig during masticatory muscle contraction.* Arch Oral Biol, 2000. **45**(2): p. 95-112.
342. Herring, S.W. and Z.J. Liu, *Loading of the temporomandibular joint: anatomical and in vivo evidence from the bones.* Cells Tissues Organs, 2001. **169**(3): p. 193-200.
343. Ateshian, G.A., M.P. Rosenwasser, and V.C. Mow, *Curvature characteristics and congruence of the thumb carpometacarpal joint: differences between female and male joints.* J Biomech, 1992. **25**(6): p. 591-607.
344. Colombo, V., S. Palla, and L.M. Gallo, *Temporomandibular joint loading patterns related to joint morphology: a theoretical study.* Cells Tissues Organs, 2008. **187**(4): p. 295-306.
345. Gallo, L.M., et al., *Stress-field translation in the healthy human temporomandibular joint.* J Dent Res, 2000. **79**(10): p. 1740-6.
346. Ettlin, D.A., et al., *Stereometric assessment of TMJ space variation by occlusal splints.* J Dent Res, 2008. **87**(9): p. 877-81.

347. Henak, C.R., et al., *Patient-specific analysis of cartilage and labrum mechanics in human hips with acetabular dysplasia.* Osteoarthritis Cartilage, 2014. **22**(2): p. 210-7.
348. Blankevoort, L., et al., *Articular contact in a three-dimensional model of the knee.* J Biomech, 1991. **24**(11): p. 1019-31.
349. Soslowsky, L.J., et al., *Quantitation of in situ contact areas at the glenohumeral joint: a biomechanical study.* J Orthop Res, 1992. **10**(4): p. 524-34.
350. Ateshian, G.A., et al., *Contact areas in the thumb carpometacarpal joint.* J Orthop Res, 1995. **13**(3): p. 450-8.
351. D'Agostino, P., et al., *In vivo biomechanical behavior of the trapeziometacarpal joint in healthy and osteoarthritic subjects.* Clin Biomech (Bristol, Avon), 2017. **49**: p. 119-127.
352. Kwak, S.D., et al., *Hamstrings and iliotibial band forces affect knee kinematics and contact pattern.* J Orthop Res, 2000. **18**(1): p. 101-8.
353. Ateshian, G.A., et al., *A stereophotogrammetric method for determining in situ contact areas in diarthrodial joints, and a comparison with other methods.* J Biomech, 1994. **27**(1): p. 111-24.
354. Kuo, J., et al., *Regional cell density distribution and oxygen consumption rates in porcine TMJ discs: an explant study.* Osteoarthritis Cartilage, 2011. **19**(7): p. 911-8.
355. Shi, C., et al., *Anisotropic solute diffusion tensor in porcine TMJ discs measured by FRAP with spatial Fourier analysis.* Ann Biomed Eng, 2010. **38**(11): p. 3398-408.
356. Abramowicz, S., et al., *Temporomandibular joint reconstruction after failed teflon-proplast implant: case report and literature review.* Int J Oral Maxillofac Surg, 2008. **37**(8): p. 763-7.
357. Scales, J.T., *Tissue reactions to synthetic materials.* Proc R Soc Med, 1953. **46**(8): p. 647-52.
358. FDA, U. *Class 2 Device Recall VITEK 2 Gram Positive Susceptibility Test Cards ASTP605 REF 22 325*. 2016 [cited 2018 1 Mar 2018]; Available from: https://www.accessdata.fda.gov/scripts/cdrh/cfdocs/cfRES/res.cfm?id=144536.
359. Roth, T.E., J.S. Goldberg, and R.G. Behrents, *Synovial fluid pressure determination in the temporomandibular joint.* Oral Surg Oral Med Oral Pathol, 1984. **57**(6): p. 583-8.
360. Wu, Y., et al., *Fluid pressurization and tractional forces during TMJ disc loading: A biphasic finite element analysis.* Orthod Craniofac Res, 2017. **20 Suppl 1**: p. 151-156.
361. Kuo, J., et al., *The region-dependent biphasic viscoelastic properties of human temporomandibular joint discs under confined compression.* J Biomech, 2010. **43**(7): p. 1316-21.
362. Berkovitz, B.K. and J. Pacy, *Age changes in the cells of the intra-articular disc of the temporomandibular joints of rats and marmosets.* Arch Oral Biol, 2000. **45**(11): p. 987-95.

363. Berkovitz, B.K. and J. Pacy, *Ultrastructure of the human intra-articular disc of the temporomandibular joint.* Eur J Orthod, 2002. **24**(2): p. 151-8.
364. Snider, G.R., et al., *Regional dynamic tensile properties of the TMJ disc.* J Dent Res, 2008. **87**(11): p. 1053-7.
365. Kang, H., et al., *[Tensile mechanics of mandibular condylar cartilage]*. Hua Xi Kou Qiang Yi Xue Za Zhi, 2000. **18**(2): p. 85-7.
366. Kang, H., et al., *[A biomechanical study on the retrodiscal tissue of human temporomandibular joint]*. Sheng Wu Yi Xue Gong Cheng Xue Za Zhi, 2000. **17**(2): p. 143-5.
367. Tanaka, E. and T. van Eijden, *Biomechanical behavior of the temporomandibular joint disc.* Crit Rev Oral Biol Med, 2003. **14**(2): p. 138-50.
368. Tanaka, E., et al., *Biomechanical response of condylar cartilage-on-bone to dynamic shear.* J Biomed Mater Res A, 2008. **85**(1): p. 127-32.
369. Tanaka, E., et al., *Dynamic shear behavior of mandibular condylar cartilage is dependent on testing direction.* J Biomech, 2008. **41**(5): p. 1119-23.
370. Fushima, K., et al., *Analysis of the TMJ intraarticular space variation: a non-invasive insight during mastication.* Med Eng Phys, 2003. **25**(3): p. 181-90.
371. Tanaka, E., et al., *Dynamic shear properties of the temporomandibular joint disc.* J Dent Res, 2003. **82**(3): p. 228-31.
372. Juran, C.M., M.F. Dolwick, and P.S. McFetridge, *Shear mechanics of the TMJ disc: relationship to common clinical observations.* J Dent Res, 2013. **92**(2): p. 193-8.
373. Kim, D.G., et al., *Sex dependent mechanical properties of the human mandibular condyle.* J Mech Behav Biomed Mater, 2017. **71**: p. 184-191.
374. Lavigne, G.J., et al., *Rhythmic masticatory muscle activity during sleep in humans.* J Dent Res, 2001. **80**(2): p. 443-8.
375. Manfredini, D. and F. Lobbezoo, *Relationship between bruxism and temporomandibular disorders: a systematic review of literature from 1998 to 2008.* Oral Surg Oral Med Oral Pathol Oral Radiol Endod, 2010. **109**(6): p. e26-50.
376. Kaplan, S.E. and R. Ohrbach, *Self-Report of Waking-State Oral Parafunctional Behaviors in the Natural Environment.* J Oral Facial Pain Headache, 2016. **30**(2): p. 107-19.
377. Glaros, A.G., et al., *Tooth contact in patients with temporomandibular disorders.* Cranio, 2005. **23**(3): p. 188-93.
378. Staude, G., et al., *Onset Detection in Surface Electromyographic Signals: A Systematic Comparison of Methods.* EURASIP Journal on Advances in Signal Processing, 2001. **2001**(2): p. 67-81.
379. Lobbezoo, F., et al., *The effect of an occlusal stabilization splint and the mode of visual feedback on the activity balance between jaw-elevator muscles during isometric contraction.* J Dent Res, 1993. **72**(5): p. 876-82.
380. Slade, G.D., et al., *Signs and symptoms of first-onset TMD and sociodemographic predictors of its development: the OPPERA prospective cohort study.* J Pain, 2013. **14**(12 Suppl): p. T20-32 e1-3.

381. Ahmad, M., et al., *Research diagnostic criteria for temporomandibular disorders (RDC/TMD): development of image analysis criteria and examiner reliability for image analysis.* Oral Surg Oral Med Oral Pathol Oral Radiol Endod, 2009. **107**(6): p. 844-60.
382. Wei, F., et al., *A pilot study of nocturnal temporalis muscle activity in TMD diagnostic groups of women.* J Oral Rehabil, 2017. **44**(7): p. 517-525.
383. McAuliffe, P., et al., *A sleep bruxism detection system based on sensors in a splint - pilot clinical data.* J Oral Rehabil, 2015. **42**(1): p. 34-9.
384. Svensson, P., A. Burgaard, and S. Schlosser, *Fatigue and pain in human jaw muscles during a sustained, low-intensity clenching task.* Arch Oral Biol, 2001. **46**(8): p. 773-7.
385. Schwarz, P.B., S. Mir, and J.H. Peever, *Noradrenergic modulation of masseter muscle activity during natural rapid eye movement sleep requires glutamatergic signalling at the trigeminal motor nucleus.* J Physiol, 2014. **592**(16): p. 3597-609.
386. Magnussen, C., S.P. Hung, and A. Ribeiro-da-Silva, *Novel expression pattern of neuropeptide Y immunoreactivity in the peripheral nervous system in a rat model of neuropathic pain.* Mol Pain, 2015. **11**: p. 31.
387. Goto, T., et al., *Recent advances in basic research on the trigeminal ganglion.* J Physiol Sci, 2016. **66**(5): p. 381-6.
388. Song, F., et al., *Lamotrigine reverses masseter overactivity caused by stress maybe via Glu suppression.* Physiol Behav, 2014. **137**: p. 25-32.
389. Spoor, C.W. and F.E. Veldpaus, *Rigid body motion calculated from spatial co-ordinates of markers.* J Biomech, 1980. **13**(4): p. 391-3.
390. Major, P.W., et al., *Tomographic assessment of temporomandibular joint osseous articular surface contour and spatial relationships associated with disc displacement and disc length.* Am J Orthod Dentofacial Orthop, 2002. **121**(2): p. 152-61.
391. Kinniburgh, R.D., et al., *Osseous morphology and spatial relationships of the temporomandibular joint: comparisons of normal and anterior disc positions.* Angle Orthod, 2000. **70**(1): p. 70-80.
392. Gossi, D.B., et al., *Dynamic intra-articular space variation in clicking TMJs.* J Dent Res, 2004. **83**(6): p. 480-4.
393. Tadej, G., et al., *Mandibular condyle morphology in relation to malocclusions in children.* Angle Orthod, 1989. **59**(3): p. 187-94.
394. Hinton, R.J., *Relationships between mandibular joint size and craniofacial size in human groups.* Arch Oral Biol, 1983. **28**(1): p. 37-43.
395. Laboratory, T.B. *Temporomandibular Joint Biomechanics and Mechanobiology*. 2018 [cited 2018 11 Mar 2018]; Available from: http://haiyao.people.clemson.edu/research.html#TMJ.
396. Kuo, J., et al., *Effect of mechanical loading on electrical conductivity in porcine TMJ discs.* J Dent Res, 2011. **90**(10): p. 1216-20.
397. Bibby, S.R. and J.P. Urban, *Effect of nutrient deprivation on the viability of intervertebral disc cells.* Eur Spine J, 2004. **13**(8): p. 695-701.